NTNU
Norwegian University of
Science and Technology

Heat pump systems adapted to highly-insulated office buildings

Comparison between simulations and field measurement

Per Martin Skjerve

Master of Energy Use and Energy Planning
Submission date: July 2016
Supervisor: Laurent Georges, EPT
Co-supervisor: Jørn Stene, EPT
Olav Rådstoga, Asplan Viak

Norwegian University of Science and Technology
Department of Energy and Process Engineering

NTNU

Norwegian University
of Science and Technology

Department of Energy
and Process Engineering

EPT-M-2016-120

MASTER THESIS

for

Student
Per Martin Skjerve

Spring 2016

Heat pump systems adapted to highly-insulated office buildings:
Comparison between simulations and field measurement

Varmepumpesystemer i nZEB: sammenligning mellom simuleringer og feltmåling

Background and objective

The goal for the project work is to analyse the change in design procedures of heat pump systems when the building energy performance is progressively improved, i.e. starting from the standard performance of today, to the passive house standard and, finally, to the nZEB level. This is done using simple modelling approaches implemented in Matlab/Simulink. This proposal is the continuation of Master student works of the academic year 2014-2015, where a Beta-version of a simulation tool has been developed. Furthermore, this work is the follow-up of a specialization project performed in fall semester. The present contribution will further focus on the validation of the Beta-version of the tool using results from measurement data. The investigated heat pump system is installed on the PowerHouse Kjørbo building.

The Master thesis is connected to the NTNU-SINTEF Zero Emission Building (ZEB) activity on development of an early-stage design tool for the selection of renewable thermal energy supply systems for nZEB (near Zero Emission Buildings) as well as the IEA HPP Annex 40 on heat pumps for nZEB.

The following tasks are to be considered:

1. Based on the procedure planned in the specialization project, compare the performance of the main heat pump system components (heat pump, boreholes and storage tanks) between simulation and measurements. Discuss results.
2. Continue the comparison at a system level where a larger number of components are interconnected together. Discuss results.
3. Based on this experience, discuss the ability of simulations to reproduce real operation, e.g.:
    a. On which aspects does it fail or does it work? What simulation is good at?
    b. How much measurement data is needed to calibrate simulations properly?

-- " --

Within 14 days of receiving the written text on the master thesis, the candidate shall submit a research plan for his project to the department.

When the thesis is evaluated, emphasis is put on processing of the results, and that they are presented in tabular and/or graphic form in a clear manner, and that they are analyzed carefully.

The thesis should be formulated as a research report with summary both in English and Norwegian, conclusion, literature references, table of contents etc. During the preparation of the text, the candidate should make an effort to produce a well-structured and easily readable report. In order to ease the evaluation of the thesis, it is important that the cross-references are correct. In the making of the report, strong emphasis should be placed on both a thorough discussion of the results and an orderly presentation.

The candidate is requested to initiate and keep close contact with his/her academic supervisor(s) throughout the working period. The candidate must follow the rules and regulations of NTNU as well as passive directions given by the Department of Energy and Process Engineering.

Risk assessment of the candidate's work shall be carried out according to the department's procedures. The risk assessment must be documented and included as part of the final report. Events related to the candidate's work adversely affecting the health, safety or security, must be documented and included as part of the final report. If the documentation on risk assessment represents a large number of pages, the full version is to be submitted electronically to the supervisor and an excerpt is included in the report.

Pursuant to "Regulations concerning the supplementary provisions to the technology study program/Master of Science" at NTNU §20, the Department reserves the permission to utilize all the results and data for teaching and research purposes as well as in future publications.

The final report is to be submitted digitally in DAIM. An executive summary of the thesis including title, student's name, supervisor's name, year, department name, and NTNU's logo and name, shall be submitted to the department as a separate pdf file. Based on an agreement with the supervisor, the final report and other material and documents may be given to the supervisor in digital format.

☐ Work to be done in lab (Water power lab, Fluids engineering lab, Thermal engineering lab)
☐ Field work

Department of Energy and Process Engineering, 13. January 2016

Olav Bolland
Department Head

Laurent Georges, Asc. Prof.
Academic Supervisor

Research Advisor:
Jørn Stene, adjunct professor NTNU, jost@cowi.no
Olav Råstoga, Asplan Viak, olav.raadstoga@asplanviak.no

Summary

The temperature in the atmosphere is rising as a cause of human influence, and it was found that the building sector in 2012 emitted 18.4 % of the greenhouse gas (GHG) emissions on the planet (Pachauri et al., 2014). A solution to reduce the GHG emissions in the sector is the zero emission building (ZEB) concept. Cost-optimisation of the heating and cooling system in a ZEB is a challenge, and therefore the NTNU-SINTEF Zero Emission Building activity and the International Energy Agency Annex 40 have been working on a design tool for the selection of renewable thermal energy supply systems for non-residential near Zero Emission Buildings (nZEB).

This design tool is called "Simulation tool for Nearly Zero Energy buildings heat Pump installations" (NZEP) and has been developed through the work of three master theses and three project works. This thesis is an continuation of a project work, written in the fall of 2015, investigated the possibilities of comparing the components in the simulation model with measured data from the CC-system of Powerhouse Kjørbo (Skjerve, 2016).

The main objective in this thesis is therefore to compare simulations performed on the main components of NZEP to field measurements from Powerhouse Kjørbo. These components are considered the heat pump block, storage tank block and ground source heat exchanger block, and the thesis therefore only deals with these components. Pressure losses and flow abilities for the chosen components are not investigated.

Comparisons for single component and multiple component simulations have been performed. For both kinds of comparisons, the inputs are gathered from and the outputs are compared to measured values from the CC-system at Powerhouse Kjørbo.

Based on the comparisons and the discussions presented in this thesis, it is concluded that:

- The heat pump block simulates nominal performance very well, but that the start-up of the block should be compared to measurements with a lower sample rate.
- The storage tank block is producing temperatures with similar trends as the measured data, but that a sensor should be mounted in order to calibrate the simulation properly.
- The GSHE block simulates similar temperatures out of the borehole in situations where the volume flow in the real borehole is constant.
- The simulation of multiple components works very well, all though there are additional complications in implementing a control strategy for the system.

Summary (Norwegian)

Temperaturen i atmosfæren øker som en konsekvens av menneskelig påvirkning, og det ble etablert at byggesektoren in 2010 sto for 18,4 % av de totale klimagassutslippene på planeten. En løsning for å redusere klimagassutslippene innenfor sektoren kan være nullutslippsbygg-konseptet. Kostnadsoptimering av varme- og kjølesystemet i nullutslippsbygg er en utfordring og derfor har NTNU-SINTEF Zero Emission Building activity og International Energy Agency Annex 40 jobbet med et verktøy for å hjelpe beslutningstaking for design av varme- og kjølesystem i planleggingsstadiet for lavutslipps yrkesbygg.

Dette verktøyet kalles «Simulation tool for Nearly Zero Energy buildings and heat pump installations» (NZEP) og har blitt utviklet gjennom tre masteravhandlinger og tre fordypningsprosjekt. Denne masteravhandlingen er en videreutvikling av et fordypningsprosjekt, utført høsten 2015, som undersøkte muligheten for å sammenligne komponentene i simuleringsmodellen mot målte data fra Powerhouse Kjørbo sitt SD-anlegg.

Målet i denne masteravhandlingen er derfor å utføre en sammenligning av hovedkomponentene i NZEP mot feltmålinger fra Powerhouse Kjørbo. Hovedkomponentene i simuleringsprogrammet anses å være varmepumpe-, akkumulatortank- og borehullkomponenten, og prosjektet konsentrerer seg derfor om disse komponentene. Trykktap i de nevnte komponentene er ikke undersøkt.

Sammenligninger for simuleringer utført med enkeltkomponenter og flere komponenter er utført. For begge sammenligningstypene er inndataene samlet fra og utdataene sammenlignet med målte verdier fra CC-system på Powerhouse Kjørbo.

Basert på sammenligningene og diskusjonene som er presentert i denne avhandlingen er det konkludert med at:

- Varmepumpe-blokken simulerer nominell ytelse meget godt, men at oppstarten for blokken bør sammenlignes med målinger med høyere måletetthet.
- Akkumulatortank-blokken produserer temperaturer som har samme trend som måledataene, men at en sensor bør monteres for å kalibrere simuleringen bedre.
- Borehull-blokken simulerer relativt like temperaturer ut av borehullet i situasjoner hvor volumstrømmen i det virkelige borehullet er konstant.
- Simulering av flere komponenter fungerer veldig bra, selv om det er flere komplikasjoner når man implementerer en kontrollstrategi for systemet.

Preface

This master thesis is the final work in my education, and is a continuation on works done by former master students of developing "Simulation tool for Nearly Zero Energy buildings heat Pump installations" (NZEP). The topic of this thesis is to compare simulations, performed with components from NZEP, to measurements from the heating and cooling system at Powerhouse Kjørbo.

There are some people I would like to thank for help they have given me in the process of writing this thesis. Laurent Georges, Jørn Stene and Olav Rådstoga have been my supervisors for the project, and I would like to thank them for helping me with information, feedback and keeping the project on track. Especially I would like to tank Laurent for being available in his office and taking the time to answer my questions. I would like to thank Randi Kalskin Ramstad for being a great source of help regarding information about boreholes. The former master students Mikkel Ytterhus, Ivar Flugekvam Nordang and Odin Budal Søgnen have been very helpful in providing me with information, for which I would like to thank them. Two of my best friends has read the thesis and have given me good feedback, and for this, I would like to thank Stian Andre Kinnunen and Øystein Sundnes.

Per Martin Lyngstad Skjerve

Inderøy 03.07.2016, Per Martin Lyngstad Skjerve

Table of contents

1 Introduction 1

1.1 Goal 2

1.2 Boundaries 2

1.3 Structure and content 2

2 NZEP 5

2.1 The development 5

2.2 Algorithm 6

2.3 Model description 7

2.4 Components 8

2.4.1 THB 9

2.4.2 Heat pump block 9

2.4.3 Storage tank block 11

2.4.4 GSHE block 13

3 Powerhouse Kjørbo 17

3.1 The heating and cooling system 17

3.1.1 Set point temperatures 18

3.1.2 System changes 18

3.2 Components 20

3.2.1 Heat pump for space heating 20

3.2.2 Heat pump for DHW 22

3.2.3 Storage tanks for space heating 23

3.2.4 Storage tanks for DHW 24

3.2.5 Boreholes 26

3.3 Measuring points 28

3.3.1 CC-system 28

3.3.2 EMS 30

4 Modifications to the matrixes 33

4.1 Tamb 33

4.2 Heat pumps 33

4.2.1 Energy consumption circulation pumps 33

4.2.2 Performance matrix HS-HP 34

4.3 Storage tanks 34

4.3.1 U-value for storage tanks 34

4.3.2 Effective vertical conductivity 35

4.3.3 Heights of inlet/outlets and measurement points 35
4.4 GHE 36
4.4.1 Average annual outdoor temperature 36
4.4.2 Thermal conductivity of the ground 37
4.4.3 Design mass flow rate 38
5 Comparison procedure 39
5.1 Input parameters 39
5.2 Single component comparison 39
5.2.1 Input and output data 40
5.2.2 Comparison period 40
5.3 Multiple component comparison 40
5.3.1 Input and output data 40
5.3.2 Comparison period 41
6 Simulation models 43
6.1 The signal builder block 43
6.2 Volume flow into mass flow 43
6.3 Heat pump for space heating 44
6.3.1 Adaptation and configuration 45
6.3.2 Simulations 46
6.4 Heat pump for DHW 47
6.4.1 Adaptation and configuration 48
6.4.2 Simulations 49
6.5 Storage tanks for space heating 49
6.5.1 Adaptation and configuration 49
6.5.2 Simulations 51
6.6 GSHE 51
6.6.1 Simulation 1 52
6.6.2 Simulation 2 54
6.7 Storage tanks for DHW 54
6.8 Space heating system 55
6.8.1 Adaptation and configuration 55
6.8.2 Simulation 57
7 Comparison 58
7.1 Heat pump for space heating 58
7.1.1 Simulation 1 58
7.1.2 Simulation 2 61

7.1.3 Simulation 3 63
7.1.4 Simulation 4 64
7.2 Heat pump for DHW 67
7.2.1 Simulation 1 67
7.2.2 Simulation 2 70
7.3 Storage tanks for space heating 72
7.3.1 Simulation 1 72
7.3.2 Simulation 2 74
7.3.3 Simulation 3 77
7.3.4 Simulation 4 80
7.4 Boreholes 83
7.4.1 Initialization period simulation 1 83
7.4.2 Comparison period 86
7.4.3 Simulation 2 89
7.5 Space heating system 92
7.5.1 Comparison 93
7.5.2 Discussion 94
7.6 Discussion 95
7.6.1 Heat pump 95
7.6.2 Storage tank 97
7.6.3 GSHE 98
7.6.4 Space heating system 98
8 Conclusion 99
8.1 Heat pump block 99
8.2 Storage tank block 99
8.3 Ground source heat exchanger block 99
8.4 System level 99
9 Proposals for future work 101
Bibliography 103
Appendix I - Matrix SH-HP 107
Appendix II - Matrix DHW-HP 109
Appendix III - Matrix SH-ST 111
Appendix IV - Matrix DHW-ST 113
Appendix V - Matrix GHE 115
Appendix VI – Equations 117

Appendix VII – Calculations **119**
Appendix VIII – Energy meters for the hydronic system **123**
Appendix IX – Timeline for the boreholes **124**
Appendix X – Missing measurements **125**
Appendix XI – Volume flow in the boreholes **126**
Appendix XII – Heat pump models **127**
Appendix XIII – Storage tank model **128**
Appendix XIV – GHE simulation model **129**
Appendix XV – Space heating system model **130**
Appendix XVI – Capacity control of the heat pump block **131**

Table of figures

Figure 1 – The algorithm (Murer, 2014) 6
Figure 2 – The model description (Ytterhus, 2015) 7
Figure 3 – Source system (Ytterhus, 2015) 8
Figure 4 – Storage system (Ytterhus, 2015) 8
Figure 5 – Heat pump block (Carnot, 2010) 9
Figure 6 – Example matrix of measurement data for heat pump 10
Figure 7 – Different storage tank blocks (Carnot, 2010) 12
Figure 8 – GSHE (Ytterhus, 2015) 14
Figure 9 – Principle system design of the thermal energy system (Nordang, 2014). 17
Figure 10 – Outdoor temperature compensation curves 18
Figure 11 – Changes in the heating and cooling system (Nordang, 2014) (modified figure) 19
Figure 12 – Heat pump for space heating (Nordang, 2014) 20
Figure 13 – SH-HP outdoor temperature compensation curve 21
Figure 14 – Heat pump water heater (Nordang, 2014). 22
Figure 15 – Storage thanks for space heating (Nordang, 2014). 23
Figure 16 – Measurements SH-ST (Oso Hotwater, 2011) (modified figure) 24
Figure 17 – Storage tanks for DHW (Nordang, 2014) 25
Figure 18 - Measurements DHW-ST (Oso Hotwater, 2011) (modified figure) 25
Figure 19 – Boreholes (Nordang, 2014) 26
Figure 20 – Borehole configuration (Nordang, 2014) 27
Figure 21 – Measuring points (Nordang, 2014) 28
Figure 22 – Heating system (Nordang, 2014) 29
Figure 23 – Energy meters (Nordang, 2015) 30
Figure 24 – Temperatures in the ground (Ramstad, 2013)(modified figure) 37
Figure 25 – Transformation blocks 44
Figure 26 – Signal modification SH-HP 46
Figure 27 – Signal modification DHW-HP 48
Figure 28 – Illustration of different coupling 50
Figure 29 – Control system 56
Figure 30 – Temperature difference radiator circuit 57
Figure 31 – Comparison SH-HP simulation 1: Power consumption 59

Figure 32 - Comparison SH-HP simulation 1: Temperature in and out of condenser 59
Figure 33 - Comparison SH-HP simulation 1: Temperature difference condenser and evaporator 60
Figure 34 - Comparison SH-HP simulation 2: Power consumption 62
Figure 35 - Comparison SH-HP simulation 2: Temperature difference condenser 62
Figure 36 - Comparison SH-HP simulation 3: Power consumption 63
Figure 37 - Comparison SH-HP simulation 3: Temperature difference condenser 64
Figure 38 - Comparison SH-HP simulation 4: Power consumption 65
Figure 39 - Comparison SH-HP simulation 4: Temperature out of condenser 65
Figure 40 - Comparison SH-HP simulation 4: temperature difference condenser 66
Figure 41 - Comparison DHW-HP simulation 1: Power consumption 67
Figure 42 - Comparison DHW-HP simulation 1: Temperature out of condenser 68
Figure 43 - Comparison DHW-HP simulation 1: Temperature difference condenser 68
Figure 44 - Comparison DHW-HP simulation 1: Temperature difference evaporator 69
Figure 45 - Comparison DHW-HP simulation 1: Mass flow evaporator and condenser 69
Figure 46 - Comparison DHW-HP simulation 2: Power consumption 71
Figure 47 - Comparison DHW-HP simulation 2: Temperature difference condenser 71
Figure 48 - Comparison SH-ST simulation 1: Tank temperature 72
Figure 49 - Comparison SH-ST simulation 1: Temperature to heat pump 73
Figure 50 - Comparison SH-ST simulation 1: Temperature to SH 73
Figure 51 - Comparison SH-ST simulation 2: U=1 W/m^{2}K 75
Figure 52 - Comparison SH-ST simulation 2: U=1.3 W/m^{2}K 75
Figure 53 - Comparison SH-ST simulation 2: U=2.5 W/m^{2}K 76
Figure 54 - Comparison SH-ST simulation 2: Temperature to heat pump 76
Figure 55 - Comparison SH-ST simulation 2: Temperature to SH 77
Figure 56 - Comparison SH-ST simulation 3: EVC=0.5W/mK 78
Figure 57 - Comparison SH-ST simulation 3: EVC=1.0W/mK 78
Figure 58 - Comparison SH-ST simulation 3: EVC=1.5W/mK 79
Figure 59 - Comparison SH-ST simulation 3: Temperature to heat pump 79
Figure 60 - Comparison SH-ST simulation 3: Temperature to SH 80
Figure 61 - Comparison SH-ST simulation 4: 2 nodes 81
Figure 62 - Comparison SH-ST simulation 4: 5 nodes 81
Figure 63 - Comparison SH-ST simulation 4: 15 nodes 82
Figure 64 - Comparison SH-ST simulation 4: Temperature to heat pump 82

Figure 65 - Comparison SH-ST simulation 4: Temperature to SH 83
Figure 66 – Comparison GSHE initialization simulation 1: Outgoing temperature 84
Figure 67 – Initialization: Measured supplied and ejected thermal power for the borehole 84
Figure 68 – Initialization: Simulated supplied and ejected thermal power for the GSHE .. 85
Figure 69 – Initialization: Difference between simulated and measured thermal power 85
Figure 70 – Initialization: Measured mass flow in the borehole 86
Figure 71 – Comparison GSHE simulation 1: Outgoing temperature..... 87
Figure 72 – Measured supplied and ejected thermal power for the borehole..... 87
Figure 73 – Simulated supplied and ejected thermal power for the GSHE..... 88
Figure 74 - Difference between simulated and measured thermal power 88
Figure 75 - Measured mass flow in the borehole 89
Figure 76 – Boreholes simulation 2: Temperature in the ground nr.1 90
Figure 77 – Boreholes simulation 2: Temperature in the ground nr.2 90
Figure 78 – Boreholes simulation 2: Temperature in the ground nr.3 90
Figure 79 – Boreholes simulation 2: Temperature in the ground nr.4 91
Figure 80 – Boreholes simulation 2: Temperature in the ground nr.5 91
Figure 81 – Boreholes simulation 2: Accumulated thermal energy in the ground..... 92
Figure 82 – Comparison SH-system simulation 1: Measured temp. to SH..... 93
Figure 83 - Comparison SH-system simulation 1: Simulated temp. to SH..... 93
Figure 84 – Comparison SH-system simulation 1: Simulated set-temp..... 94
Figure 85 Comparison SH-system simulation 1: Energy consumption heat pump..... 94
Figure 86 – Heat pump cycle (Karlsson and Fahlén, 2007) 97

Table of tables

Table 1 – Short explanation of the algorithm 6
Table 2 – The model description 7
Table 3 – Input parameters of the heat pump block 11
Table 4 – Input parameters for storage tanks (Carnot, 2010) 13
Table 5 – Input parameters GSHE 15
Table 6 – Performance data Carrier 61WG-070 (Carrier SCS, 2012) 21
Table 7 – Performance data NIBE F1145-10 23
Table 8 – Parameters Maxi Accu 51R 1000 24
Table 9 – Parameters OSO Maxi Standard 17R/RE 600 26
Table 10 – Sensor accuracy (Nordang, 2015) 30
Table 11 – Extrapolated performance curve 34
Table 12 – Simulations SH-HP 47
Table 13 – Simulations DHW-HP 49
Table 14 – Simulations SH-ST 51
Table 15 – Input parameters for simulation 1 52

Nomenclature

Abbreviations

CC-system	**C**entral **C**ontrol-System
COP	**C**oefficient **o**f **P**erformance
DHW	**D**omestic **h**ot **w**ater
DHW-HP	Heat pump for heating of domestic hot water
DHW-ST	Storage tanks for domestic hot water
EMS	**E**nergy **M**onitoring **s**ystem
ETC	**E**ffective **T**hermal **C**onductivity
EVC	**E**ffective **V**ertical **C**onductivity
EWS	**E**rd**w**ärme**s**onden (Which in English means “ground source heat exchanger”)
GHG	**G**reen **H**ouse **G**as
GSHE	**G**round **S**ource **H**eat **E**xchanger
LMTD	**L**ogarithmic **m**ean **t**emperature **d**ifference
nZEB	**n**early **Z**ero **E**mission **B**uilding
NZEP	Simulation tool for **N**early **Z**ero **E**nergy buildings heat **P**ump installations
SH-HP	Heat pump for space heating and heating of ventilation air
SH-ST	Storage tanks for space heating
SPF	**S**easonal **P**erformance **F**actor
THB	**T**hermo-**H**ydraulic **B**us
ZEB	**Z**ero **E**mission **B**uilding (also used for “**Z**ero **E**nergy **B**uilding”, but not in this thesis)

Terms

Energy meter	Energy measurement sensor
Heating and cooling system	This includes the system for space heating and cooling, DHW, heating and cooling of ventilation air in addition to their control system.
Intermittent control	On/off control
Charge and discharge circuit for a storage tank	The charge circuit is the circuit where the component heating up the storage tank is placed. The discharge circuit is the circuit that is using the heat of the heat pump.

1 Introduction

In the Fifth Assessment Report (Pachauri et al., 2014) made by the IPCC, it is concluded that the atmospheric temperature is rising and that they are 90 % sure that humans are a major influence in this climate change. Some of the consequences associated with rising global temperatures presented in this report are: loss of species, extreme weather events, decrease in regional crop yields and acidification of oceans. The building sector emitted, according to the Fifth Assessment Report, 18.4 % of the greenhouse gas (GHG) emissions in 2010.

A solution to reduce GHG emissions in the building sector is to implement the zero emission building (ZEB) concept. Although a ZEB standard has yet to be made, it is commonly agreed upon as a building that in sum over its lifetime produces close to zero GHG emissions. In order to emit no GHG' the ZEBs have to produce energy to account for the GHG emissions in the making, in the operation and in the demolition of the building. Emissions from technical equipment not connected to the buildings energy system are usually not included in the calculations. Since energy producing systems and energy efficient heating and cooling systems are expensive, finding the most cost-efficient solution is often the biggest challenge.

In this context, the NTNU-SINTEF Zero Emission Building activity and the International Energy Agency have been working on an early-stage design tool for the selection of renewable thermal energy supply systems for near Zero Emission Buildings (nZEB). This design tool is called "Simulation tool for Nearly Zero Energy buildings heat Pump installations" (NZEP) and the first version was made in a master thesis written in 2013 (Småland, 2013). Through development, the simulations have become faster, obtained new components and become tidier (Murer, 2014, Ytterhus, 2015).

A master thesis written in the spring semester of 2015 (Ytterhus, 2015) suggested that the next step in the development of NZEP was validation of the simulation components. A project work was therefore written in the fall of 2015 investigating the possibilities of comparing the components in the simulation model with measured data from the CC-system of Powerhouse Kjørbo (Skjerve, 2016). This thesis is based on the project work written in the fall semester of 2015, and performs a comparison between components in NZEP and field measurements.

1.1 Goal

The goal of this thesis is to answer these following tasks, which are proposed in the description of the thesis:

1. Based on the procedure planned in the specialization project, compare the performance of the main heat pump system components (heat pump, boreholes and storage tanks) between simulation and measurements. Discuss results.
2. Continue the comparison at a system level where a larger number of components are interconnected together. Discuss results.
3. Based on this experience, discuss the ability of simulations to reproduce real operation, e.g.:
    a. On which aspects does it fail or does it work? What simulation is it good at?
    b. How much measurement data is needed to calibrate simulations properly?

1.2 Boundaries

The material in this thesis only deals with boreholes, heat pumps and storage tanks. Other components are not considered. Pressure losses and flow abilities in the chosen components are not investigated either.

It is also assumed that the reader has basic knowledge about heat pumps, storage tanks, boreholes, Matlab and Simulink.

1.3 Structure and content

Chapter 2: Presents information about NZEP, which is based on chapter 2 from the project work. The information about NZEP is mostly gathered from the master thesis and project work of Mikkel Ytterhus (Ytterhus, 2014, 2015).

Chapter 3: Presents information about Powerhouse Kjørbo, which is based on chapter 3 the project work. The information about Powerhouse Kjørbo is mostly gathered from the master thesis and project work of Ivar Flugekvam Nordang (Nordang, 2014, 2015)

Chapter 4: Presents changes that have been done to the matrixes that were presented in the project work.

Chapter 5: Presents the procedure for comparing the simulations to the field measurements. It also gives some general information about the input and output data for each of the simulation components.

Chapter 6: Presents the set up for each of the simulations that is performed in this thesis, and which values that are compared for each simulation. The results of the simulations are presented Chapter 7.

Chapter 7: Presents the results from the simulations and compares them to the measured values at Powerhouse Kjørbo. The comparisons and the simulation components are then discussed.

Chapter 8: Sums up the conclusions that can be drawn from Chapter 7.

Chapter 9: Describes proposals for future work within NZEP.

Equations are explained in Appendix VI.

2 NZEP

*"This tool is termed NZEP, for simulation tool for **N**early **Z**ero **E**nergy buildings heat **P**ump installations" (Alonso et al., 2015).*

As mentioned in the introduction, the NZEP is an early-stage decision-making tool to help choosing renewable electrical and thermal energy sources for nZEB. With the use of an algorithm the program approximates the annual energy consumption, costs and GHG emissions for different heat pump sizes, and thus makes it possible to make decisions regarding the buildings energy system (Ytterhus, 2015).

2.1 The development

The first version of the program was developed during the project work and master thesis of Leif Småland. This program was made in Matlab and presented an algorithm that calculated annual energy use, emissions and cost (Småland, 2013).

Thomas Murer then made a new version of the tool, using Simulink to simulate the hydronic system and Matlab as the executing program. Components from the Carnot library, developed at the Solar Institut Jülich, were also implemented into the model. This led to a model with a graphical interface and more advanced components. The algorithm was among other changes modified to tie the two programs together (Murer, 2014).

Mikkel Ytterhus did the next development of the program. During his project work and master thesis he made the model description of the algorithm tidier and also reduced computation time by making modifications to the model and to the components (Ytterhus, 2015).

Simon Aldebert wrote his project work simultaneously as Mikkel Ytterhus wrote his master thesis. In this project thesis Aldebert developed an air sourced heat pump for the model (Aldebert, 2015).

2.2 Algorithm

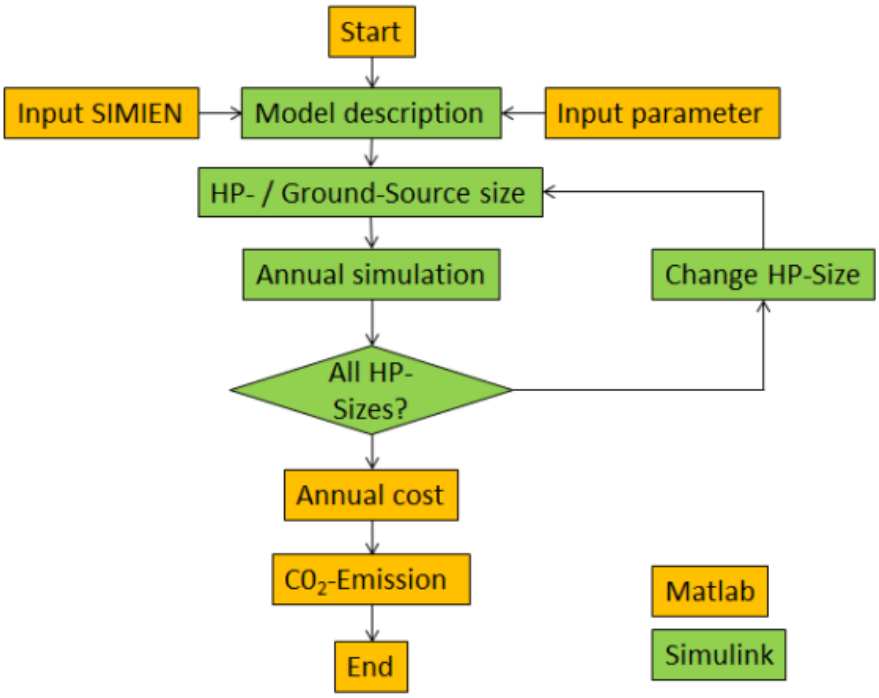

Figure 1 – The algorithm (Murer, 2014)

Figure 1 shows the algorithm that Thomas Murer presented in his master thesis. A short description of the blocks is given in Table 1.

Table 1 – Short explanation of the algorithm

Block	Description
Input SIMIEN	The energy need for heating and cooling per time unit for a year.
Input parameter	The different parameters for the used components.
Model description	The model of the heating and cooling system.
HP-/Ground – Source size	A function that is changing both the heat pump size and the number of boreholes.
Annual simulation	Calculates the annual energy use for the heating and cooling system.
All HP-Sizes?	Checks if the annual simulation has been performed for all of the heat pumps. If yes, it goes to annual cost. If no, it starts a new simulation with a new heat pump.
Change HP-Size	Sets up the model with a heat pump that has not yet been simulated.
Annual cost	Calculates annual costs based on the total annual energy consumption, estimated maintenance costs and investment cost for the heating and cooling system.
CO_2-Emission	Calculates the annual GHG emissions based on the energy consumption for the heating and cooling system.

2.3 Model description

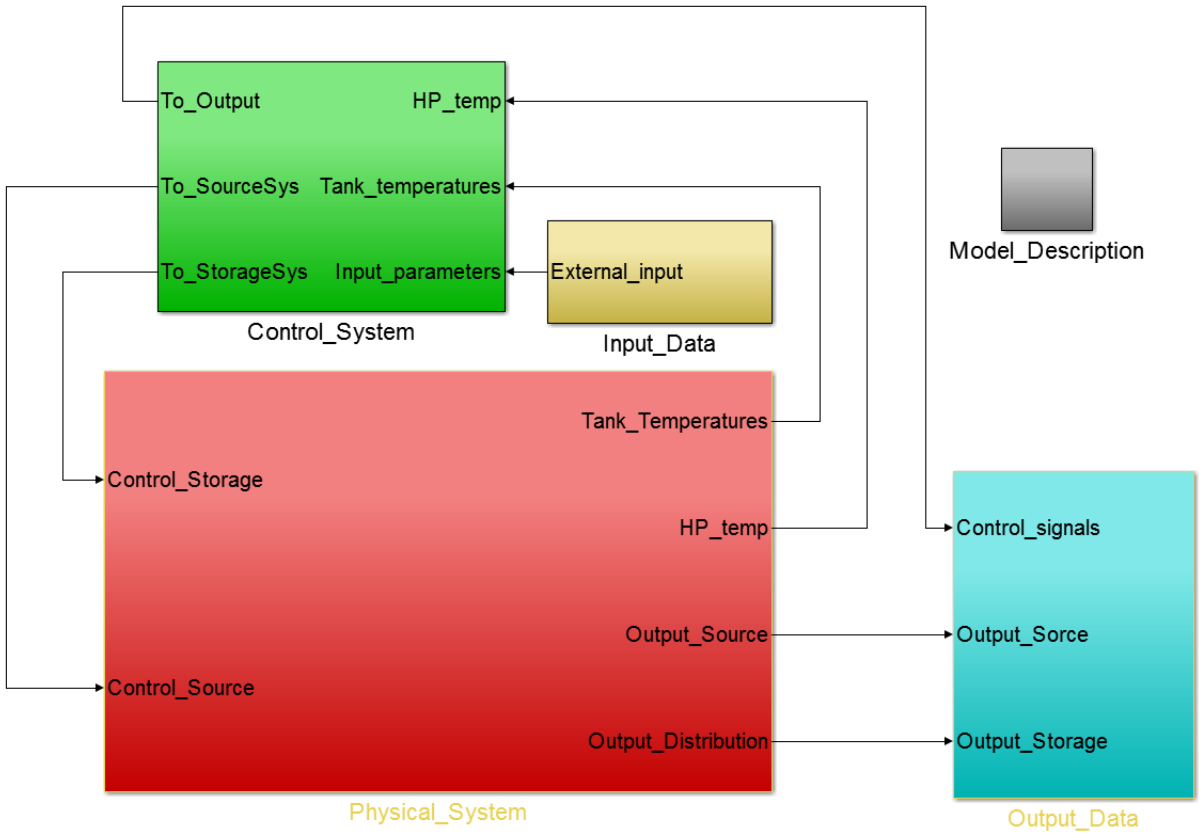

Figure 2 – The model description (Ytterhus, 2015)

As mentioned in Chapter 2.2, the model description of the algorithm is the model of the heating and cooling system. Figure 2 shows the first layer of the model description, where the heating and cooling system are divided into subsystem blocks. A short description of the blocks is given in Table 2.

Table 2 – The model description

Block	**Description**
Input_Data	Contains the power needed for heating and cooling per time unit.
Control_System	Contains the signal processing and control strategy for the system.
Physical_System	Contains two subsystems called "Source_System" and "Storage_System", which are the heat and cooling producing and storing parts of the system.
Output_Data	Contains the processing of the output data.
Model_Description	Contains information about the system and abbreviations. This block is not connected to the other blocks

2.4 Components

The components can be connected to simulate different heating and cooling systems. Figure 3 shows an example of a source system containing a ground source heat pump, and is the source system Mikkel Ytterhus assembled during his master thesis. The green square shows the ground source heat exchanger block and the red one to the right shows the heat pump block.

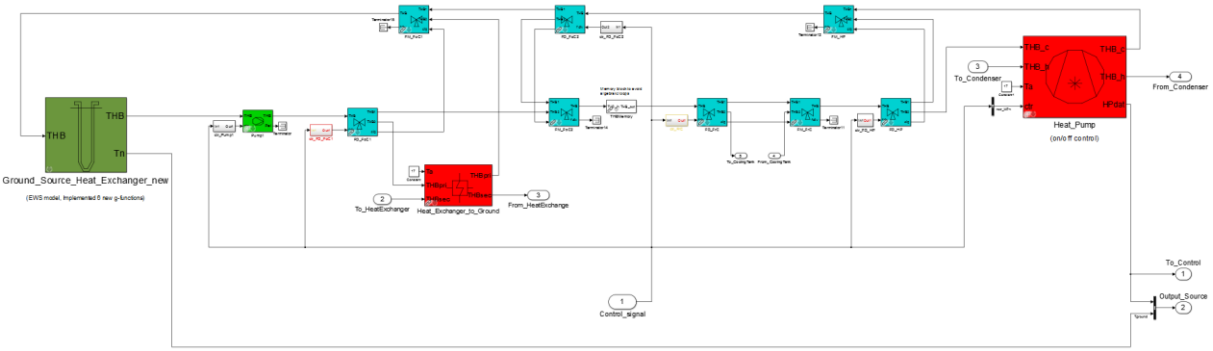

Figure 3 – Source system (Ytterhus, 2015)

Figure 4 shows an example of a thermal energy storage system. This storage system has a storage tank for space heating and heating of ventilation air, a tank for DHW and a tank for the cooling system, which are shown in the red squares to the right of the figure.

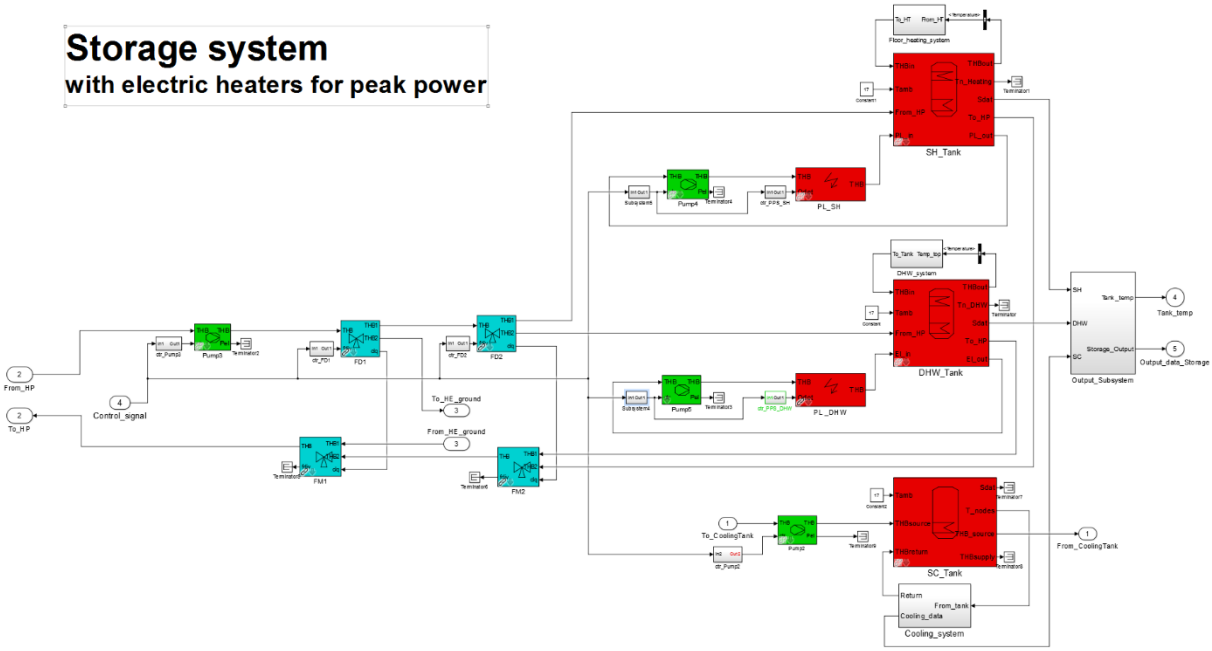

Figure 4 – Storage system (Ytterhus, 2015)

Except for the ground heat exchanger, none of the blocks illustrated in Figure 4 are changed from the Carnot library. The ground source heat exchanger block is originally from the Carnot library, but was modified during the master thesis of Mikkel Ytterhus by Laurent Georges (Ytterhus, 2015).

2.4.1 THB

In order to simulate the fluids circulating between the component blocks, a signal called Thermo-Hydraulic-Bus (THB) is used. The THB is a vector consisting of 12 parameters, which gives information about the fluids that are entering and leaving the block. Some of the information these parameters are giving is the temperature, mass flow rate, fluid type, fluid mix and pressure. Other blocks in the Carnot library can be used to calculate values such as the heat capacity or the density from the information in the THB (Ytterhus, 2015).

2.4.2 Heat pump block

The heat pump block uses the control signal, temperature of the fluid entering the evaporator, in addition to the temperature and the mass flow of the fluid entering the condenser to calculate the power consumption and the heating and cooling capacity of the heat pump (Murer, 2014). Figure 5 is gathered from the Carnot library (Carnot, 2010), and shows the heat pump block.

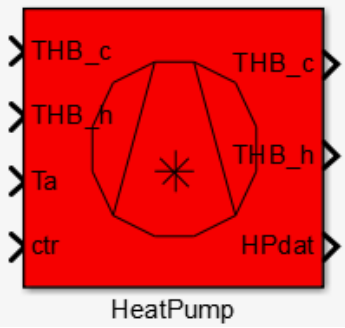

Figure 5 – Heat pump block (Carnot, 2010)

2.4.2.1 Inputs and outputs

As it can see from Figure 5, the block has four inputs and three outputs. The *THB_c* represents the fluid circulating on the cold side of the heat pump (evaporator) and the *THB_h* represents the fluid circulating on the hot side of the heat pump (condenser). *Ta* is an input for the ambient temperature in the machinery room and is a value that is necessary in order to calculate the heat loss from the heat pump. The *ctr* input is the signal input, and the block is developed to be intermittent controlled by the input signals 0 or 1, which means off and on respectively. *HPdat* is an output of various data, such as power consumption, heat capacity, cooling capacity, temperatures in and out of the condenser and evaporator and mass flows, which can be used to log different parameters in the heat pump (Ytterhus, 2015).

2.4.2.2 Black box

The heat pump block can be viewed as a “black box” which makes no physical calculations of the heat pump circle. It performs linear regression of data measured in accordance with NS-

EN 14511 in order to determine power consumption and the heating and cooling capacity according to given inlet fluid temperatures of the evaporator and outlet fluid temperatures out of the condenser (Murer, 2014). In the standard rating conditions given in NS-EN 14511-2:2013, the measurements must be done at 0°C and 10°C inlet fluid temperatures for the evaporator and 35°C, 45°C, 55°C and 65°C outlet temperature out of the condenser. The fluid temperature difference over the evaporator is set at 3 K and the fluid temperature difference in the condenser is set at 5 K for 35°C and 45°C, 8 K for 55°C and 10 K for 65°C outgoing condenser temperature (Standard Norge, 2013). The block then calculates the temperature of the fluid going out of the evaporator/condenser by using the temperature, heat capacity and the inlet mass flows for the evaporator/condenser along with the power in the evaporator/condenser.

Heating power [W]	Source power [W]	Electric power [W]	Temperature of brine coming into the evaporator [°C]	Temperature of water coming out of the condenser [°C]
9 660	7 650	2 010	0	35
8 550	6 280	2 270	0	45
7 580	5 200	2 380	0	55
6 490	4 010	2 480	0	65
12 820	10 630	2 190	10	35
11 800	9 250	2 550	10	45
10 940	8 150	2 790	10	55
9 650	6 640	3 010	10	65

Figure 6 – Example matrix of measurement data for heat pump

The heat pump measurement data can typically look like the matrix in Figure 6. For a brine to water heat pump, NS-EN 14511 also specifies that the values in the electric power matrix contain the pump power that is needed to account for the pressure losses in the evaporator and condenser.

2.4.2.3 Control

A simulation specified in Appendix XVI demonstrates that the heat pump block can be capacity controlled from 0-100 % with an input signal from 0 to 1. The COP of the heat pump is however changing over the capacity area and, all though some heat pumps might have a

similar part load performance curve, it is certain that this part load performance curve does not apply to all heat pumps both because of different compressor types and part load solutions (Stene, 1997). In the accompanying Carnot manual (Solar Institute Juelich, 2014), it is described that the input signal should be 0 or 1 and, all though this is not explained, it is assumed that this is specified because it yet is not implemented a good method to compensate the part load operation of the heat pump block.

2.4.2.4 Input parameters

The input parameters for the heat pump block that are relevant for the task are listed in Table 3 along with explanations where necessary.

Table 3 – Input parameters of the heat pump block

Input parameter	Explanation
Inlet source temperature vector [℃]	The inlet fluid temperature for the evaporator.
Outlet load temperature vector [℃]	The outlet fluid temperature for the condenser.
Source power matrix [W]	The power matrix for the evaporator.
Heating power matrix [W]	The power matrix for the condenser.
Electric power matric [W]	The matrix for the heat pumps energy consumption.
Thermal capacity hot loop [J/K]	A value for the thermal mass of the condenser.
Thermal capacity cold loop [J/K]	A value for the thermal mass of the evaporator.
Heat loss coefficient [W/K]	-
Pressure drop parameters for the condenser and the evaporator	Is not used in this task

2.4.3 Storage tank block

The storage tank blocks estimates the temperature at different heights in storage tanks by dividing the tank into horizontal nodes, which then are restricted by the inner wall of the storage tank and internal heat exchangers. For each node, the temperature is found by calculating the energy balance using differential equations (Murer, 2014). The blocks in Figure 7 is gathered from the Carnot library (Carnot, 2010), and shows some of the various types of storage tanks that can be found in the library.

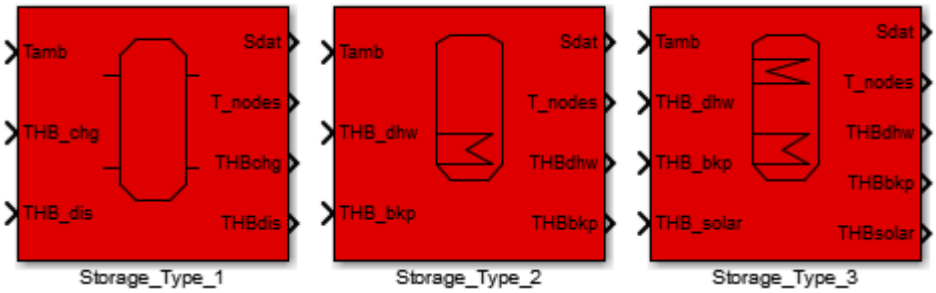

Figure 7 – Different storage tank blocks (Carnot, 2010)

2.4.3.1 Inputs and outputs

The *Tamb* input is the temperature of the ambient air, and is an input that is necessary to calculate the heat loss of the storage tank. *Sdat* is an output of various data, which could be used for measuring purposes. *T_nodes* is an output vector, which gives the temperature per node, and can be used to measure the temperature in different heights of the tank. The THB is explained in Chapter 2.4.1, and represents the connection of the fluids going in and out of the storage tanks (Murer, 2014).

From Figure 7 it is possible to see that the tanks have either direct liquid flow through the storage tank or indirect liquid flow through heat exchangers. The connection height of the different inputs and outputs can be adjusted inside the block (Murer, 2014).

2.4.3.2 S-function

The calculation of the nodes are done by an S-function block, which is a block that in this case is programmed in Microsoft Visual Studio 10 compiler, but also can be programmed in programs such as Matlab. In order to solve the differential equations the S-function requires information such as the fluid mass flows, temperatures, type and mix, geometry of the storage tank and surface areas and U-values of the storage tank and potential heat exchangers. The equation for this S-function can be found in the Carnot help (Hafner, 1999).

2.4.3.3 Input parameters

The storage tanks in Figure 7 have the same block parameters, but have different input parameters that can be changed inside the subsystem of the blocks. The different block parameters can be seen in Table 4, and a short explanation of the block parameters is given where it seems necessary.

Table 4 – Input parameters for storage tanks (Carnot, 2010)

Input parameter	Explanation
Heat loss coefficient cylinder wall, bottom and top cover in W/(m²K)	-
Effective vertical conductivity (EVC) in W/(m*K)	Gives the heat transfer capacities in the wall of the tank. Equation 1 can be used to calculate this value (Hafner, 1999).
Initial temperature (vector or scalar) in℃	The temperature in the tank at the start of the simulation.
Volume in m³	-
Diameter in m	Gives the inner diameter of the storage tank
Position	If the tank are standing or laying
Number of connections	The number of input and output pairs.
Number of nodes	-
Number of measurement points	Sets the number of measurement points, where the measurement points are distributed equally through the height of the tank.

The parameters that can be changed inside the subsystem of the blocks are heights for inlets and outlets, and heat transfer and pressure drop parameters for heat exchangers.

2.4.4 GSHE block

The ground source heat exchanger (GSHE) block calculates the heat transfer between the ground and the brine circulating in the boreholes according to the calculated temperatures in the ground and the brine temperature going into the block. From this, the block calculates the outlet brine temperature from the borehole. The block is a modified version of the GSHE block from the CARNOT block set, which is based on a Erdwärmesonden (EWS) model (Ytterhus, 2014, 2015).

2.4.4.1 Inputs and outputs

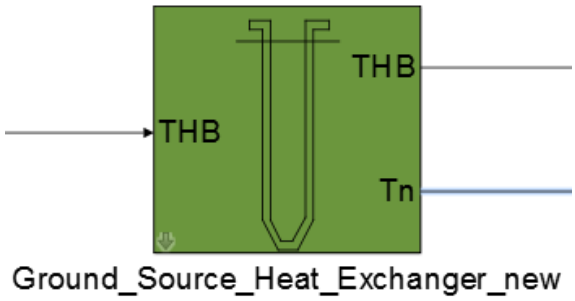

Figure 8 – GSHE (Ytterhus, 2015)

Figure 8 shows the vertical ground heat exchanger block. It has an input and output for the THB bus, which are explained in chapter 2.4.1, and a Tn output, which is giving the temperature for each of the nodes in the ground.

2.4.4.2 The g-function

As mentioned earlier in this chapter, the GSHE block is based on something called the EWS model, which is a model made for simulation of a single grouted boreholes with twin U-tubes. However, when using more than one borehole, the EWS model needs to take into account the change in the thermal response of the boreholes. Pre-defined response factors called g-functions have therefore been developed in order to correct the thermal response of the boreholes. For the GSHE block, the different pre-defined g-functions can be chosen in the field geometry menu in the block parameters (Ytterhus, 2014).

For more extensive information about both the EWS model and the g-functions, check out the project work of Mikkel Ytterhus (Ytterhus, 2014).

2.4.4.3 Input parameters

The different input parameters for the ground heat exchanger block are presented in Table 5, where some explanation also is given where necessary.

Table 5 – Input parameters GSHE

Input parameter	Explanation
Average annual outdoor temperature in℃	-
Temperature gradient in K/m, typical 0.025..0.04	-
Thermal conductivity ground in W/m/K	-
Heat capacity of the ground in J/kg/K	-
Density of the ground in kg/m^3	-
Thermal conductivity filling in W/m/K	-
Heat capacity of the filling in J/kg/K	-
Density of the filling in kg/m^3	-
H: Length of earth probe in m	The length of the borehole
B: probe distance in m	The distance between the boreholes
Diameter of tube in m	-
Diameter of drilled hole in m	-
Field geometry	A menu where a variety of pre-defined g-functions can be chosen.
Number of parallel tubes	The number of boreholes in the system.
No. of nodes in axial direction (typical 10)	Decides how many differential equations that is calculated in the axial direction of the borehole.
No. of nodes in radial direction (typical 10)	Decides how many differential equations that are calculated in the radial direction of the borehole.
Grid factor (typical 2.5)	The grid factor indicates the spreading of the radial nodes. A high number indicates that the nodes are close to the walls of the hole (Ytterhus, 2014).
Design mass flow rate [kg/s]	-

3 Powerhouse Kjørbo

Powerhouse Kjørbo consists of two refurbished office buildings placed in Sandvika outside Oslo. With being in accordance with the Passive house standard, having a solar cell plant mounted on rooftops and having an energy efficient heating and cooling system, the buildings are supposed to produce more energy than they are using during their lifespan. The building were officially inaugurated in April 2014 and is at the time of this writing featured as the most environmentally friendly building in the world (Nordang, 2015).

3.1 The heating and cooling system

Figure 9 shows a principle system design of the heating and cooling system at Powerhouse Kjørbo as it was originally built.

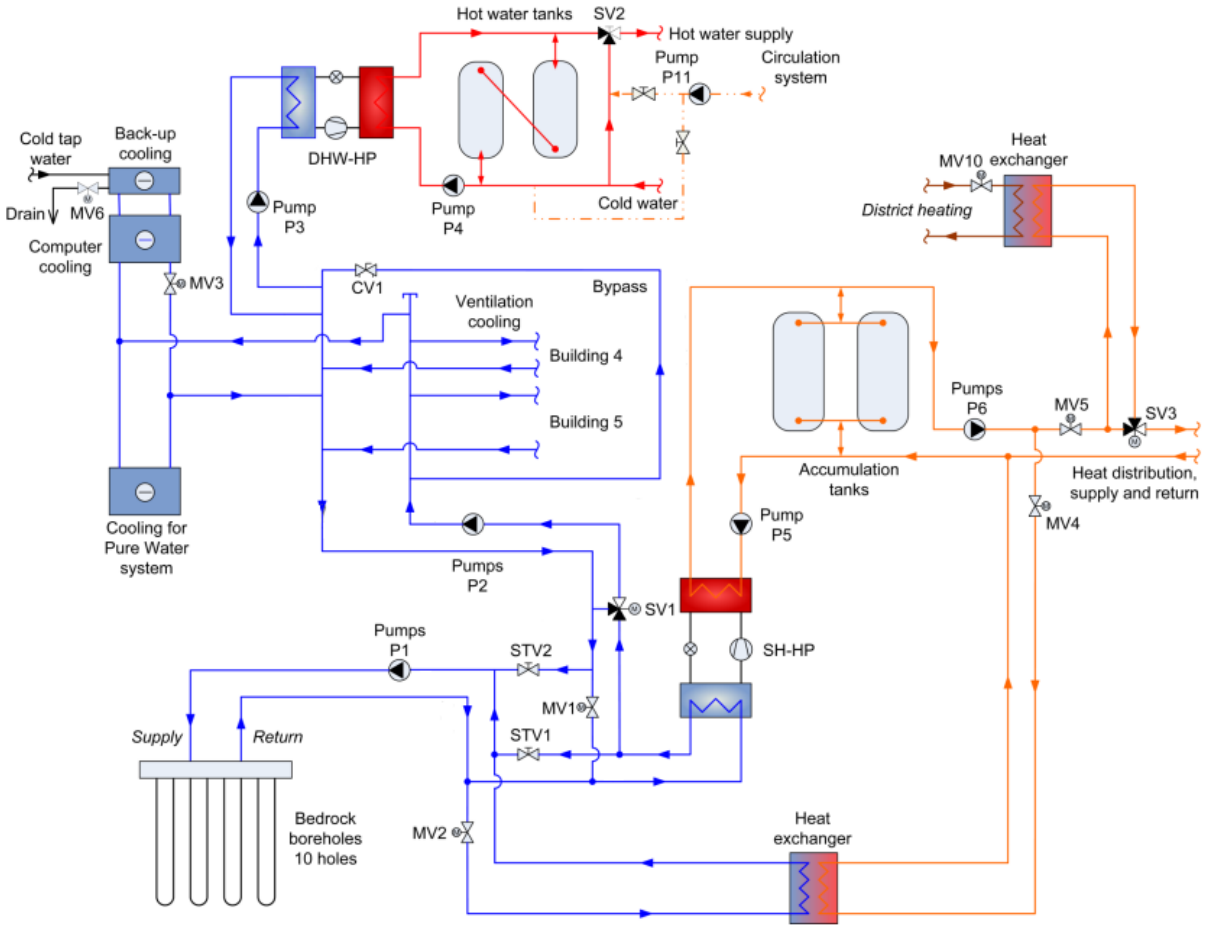

Figure 9 – Principle system design of the thermal energy system (Nordang, 2014).

The heating and cooling system can be divided by function into three parts. These parts are; heating system for space heating and heating of ventilation air, heating of DHW as well as space cooling, cooling of ventilation air, cooling of computers and cooling of pure water. All of these

parts are connected to the 10 boreholes, which are dimensioned to cover the entire cooling demand with free cooling.

The space heating and heating of ventilation air is done by a heat pump, which could also be used in cooling mode by rejecting the excess heat from the condenser through a heat exchanger and to the boreholes. This heat pump is dimensioned to cover the peak heating demand, but the system has also a heat exchanger connected to the district heating network in case of heat pump failure. Two storage tanks connected in parallel are used to accumulate the heat for the space heating and heating of ventilation air.

A separate heat pump does the heating of DHW, which is stored in two accumulation tanks coupled in series.

3.1.1 Set point temperatures

The outdoor temperature compensation curves for the water circulating in the hydronic space heating system follows the lines shown in Figure 10. Figure 22 shows a layout of the space and ventilation heating system, and it is therefore recommended to look at this figure in order to understand the system. From the inception of the space heating system, several changes have been done to the outdoor temperature compensation curves. These compensation curves is gathered from the CC-system the 29.04.2016.

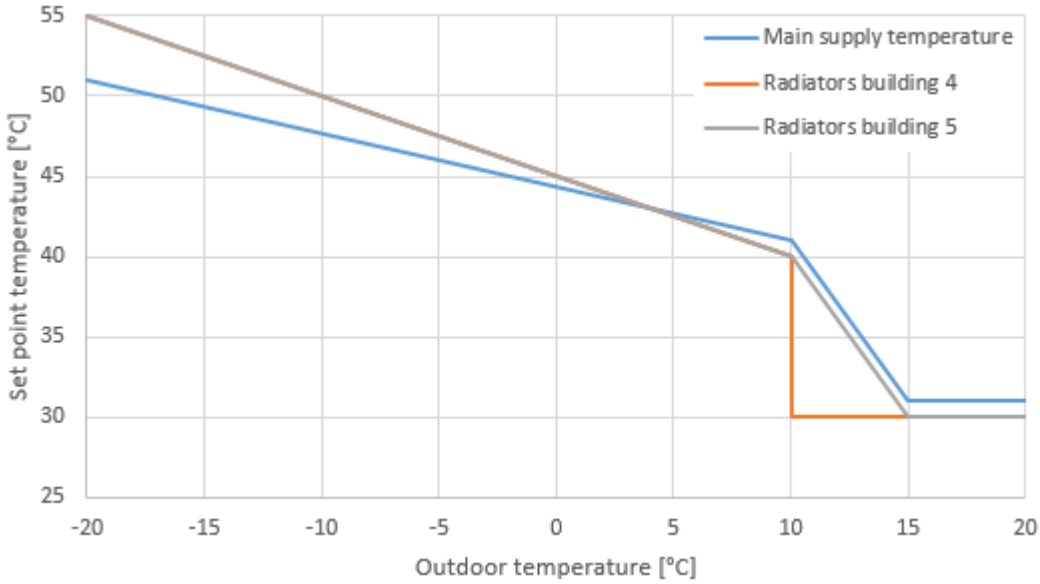

Figure 10 – Outdoor temperature compensation curves

3.1.2 System changes

Changes have been made to the heating and cooling system since it was built. One change is that the electric heating coil in the DHW storage tanks has been disconnected. This was done

because the electric heating coil turned on at temperatures where the heat pump should cover the temperature lift.

The other change was to alter the inlet from to the DHW heat pump, which is shown in Figure 11.

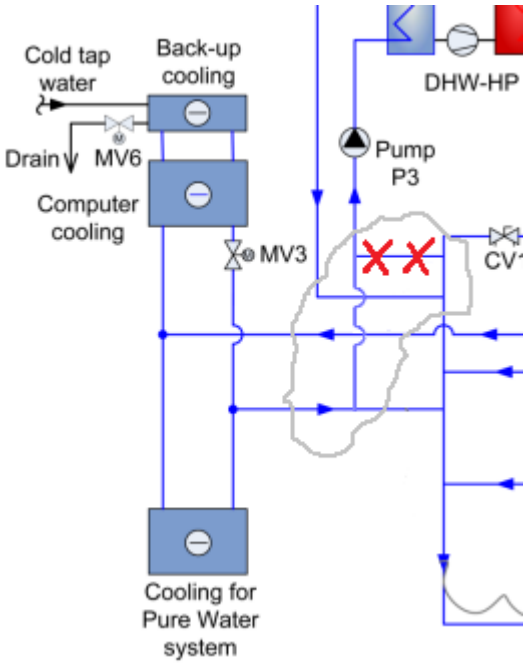

Figure 11 – Changes in the heating and cooling system (Nordang, 2014) (modified figure)

This changes the brine entering the evaporator from being drawn from the bypass circuit to be drawn from the return of the cooling for computers and pure water. The brine coming from the computer cooling has a higher temperature, which gives the heat pump a lower temperature lift and therefore a better COP (O Rådstoga 2015, pers. comm., 16. Nov.).

3.2 Components

3.2.1 Heat pump for space heating

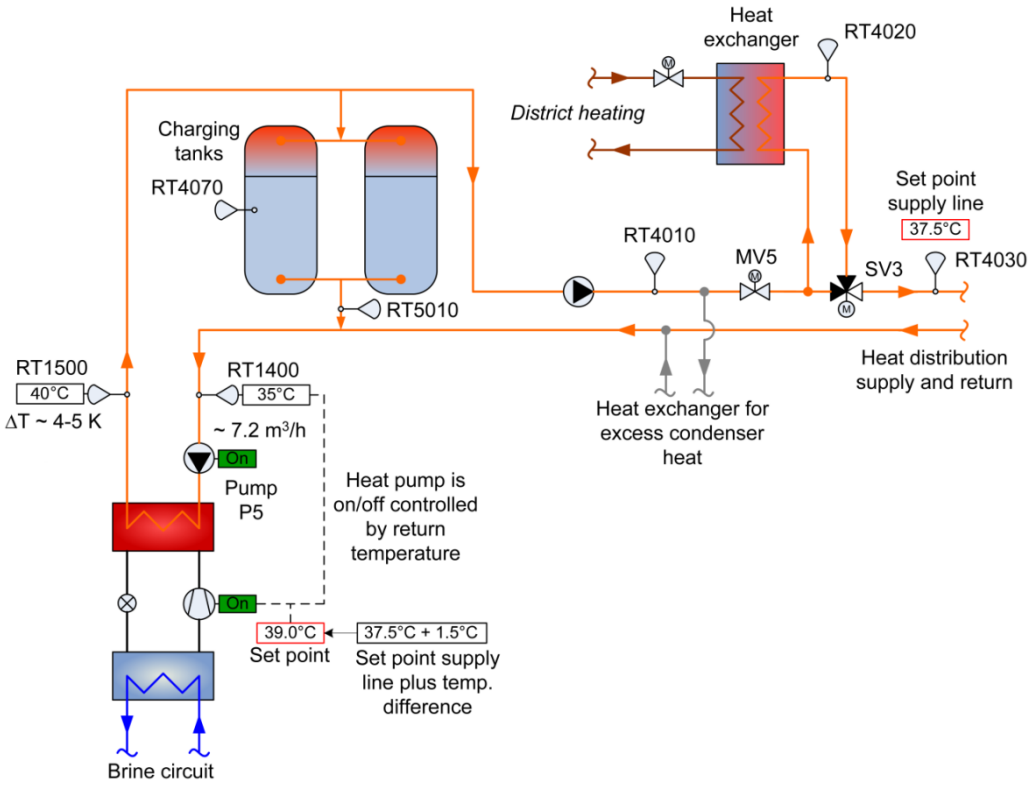

Figure 12 – Heat pump for space heating (Nordang, 2014)

The heat pump for space heating and heating of ventilation air is a Carrier 61WG-070 with option 272. Option 272 means that the evaporator is a brine heat exchanger. R410A is used as working fluid for the heat pump. There are two compressors in the heat pump, which both are intermittently controlled (on/off). The heat pump therefore has two capacity steps (Nordang, 2014).

3.2.1.1 Control strategy

The heat pump has an integrated control system, where the heat pump in heating mode is set to keep the water temperatures according to a set point. It uses the inlet water temperature for the condenser to determine when to start and stop, and uses the outlet water temperature for the condenser to determine the number of compressors that is used. In addition, the heat pump control is counting the amount of starts and stop cycles per hour for each compressor, and is comparing this value to a set maximum amount of start/stop cycles. If the number of start/stop cycles for a compressor exceeds the maximum start/stop cycles set for the system, the control system is increasing the minimum cycle time for the compressors, and then decreasing it when the start/stop rate drops (Carrier SCS, 2014). The set point for the heat pump is 1.5℃ higher

than the set point for the supply line and, did the 29.04.2016, follow the line shown in Figure 13.

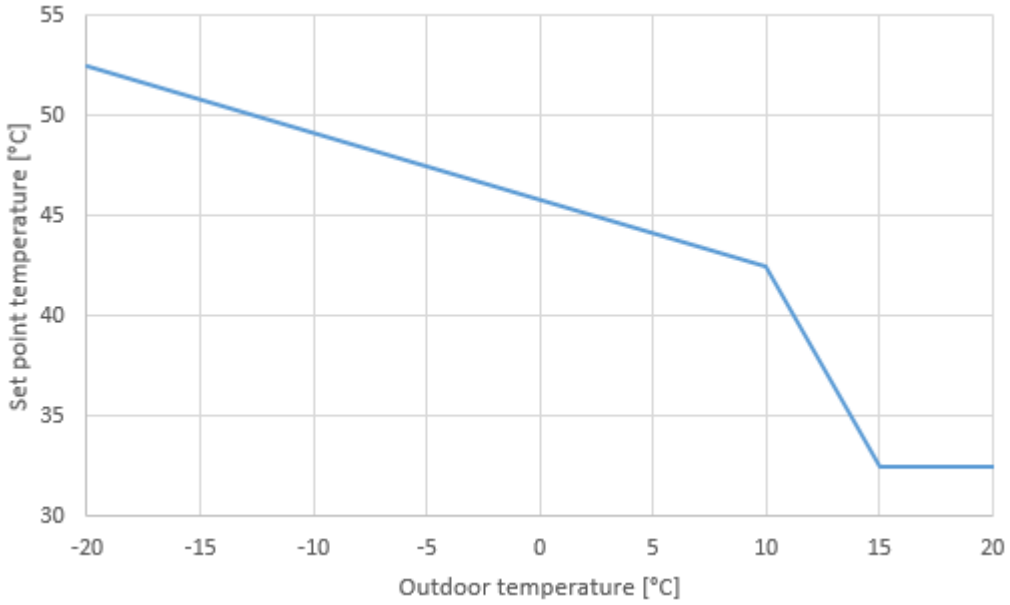

Figure 13 – SH-HP outdoor temperature compensation curve

3.2.1.2 Performance data

Performance data measured according to the standard rating conditions described in NS-EN 14511 is not found for this heat pump. There is however found performance data for the Carrier 61WG-070 with option 272 given in the temperature range of -2°C to 3°C inlet temperature for the evaporator and with 25°C, 35°C, 45°C, 55°C and 65°C outlet temperature for the condenser. Performance data is also given in the temperature range of 8°C to 18°C for the standard Carrier 61WG-070, which have a water heat exchanger as evaporator. Performance data, given in kW, measured in accordance with EN 14511 is shown in Table 6. The temperature differences for these measurements are 3 K for the evaporator and 5 K for temperatures up to and including 45°C and 10 K for temperatures over 45°C for the outlet temperature of the condenser.

Table 6 – Performance data Carrier 61WG-070 (Carrier SCS, 2012)

			T_{hout}															
			25°C			35°C			45°C			55°C			65°C				
			Heat	Pin	COP	Heat	Pin	COP	Heat	Pin	COP	Heat	Pin	COP	Heat	Pin	COP	
T_{cin}	With option 272	-2°C	65.9	12.6	5.21	63.1	15.5	4.07	60.8	19.2	3.17	59.3	22.4	2.65	56.6	26.8	2.11	
		3°C	76.0	13.3	5.7	72.7	16.2	4.5	69.3	19.6	3.55	67.1	22.5	2.98	64.7	26.9	2.4	
	Without option 272	8°C	86.8	13.5	6.42	83.4	16.0	5.21	79.5	19.2	4.14	76.4	21.8	3.51	72.4	25.6	2.82	
		13°C	99.7	14.4	6.93	95.1	16.5	5.77	90.8	19.6	4.63	87.0	21.9	3.98	82.3	25.4	3.24	

3.2.2 Heat pump for DHW

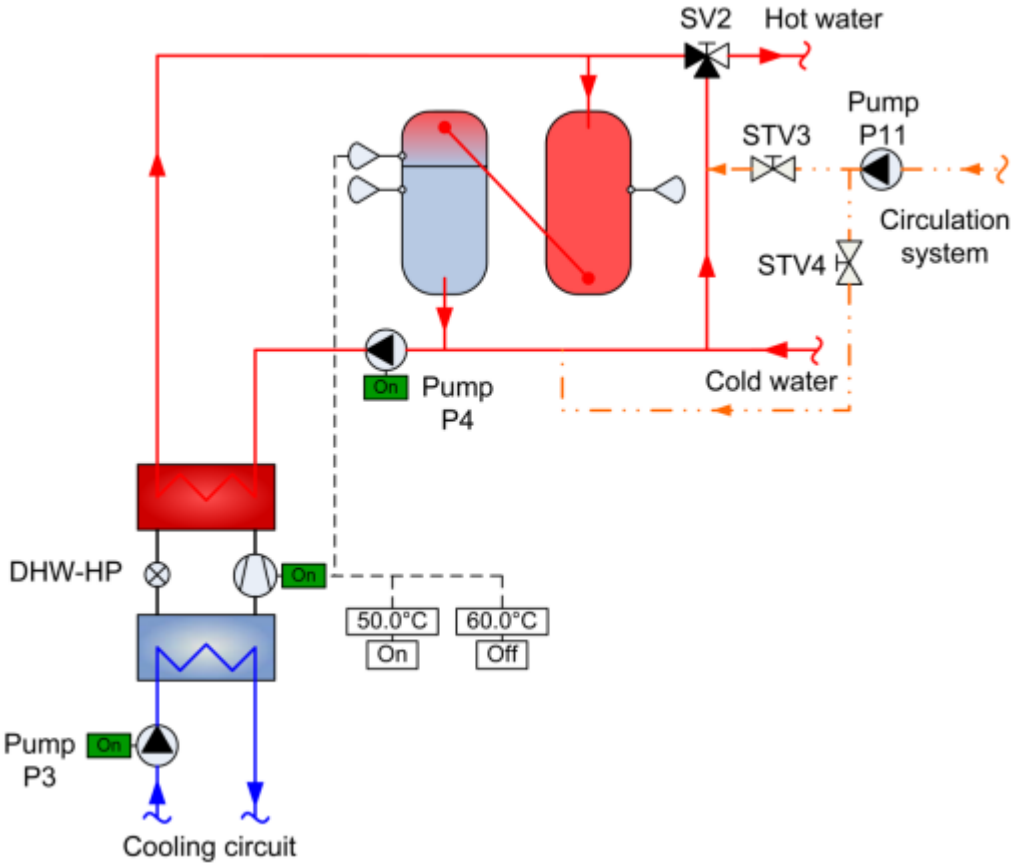

Figure 14 – Heat pump water heater (Nordang, 2014).

The heat pump for heating of DHW is a Nibe F1145-10 and is intermittently controlled by the temperatures from the first accumulation tank. R407C is used as working fluid for the heat pump. The set-point temperature for the switch-on of the heat pump is 50°C and the switch-off temperature is 60°C.

3.2.2.1 Control strategy

The control of the heat pump also controls the integrated circulation pumps, which are circulating the brine in the evaporator and the water in the condenser. The flowrate for the circulation pump, which is circulating water between the condenser and the storage tanks, is 1060 l/h. For the circulation pump circulating brine in the evaporator, the flowrate is 960 l/h. These circulation pumps have the possibility of variable speed control, but are set at a fixed speed (Nordang, 2014).

3.2.2.2 Performance data

Table 7 – Performance data NIBE F1145-10

	0°C/35°C	0°C/45°C	0°C/55°C	0°C/65°C	10°C/35°C	10°C/45°C	10°C/55°C	10°C/65°C
Heat cap [kW]	9.66	8.55	7.58	6.49	12.82	11.8	10.94	9.65
Power input [kW]	2.01	2.27	2.38	2.48	2.19	2.55	2.79	3.01
COP [-]	4.81	3.77	3.19	2.62	5.86	4.63	3.93	3.21

Table 7 was acquired by contacting Nibe (D Kroon, 2015, pers. comm., 02. Nov.), and contains measured data for the DHW-HP, which is measured at standard rating conditions in accordance with EN 14511.

3.2.3 Storage tanks for space heating

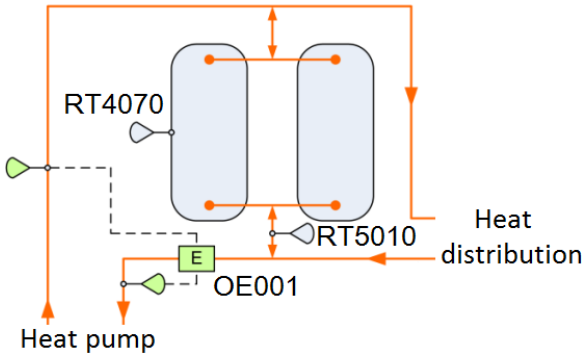

Figure 15 – Storage thanks for space heating (Nordang, 2014).

The thermal storage system for space heating and heating of ventilation air consists of two accumulation tanks that are connected in parallel. A temperature measurement point is mounted on one of the tanks, as shown in Figure 15. Figure 16 shows the heights of the inlets and outlets, in addition to the height of the measurement point, which is obtained from OSO hotwater (2016, pers. comm., 2. Feb.).

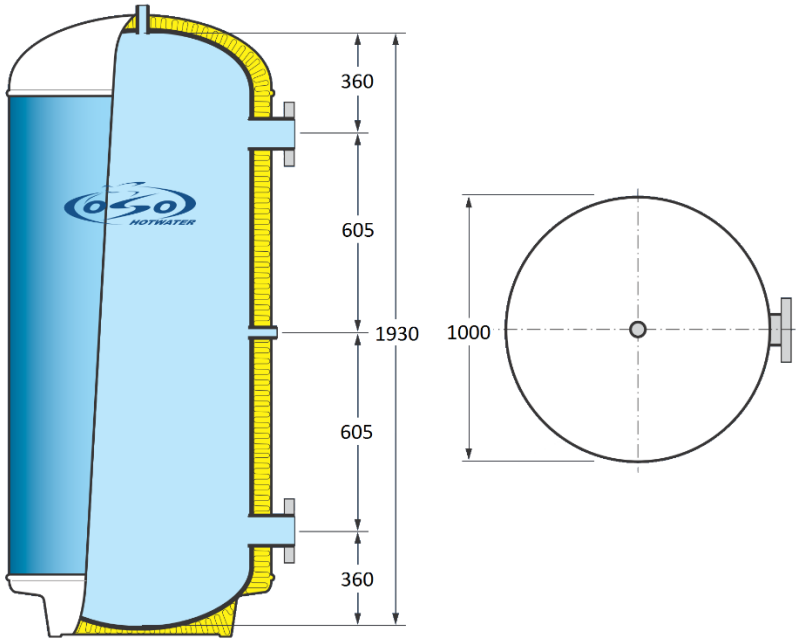

Figure 16 – Measurements SH-ST (Oso Hotwater, 2011) (modified figure)

Water is circulating with a constant flow of roughly 7.2 m^3/h between the condenser of the heat pump and the storage tank, while the circulation pump for space heating and heating of ventilation air have a variable flowrate.

Table 8 – Parameters Maxi Accu 51R 1000

Parameter	**Value**
Type	Maxi Accu 51R 1000
Volume	900 litres each
Geometry	Ø1000 x 2200 H
Insulation	100 mm mineral wool (OSO Techn. sec. 2015, pers. comm., 9. Nov.)
Number of connections	Can be seen in Figure 15

3.2.4 Storage tanks for DHW

No simulations is performed for the storage tanks for DHW, but it is nevertheless assumed that information about the components is relevant for the thesis because it, with the correct sensors installed, could be useful in the future work of comparing the storage tanks of NZEP to field measurements. The reason why no simulations are performed on the DHW-ST is explained in Chapter 6.7.

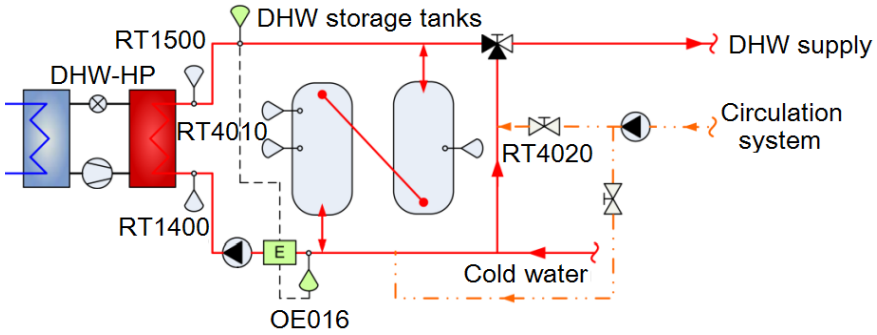

Figure 17 – Storage tanks for DHW (Nordang, 2014)

The storage tanks for heating of DHW consist of two accumulation tanks that are connected in series. These storage tanks are of the type Oso Maxi Standard 17R and Oso Maxi Standard 17RE, where the difference is that the 17RE version has an electrical heating coil. From Figure 17, it is possible to see that the accumulation tanks have three measurement points. Figure 18 gives the height of the inlets and outlets and the measurement points of the storage tanks, in addition to where the measurement sensors are placed on the two storage tanks. The measurements have been obtained from OSO hotwater (2016, pers. comm., 2. Feb.), and the figure visualising where the sensors are placed is a figure made by Nordang (Nordang, 2014).

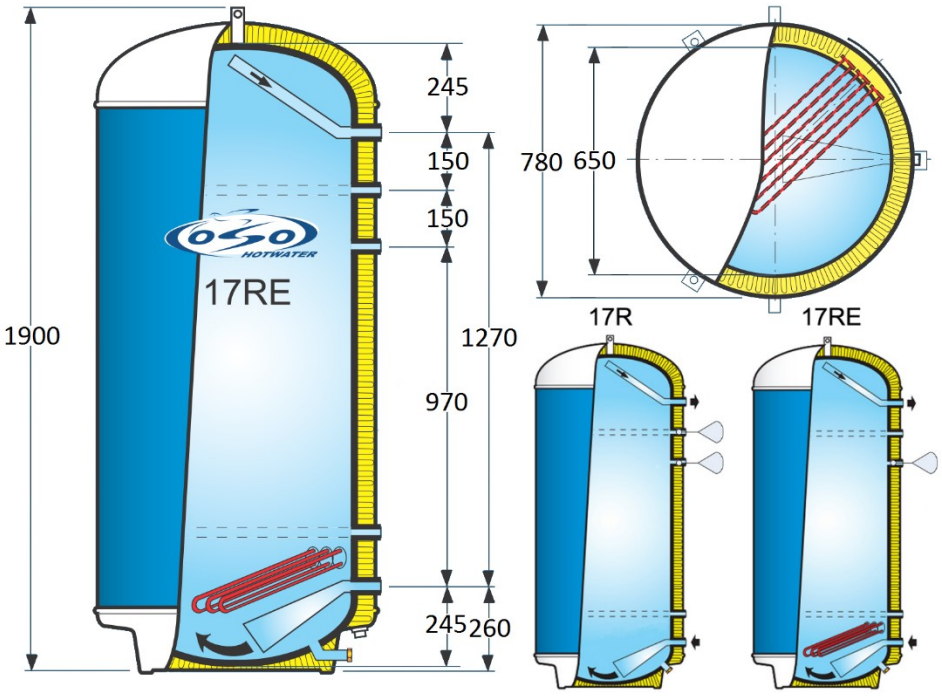

Figure 18 - Measurements DHW-ST (Oso Hotwater, 2011) (modified figure)

Flowrates and control strategy for the circulation pump, which is circulating water between the condenser of the heat pump and the storage tanks, is given in chapter 3.2.2. In Table 9, some parameters for the storage tank are presented.

Table 9 – Parameters OSO Maxi Standard 17R/RE 600

Parameter	Value
Type	Maxi Standard 17R 600
Volume	550 litres each
Geometry	Ø780 x 1900 H
Insulation	65 mm mineral wool (OSO Techn. sec. 2015, pers. comm., 9. Nov.)
Number of connections	Can be seen on Figure 18

3.2.5 Boreholes

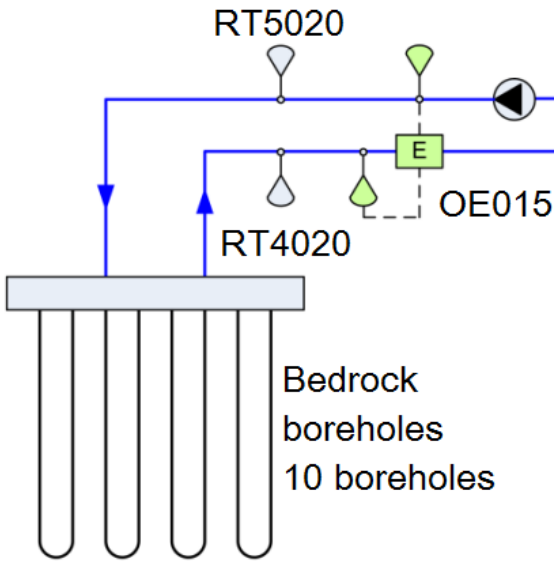

Figure 19 – Boreholes (Nordang, 2014)

The borehole system consists of ten Ø115mm vertical boreholes, where each borehole contains a single U-collector turbulence tube in the dimension Ø40x2.4mm. Eight of the boreholes have a depth of 225 m, while two are shorter and have a length of 192 m and 177 m. The distance from the ground level to the bedrock is 3 meters, and is covered with a steel casing. This means that the total borehole length is 2169 m, while the average effective borehole depth is 215 m (Ramstad, 2013).

The brine circulating in the boreholes is a water-ethanol mixture of 35 % ethanol. The outlet brine temperature from the borehole in the maximum power extraction and the maximum power injection, was found by Nordang in his master thesis to be between 5.7℃ and 15.2℃ (Nordang, 2015).

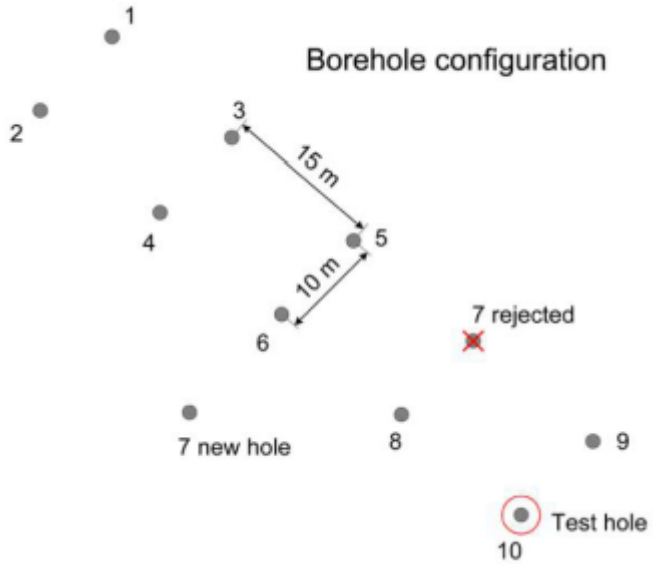

Figure 20 – Borehole configuration (Nordang, 2014)

The configuration of the boreholes is shown in Figure 20. It is possible to see that each borehole, except of hole number 8, has a 10 meter distance to another borehole.

A thermal response test was performed on borehole number 10, and the temperature profiles of the test are shown in Figure 24. From the thermal response test, it was found that the effective thermal conductivity (ETC) is 1.9 W/mK. Dry laboratory tests performed on the same ground types have an ETC in the range of 1.9 – 4.4 W/mK, which shows that the ETC in the test hole is low (Ramstad, 2013).

In the thermal response test, a flow of groundwater at 170-190 meters depth was found. It was concluded that the groundwater flow is quite small and influences the borehole negligible since the measured thermal conductivity is quite low. Since there is a relatively high groundwater level in the area, the groundwater is also used as a filling in the borehole (Ramstad, 2013).

The pump circulating brine through the boreholes has variable speed drive and has a minimum and maximum capacity of 2.5 and 5 l/s respectively. In heating mode, the circulation pump is set to maintain a constant temperature difference of 4 K higher temperature of the outlet brine compared to the inlet brine. The control strategy for the circulation pump in cooling mode is to maintain a temperature difference of 5 K (Nordang, 2015).

3.3 Measuring points

Figure 21 shows some of the measurement points in the heating and cooling system. Measurements are done by two systems, which are explained in this chapter.

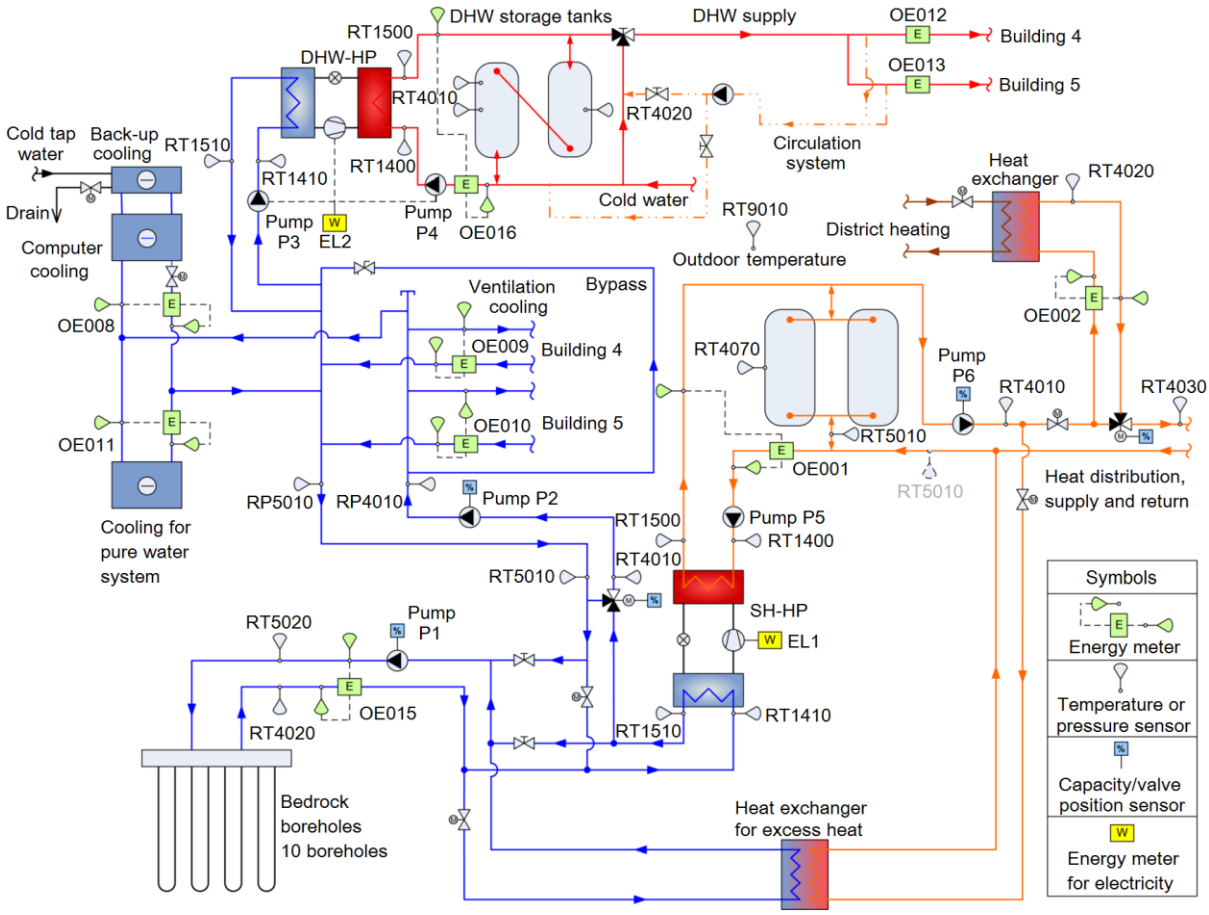

Figure 21 – Measuring points (Nordang, 2014)

3.3.1 CC-system

In the central control system, measurements from an extensive amount of sensors are logged. From Figure 21 it is possible to see that there are RT, RP, and OE sensors, which are measuring temperature, pressure and energy use respectively. To measure the energy use the OE sensors are measuring temperatures and flow, which are also being logged in the CC-system. The CC-system is also including set points, signals and operating modes in addition to power usage for the different components.

There are 17 thermal energy meters in the hydronic system, which are placed in the heating and cooling system of the building. A print screen from the CC-system, which shows the energy meters for the hydronic system, can be found in Appendix VIII. Figure 22 shows the energy meters in the heating system.

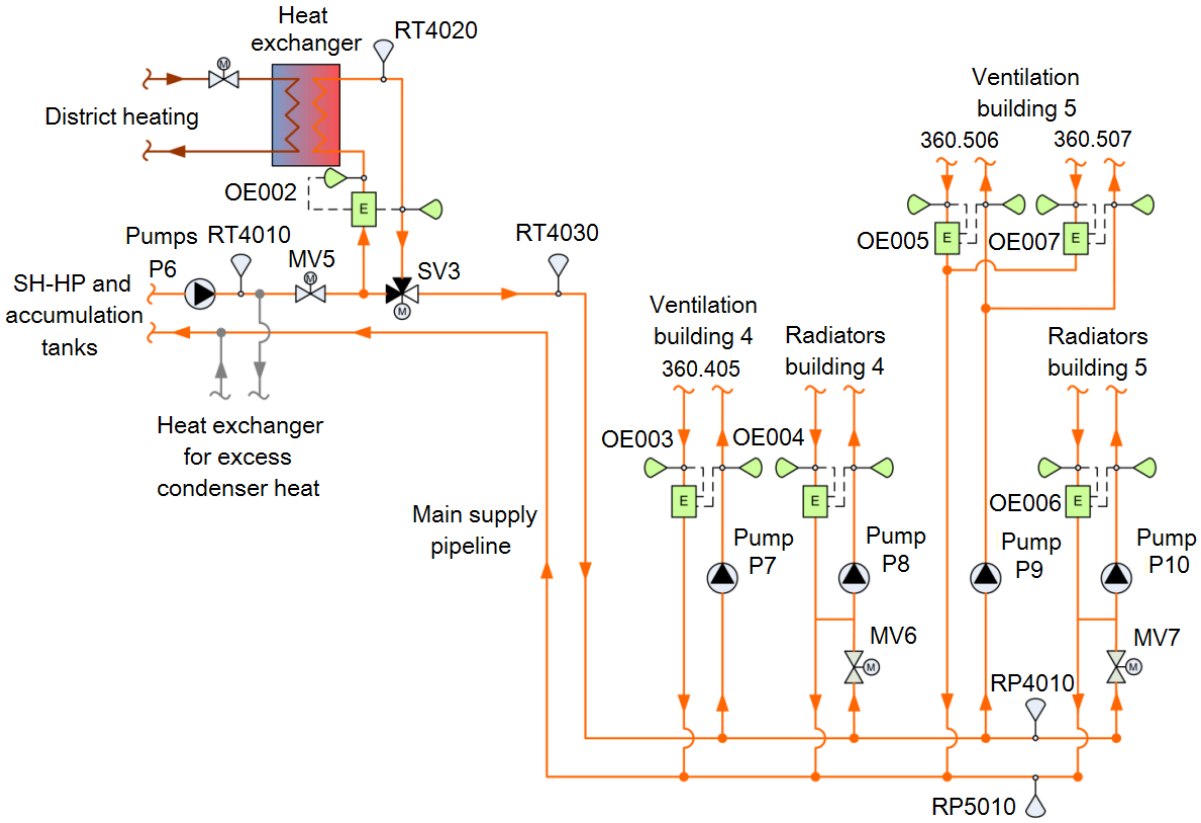

Figure 22 – Heating system (Nordang, 2014)

The extent of temperature sensors in addition to the ones included in the energy meters are not known, but it is considered by the writer of this thesis to be about 17 sensors. These sensors are either additional sensors delivered by Jonson Controls or internal sensors in the heat pumps. The DHW-HP and the SH-HP have internal temperature sensors that measure the fluid temperatures at the inlet and outlet of the heat pump, where the DHW-HP also has a sensor measuring the temperature of the superheated gas for the compressor. Other measurement sensors are placed in storage tanks and pipes (CC-system 2015, 16.12).

The sensors have mainly been delivered from the manufacturers Kamstrup and Johnson Controls, except for some, which are integrated in the heat pump units. Therefore, the documented accuracy of the sensors do not exist for some, and varying for others. Table 10 shows the accuracies of the energy meters, which are in the upper field, and for the general temperature sensors, which are in the bottom field.

Table 10 – Sensor accuracy (Nordang, 2015)

Sensor	Type	Accuracy
Energy meters	Kamstrup Multical 801	$E_C = (\pm 0.15 + 2/\Delta T)\%$[a] $E_T = (\pm 0.4 + 4/\Delta T)\%$[a]
Temperature sensor	Four wire connection	-
Flow sensor	Ultrasound	-
Energy meter for electrical equipment	Kamstrup 382 Generation M	+0.1%
General temperature sensors	PTC-Thermistor A99 series, Johnson control	±0.5°C (for -15°C <t<75°C)
[a] E_C=Accuracy energy calculation, E_T=Accuracy energy measurement.		

There are also some different time steps for logging of the different sensors and signals. Some of the energy meters had a one-hour logging interval up to the 27th of January 2015, where the logging intervals were changed to 5 minutes. The logging intervals of the sensors used in this thesis can be seen in the matrixes presented in Appendix I to Appendix V. Most sensors also have a period of missing measurements between the 11th and the 21th of November 2015.

3.3.2 EMS

The energy monitoring system (EMS) is logging the accumulated hourly energy data collected from the energy meters, which are marked with the letters OE in Figure 21. Some information about these sensors is given in Chapter 3.3.1 and accuracy of the measurements in addition to the production name of the sensors can be found in Table 10.

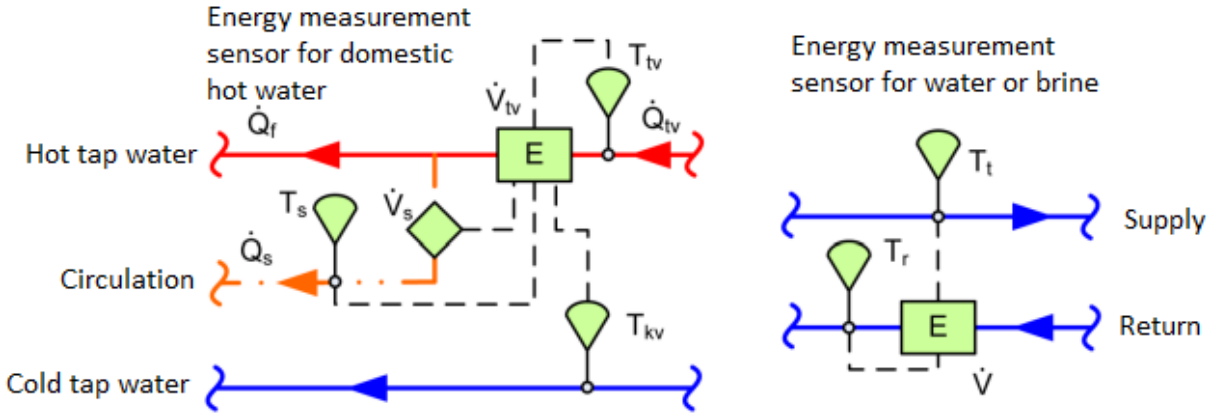

Figure 23 – Energy meters (Nordang, 2015)

Figure 23 shows the two types of thermal energy meters installed in the system. It is however found that the energy meters for the DHW is measuring a much lower value compared to the

energy given from the condenser of the heat pump and that some of the sensors for the DHW energy meter is not present in the CC-system (Nordang, 2015, Skjerve, 2016).

4 Modifications to the matrixes

The matrixes presented in Appendix I to Appendix V give the input parameters and the measurement sensors that are used in the simulations of this thesis. The background for the input parameters and measurement sensors that are presented in these matrixes can be found in either this chapter or in the project work in which this thesis is built on (Skjerve, 2016).

It was concluded in the project work that some of the values in these matrixes should be investigated further, and that there was a need for a correction of certain values because of both faults in calculation methods and that additional information now are gathered. It was for example found that the methods used to calculate the U-values and the EVC of the storage tanks in the project work were somewhat incorrect. Changes done to the matrixes that were presented in the project work are given in this chapter and in the matrixes in Appendix I to Appendix IV.

4.1 Tamb

Investigations done in the project work and in the research for this thesis reveal that there is no sensor measuring the temperature in the machinery room, where the heat pumps and storage tanks are placed at Powerhouse Kjørbo. However, a manual measurement of the ambient temperature in the machinery room, performed the 17.02.2016, shows a temperature of 23.4℃.

For both the components mentioned, the heat loss is a product of the temperature and heat loss factors. For the storage tanks in this thesis, different U-values is investigated, and it is therefore considered that it is not necessary to vary the ambient temperature in the machinery room in order to investigate the heat loss of the storage tanks. Also, there are found no documented heat loss factors for either of the two heat pumps investigated in this thesis, and the heat loss of the heat pumps is therefore not investigated.

The influence of this parameter on the simulation blocks are therefore not investigated in this thesis, but the measured temperature is placed in the matrixes of Appendix I to Appendix IV as an input parameter.

4.2 Heat pumps

4.2.1 Energy consumption circulation pumps

In the project work, it was proposed that the power consumption of the circulation pumps in the Nibe F1145 should be investigated. This is because the measured power consumption of the heat pump includes the power consumption of the circulation pumps. From an installation manual produced by Nibe, the power consumption of the circulation pumps is 35-185 W for

the evaporator side and 7-67 W for the condenser side (Nibe, -). A value of 42-252 W is therefore subtracted from the measured power consumption of the heat pump in the simulations.

4.2.2 Performance matrix HS-HP

In the project work, it was concluded that the performance data of the Carrier 61WG-070 presented in Chapter 3.2.1 should be investigated further before it is used in the comparison. In this thesis, no new information is found about the performance data, but it is decided that one simulation should be done using performance data produced by extrapolation of the existing data. Since the performance curve for the Carrier 61WG-070 with option 272 is only given for the inlet brine temperatures of -2℃ and 3℃ for the evaporator, the performance data for the values 8℃ and 13℃ is found by extrapolating the data measured for the other two inlet brine temperatures. Table 11 shows the extrapolated performance data for the heat pump.

Table 11 – Extrapolated performance curve

			Thout													
			25°C			35°C			45°C			55°C			65°C		
			Heat	Pin	COP	Heat	Pin	COP	Heat	Pin	COP	Heat	Pin	COP	Heat	Pin	COP
T_{cin}	Tcin	-2°C	65.9	12.6	5.23	63.1	15.5	4.07	60.8	19.2	3.17	59.3	22.4	2.65	56.6	26.8	2.11
		3°C	76.0	13.3	5.71	72.7	16.2	4.49	69.3	19.6	3.54	67.1	22.5	2.98	64.7	26.9	2.41
	CTcin	8°C	86.1	14.0	6.15	82.3	16.9	4.87	77.8	20.0	3.89	74.9	22.6	3.31	72.8	27.0	2.70
		13°C	96.2	14.7	6.54	91.9	17.6	5.22	86.3	20.4	4.23	82.7	22.7	3.64	80.9	27.1	2.99

4.3 Storage tanks

As mentioned in Chapter 3.2.4, no simulations are performed on the storage tanks for DHW, but information about the storage tanks is nevertheless presented in this chapter because it might be useful in the future work for comparing the storage tanks of NZEP to field measurements.

4.3.1 U-value for storage tanks

In the project work, the U-values for cylinder wall, bottom and top cover for the storage tanks was calculated to be 0.33 $W/m^2 \cdot K$ for the ST-SH and 0.49 $W/m^2 \cdot K$ for the ST-DHW. The method that was used to calculate these values did only take into account the thickness of insulation, and did not include the transmission losses in couplings or other details on the storage tanks. It was therefore decided that the U-value should be calculated by a new method.

In the product data sheets that is given on the homepages of the producer (OSO Hotwater, 2016a, 2016b) the 24 hour heat loss for the storage tanks is given. The heat loss is measured and corrected in accordance with the standard NS-EN 12897:2006 (Dyreng, Vegar 2016, pers.

comm., 22. Feb.), and is regarded as possible to use in order to calculate more realistic U-values.

New U-values are calculated in Appendix VII too be 1.73 $W/m^2 \cdot K$ for the ST-SH and 1.58 $W/m^2 \cdot K$ for the ST-DHW. Compared to the U-values calculated in the project work these U-values are considerably higher, but it is considered that they are closer to the real value, and they are therefore placed in the original matrix' of Appendix III and Appendix IV.

4.3.2 Effective vertical conductivity

In the project work, some assumptions were made in order to calculate the EVC for the storage tanks. The equation that was used in the project work and is used in this thesis is equation 1.

$$\lambda_{eff} = \frac{4 \cdot A_{wall} \cdot \lambda_{wall}}{\pi \cdot D^2} + \lambda_{fluid} \left[\frac{W}{mK}\right] \quad 1$$

After doing some research, it became apparent that the formula was misunderstood, and that some of the values that was used in the project work were wrong. One thing that was misunderstood is that the area of the walls meant the horizontal area, not the total wall area of the storage tank cylinder. In the case of a standing storage tank this therefore means the cross sectional area of the steel walls. The EVC is therefore calculated in Appendix VII. The EVC is calculated to be 0.772 W/mK for the SH-ST and to be 0.741 W/mK for the DHW-ST. Compared to the default value, which is 1 W/mK, the calculated values is assumed to be realistic estimates for the EVC.

4.3.3 Heights of inlet/outlets and measurement points

As mentioned earlier in the chapter, more accurate information concerning the heights of inlets/outlets and measurement points for the storage tanks are gathered. From contacting OSO Hotwater (2016, pers. comm., 2. Feb.), measurements that are more accurate are gathered for the storage tanks. Figure 16 and Figure 18 is updated to the new measurements.

4.3.3.1 SH-ST

Figure 16 shows the heights of the inlets/outlets and measurement points. From these measurements, the relative height of the highest inlet/outlet is calculated to be 0.813, and 0.187 for the lowest inlet/outlet. From Figure 16 it is also possible to see that the measurement point is placed in a relative height of 0.5.

4.3.3.2 DHW-ST

In the project work, it was assumed that the height of the highest and lowest inlet/outlet should have the values of respectively 1 and 0 because of internal tubing in the storage tank. This assumption is regarded as decent, and these values are therefore not changed. From Figure 18, the height of the measurement points is calculated to be 0.78 and 0.69, which means that the measurement points in the simulation should be taken from about the same relative height.

4.4 GHE

4.4.1 Average annual outdoor temperature

Closer investigation into the mask of the GSHE shows that this parameter is being used as a reference point to determine the temperature at certain depths in the ground. The block is using equation 2 to calculate the temperature at different depths in the ground follows equation.

$$T(z) = \overline{T_{amb}} + 1 + \frac{dT}{dz} \cdot z[℃] \qquad 2$$

Where, $\overline{T_{amb}}$ is the average annual outdoor temperature, $\frac{dT}{dz}$ is the temperature gradient and z is the depth in the ground.

In the project work, $\overline{T_{amb}}$ was found to be 5.4℃, and the temperature gradient was found to be 0.0173 K/m. Figure 24 shows two calculated ground temperature curves calculated with average annual outdoor temperatures of 5.4℃ and 7℃, in addition to the measured temperatures in the ground. The 7℃ annual outdoor temperature is found by the trial and error approach.

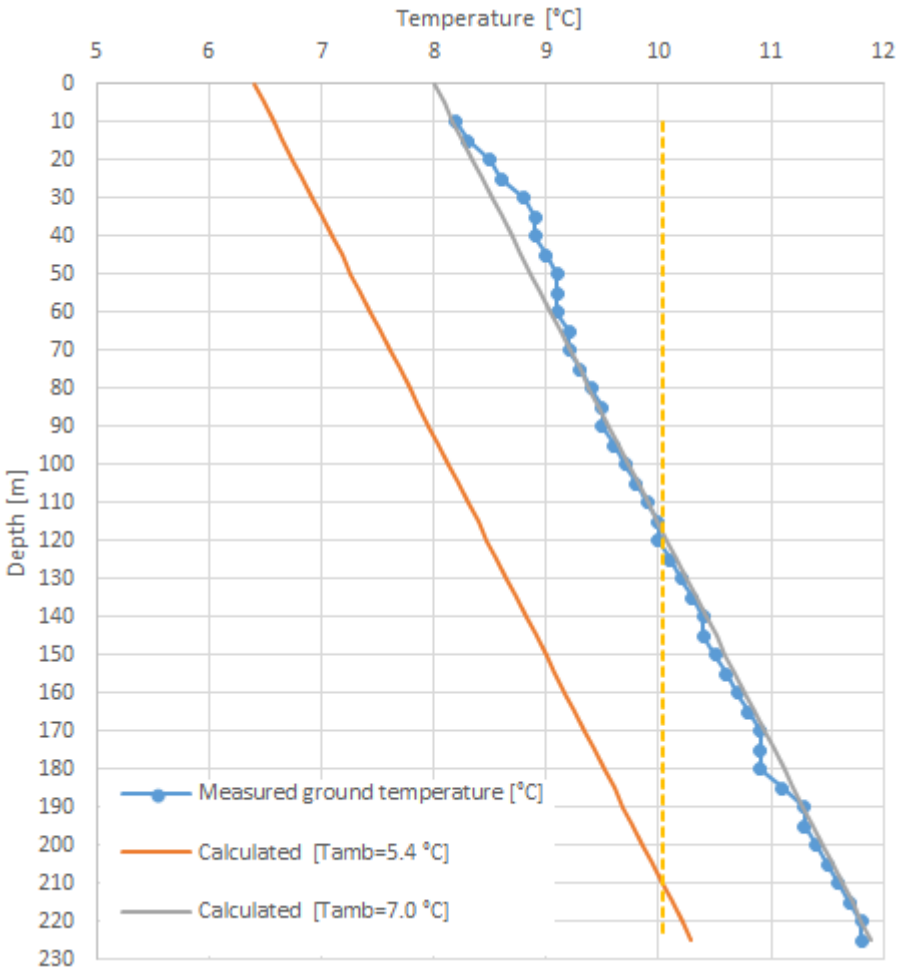

Figure 24 – Temperatures in the ground (Ramstad, 2013)(modified figure)

From Figure 24 it can be seen that the calculated temperatures using 5.4℃ as an average annual outdoor temperature gives roughly 1.6℃ lower temperatures compared to the measured temperatures. This is something that is assumed to have an impact on the results of the simulations, and it is therefore decided that another value is used. The calculated temperature line using 7.0℃ as an average annual outdoor temperature is therefore considered a better fit to the measured data compared to the calculated temperature line using the average annual temperature of 5.4℃. An average annual temperature of 7.0℃ therefore replaces the previous value of 5.4℃ in the original matrix in Appendix V.

4.4.2 Thermal conductivity of the ground

In the project work, it was proposed that it should be looked into if it is possible to calculate the thermal conductivity of the ground. The idea was to investigate whether it is possible to divide the given effective thermal conductivity into thermal conductivity of the filling, collector tubes and the ground. However, there are laboratory tests of the same ground type, it is therefore concluded that this is not necessary. This is also because a small literature search in the subject

reveals that dividing the effective heat conductivity is very complex and not regarded as necessary to run the simulations (Beier et al., 2012).

4.4.3 Design mass flow rate

The function of this parameter was not discussed in the project work, because it was assumed without doubt that this parameter was an input for the maximum-dimensioned mass flow in the borehole. However, an investigation of the function of this input parameter reveals that the input parameter is an input for the constant mass flow in the borehole (Ytterhus, 2014, Ytterhus, 2015). This means that the borehole block is not able to calculate the outlet brine temperatures for the borehole according to the mass flow that is given in the THB. The value for this parameter is therefore chosen according to the measured mass flow for the specific simulation period, which is given in Chapter 6.6. The design mass flow rate parameter spot in Appendix V is hence blank.

5 Comparison procedure

This chapter explains, based on the writers own assessment, which comparisons that are performed, what are the basis of comparison for the different components and systems in this thesis, in addition to the periods for these comparisons. As mentioned in Chapter 1.1, the goal of this thesis is to compare simulations performed at a single component level and at a multiple component level. Consequently, it is developed two slightly different approaches for these two types of comparisons. These two methods are presented in Chapter 5.2 and 5.3.

In order to perform these comparisons, the simulation models are in need of various amounts of inputs, and, in this thesis, these inputs are divided into two categories: input data and input parameters. Input data are time-based measurements, which for example gives the inlet brine temperature for the evaporator of a heat pump (for a given time). The input parameters are inputs that are constant, and either can be set for a block trough the THB, block parameters, inside the mask of the block or inside the subsystem of the block.

5.1 Input parameters

The matrix' in Appendix I to Appendix V shows an overview of the data and parameters that are needed, in addition to the values that are used as a foundation for the simulations. Some input parameters and sensors are however missing, which makes the simulations rely on default values, or approximated ones. Where input parameters is missing, simulations are performed in order to investigate at which rate the simulation component is dependent to the specific input parameter or input data. Which input parameters that are investigated are, for each component, explained in Chapter 6.

5.2 Single component comparison

Comparison of simulations containing a single component is a comparison at a component level, and gives information about whether the model is simulating the component in a realistic way. This kind of comparison is performed by simulating the component at the same conditions as the real component, and then investigating the simulation results against measurements from the real component. It is considered that this comparison approach is the best for investigating changes in input parameters since the consequence of changing the parameters should be visible from comparing the characteristics of the simulated component against the real component.

5.2.1 Input and output data

For the comparison of single components, a simulation is performed where the simulated and real component has the same inputs, and the outputs from the simulation are then compared to measurements from the outputs of the real component. Appendix I to Appendix V gives an overview of the measurements needed as inputs and outputs in order to compare each component. The appendixes also give an overview of the measurement sensors available in the CC-system at Powerhouse Kjørbo.

5.2.2 Comparison period

The components are divided into two groups based on the time period that the comparisons require in order to investigate the characteristics of the component. The heat pump block and the storage tank block is compared for one on/off or charging/discharging cycle, is therefore defined as components that need short comparison time since their cycles is relatively short.

The GSHE block however, is a block where the temperature in the ground is evolving based on the sum of the supplied and ejected thermal energy. Consequently, it is considered that the simulation period should be as long as possible in order to compare the temperature development of the model.

5.3 Multiple component comparison

The comparison of simulations containing multiple components compared the components at a system level. This means that the components are coupled in order to replicate certain parts of the system, and then compared to the real system. In this kind of simulations, it is considered that it would be difficult to compare the characteristics of the simulated and real components since the same working conditions should be present. It is therefore decided that the energy consumption and the overall temperature characteristics in certain parts of the system is compared when simulating multiple components.

5.3.1 Input and output data

For multiple component comparisons, the component blocks are arranged so that they replicate certain parts, or the whole the heating and cooling system at Powerhouse Kjørbo. Examples of parts that can be compared are the space heating system and the domestic hot water system. The input data into such a simulation model is the loads of the system, which can be the measured energy for space heating, ventilation heating, DHW, room cooling, and so on, while the output could be the measured energy consumption of a heat pump or the temperature sensors at different places of the system.

5.3.2 Comparison period

It is assumed that the period for a multiple component comparison should be for a year. This is because it would test the system at different working conditions caused by the changing outdoor temperatures and usage pattern of a year. A comparison over a relatively long period (for a month or more) is nonetheless considered an advantage for comparing outputs such as the energy consumption.

6 Simulation models

This chapter explains how the simulation models are set up and describes which simulations that are performed for each component or system. The result of the simulations described in this chapter is visualised in Chapter 7.

The simulations of the components described in this chapter use, as mentioned in Chapter 5, the measurement sensors and the input parameters given for each component in the matrixes of Appendix I to Appendix V as a basis. These matrixes are referred to as the original matrix. In the description of the simulations, it is given that the original matrix is used or that some parameter is changed. When it is given that some parameter is changed, it means that it is the only parameter, or parameters, that are changed from the original matrix.

The Matlab/Simulink version that is used for the simulations of this thesis is the 64-bit version of R2016a. Print screens from Simulink displaying the simulation models can be seen in Appendix XII to Appendix XV.

6.1 The signal builder block

The measurements are inserted into the simulation models using a block called "Signal builder". This block is able to *"create and generate interchangeable groups of signals whose waveforms are piecewise linear"(The MathWorks Inc., 2016a).* This means that the block can import measurements from several sensors and generate a piecewise linear waveform, which provides a value for each sensor according to the time step of the simulation. The values between each measuring point are thus generated by performing a linear interpolation between the measuring points (The MathWorks Inc., 2016b).

6.2 Volume flow into mass flow

The investigations performed in the project work (Skjerve, 2016) shows that there is no mass flow sensors in the CC-system. There is however found a number of volume flow sensors in the system, and their placement can be seen on Figure 21. In Appendix I to Appendix V it is shown which of these sensors that can be used for the specific components, in addition to the equation for transforming the specific volume flow into a mass flow. All of the components compared in this thesis require mass flow as an input, and it is therefore developed blocks that transform the volume flow into a mass flow.

Equation 3 and equation 4 is used for transforming the volume flows into mass flow depending on whether the volume flow is given in litres per hour or cubic metres per hour respectively.

$$\dot{m} = \frac{0.001}{3600} \cdot \dot{V} \cdot \rho(t) \left[\frac{kg}{s}\right] \quad 3$$

$$\dot{m} = \frac{1}{3600} \cdot \dot{V} \cdot \rho(t) \left[\frac{kg}{s}\right] \quad 4$$

The blocks that are used to in order to perform these transformations in the simulations are shown in Figure 25. Here the volume flow, density and the constant 1/3600 is multiplied in the multiply block. Measured volume flow is inserted into the model trough the block called Flow. The density is found in the Density block, which acquire the density of the fluid with the input parameters temperature, pressure, fluid type and fluid mix. A block called Input_Water_Glycol is used to give information about pressure, fluid type and fluid mix to the Density block. The basic_create_THB is then creating a THB using the mass flow, temperature and input parameters, which is connected to either the input of the evaporator or the condenser.

The blocks marked Input_Water_Glycol, Density and basic_create_THB is obtained from the Carnot library, while the other blocks are obtained from the Simulink block library.

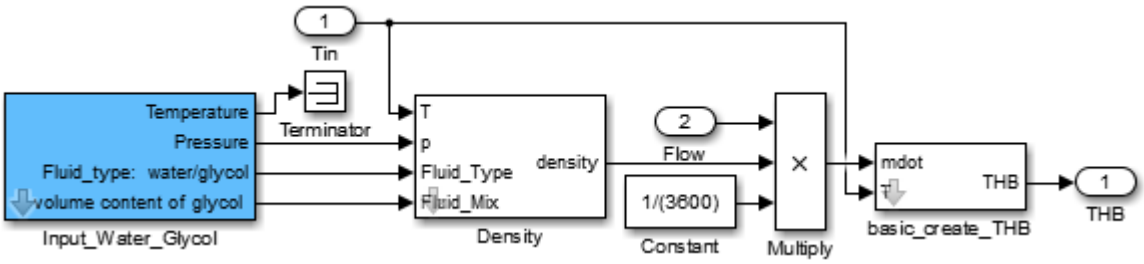

Figure 25 – Transformation blocks

6.3 Heat pump for space heating

In the project work, it was concluded that there is enough data to compare the heating capacity of the heat pump. It was also concluded that the performance data should be investigated in order to decide whether it could be used for the simulations. However, in this thesis, it is decided that both the heating capacity and the power usage are compared both with performance data from the manufacturer and with the extrapolated performance data presented in Chapter 4.2.2.

The block is, as mentioned in Chapter 2.4.1, not recommended for simulating part load operation, but the simulations described in Chapter 6.7 is using part load operation and it is therefore considered necessary to investigate this feature of the block. A comparison of the part load operation is therefore also performed for the block.

The cooling capacity is not investigated for this block, as it was concluded in the project work, since there is no volume flow sensor on the evaporator side and that no performance data measured for the evaporator is found.

6.3.1 Adaptation and configuration

For this component, it is considered that the control signal for the heat pump needs to be adapted. This is because the signal from the signal builder block has values that are other than 0, 0.5 and 1. From Chapter 3.2.1, it can be found that the real heat pump has two compressors, which gives the heat pump the capacity steps of 0%, 50% and 100%. It is therefore considered that input signals other than 0, 0.5 and 1 should not be given to the heat pump block.

6.3.1.1 Input data

As it can be seen in Appendix I, the inputs into this simulation model are the capacity signal, the temperatures of the brine entering the evaporator and of the water entering the condenser and volume flow of water coming in to the condenser. There is no volume flow sensor to measure the brine flowing through the evaporator. However, as mentioned in Chapter 2.4.2, the heat pump block does not use the mass flow in the evaporator to decide the power consumption and the heating and cooling capacities. It is therefore considered that it should be no problem using alternative values. It is assumed, from studying Figure 21, that the measured volume flow of brine through the boreholes is in the same magnitude as the volume flow through the evaporator, and the measured volume flow for the boreholes are therefore used as volume flow into the evaporator in the simulations. For the simulations, the mass flows into the block are found using the method described in Chapter 6.2.

6.3.1.2 Signal modification

As it is described in Chapter 3.3.1, the signals measured at Powerhouse Kjørbo has a measuring interval of 5 minutes, which leads to situations where the signal builder delivers signals that is other than 0, 0.5 and 1, which again is the signals given to the SH-HP.

The 5 minutes between each measurement makes it impossible to know exactly when, within the 5 minutes period, the signal changes and, as mentioned in Chapter 6.1, the signal in this period is found using linear interpolation between the two measurements. The scope of the signal processing, for this heat pump, is therefore to transform the measured signal into values that are either 0, 0.5 or 1, and to choose when the change between these values are.

It is decided that the change between the signals should happen half way of the 5 minutes period where the signals change. This is done because it is assumed that it would be the point of change that would be the least incorrect for all of the signal changes. The signals to the heat pump are modified using the blocks illustrated in Figure 26.

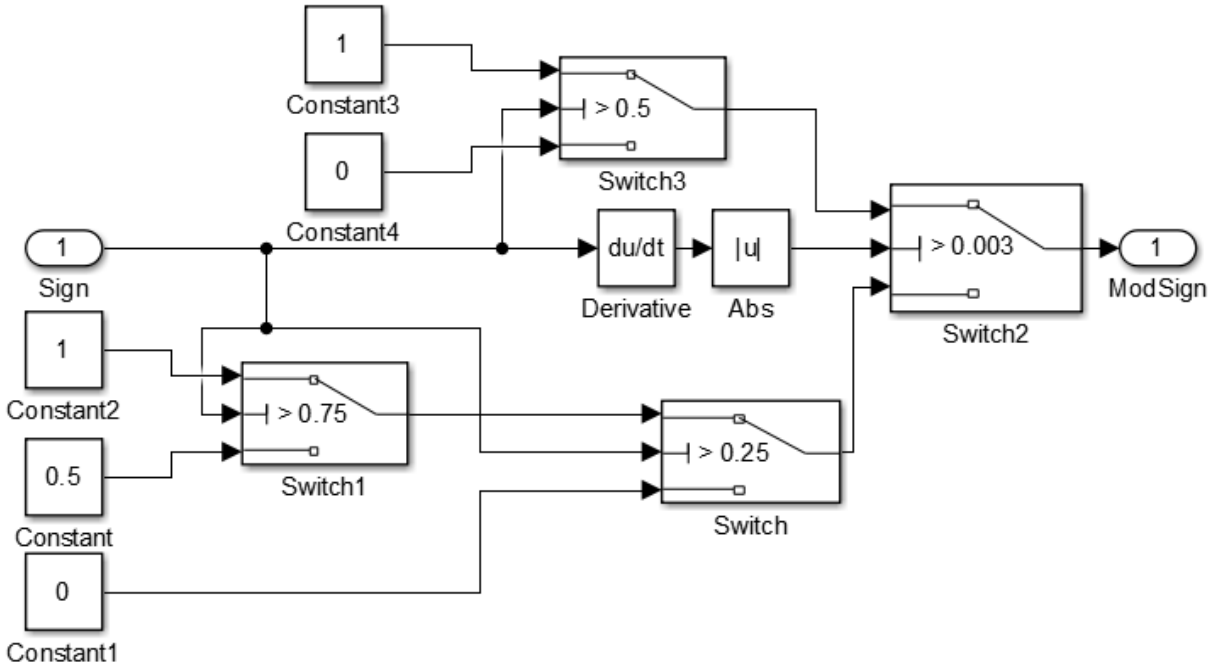

Figure 26 – Signal modification SH-HP

The Sign block is sending out the measured signal, and the ModSign block is sending the processed signal to the heat pump. The signal can then take two paths depending on whether the absolute value of the derivative of the incoming signal is higher than 0.003 or lower than 0.003. If the absolute derivative value is higher than 0.003, it means that the signal is changing between 0 to 1, which means that the signal changes directly from 0 to 1 or opposite. This is done in order for the signal to change directly between 0 and 1 in situations where the measured signal is changing between 0 and 1. If the absolute of the derivative is lower than 0.003 it means either that the signal is not changing or that the signal is changing between 0 and 0.5 or 0.5 and 1, and the signal then changes directly from 0 to 0.5, 0.5 to 1, 1 to 0.5 or 0.5 to 0.

6.3.2 Simulations

Four simulations are performed for the SH-HP, and these simulations are given in Table 12. As mentioned in Chapter 5.1, simulations are performed in order to investigate the blocks behaviour when changing input parameters where the values are regarded uncertain. Input parameters that are regarded as uncertain for the SH-HP, are the performance matrix and the thermal capacity in the hot loop.

Table 12 – Simulations SH-HP

Simulation	Description
1.	Original matrix
2.	Change in the performance matrix (a matrix based on extrapolation are compared)
3.	Change in thermal capacity hot loop (the values of 40 000 J/K and 160 000 J/K are compared)
4.	Simulation of the part load operation with original matrix

6.3.2.1 Simulation period

The simulation period for simulation 1, 2 and 3 is decided to be the period 27.04.2015 17:15-17:30. In the data extracted from the CC-system, ranging from 01.12.2014 to 30.11.2015, the longest period of 100 % capacity is found over four measurements. There is four instances where this happened: 27.04.2015 17:15-17:30, 01.08.2015 03:00-03:15, 22.08.2015 04:05-04:20 and 24.09.2015 22:45-23:00. For the simulations, the period 27.04.2015 17:15-17:30 is used since it is the only instance where the capacity goes directly from 0 to 100 %, which is assumed to be the most accurate for the comparison of the component. The heat pump is in this period running in cooling mode, but it is assumed that this is not a problem for the comparisons.

The period for the comparison of the part load performance of the heat pump is decided to be the 27.02.2015 between 07:10 and 10:35, since it is found to be the longest period where the pert load input signals and the measured power consumption is consistent.

6.3.2.2 Comparison data

As mentioned in Chapter 6.3, the heating capacity and the power consumption of the heat pump are compared. It is however regarded that comparing the temperature difference between the incoming and outgoing water in the condenser gives more information than comparing the heating capacity of the heat pump. Consequently, in the interest of limiting the number of figures, the outgoing temperature of the condenser is hence compared instead of the heating capacity. The outputs from the simulation are therefore the temperature coming out of the condenser and the power consumption of the heat pump.

6.4 Heat pump for DHW

From the project work, it was concluded that there is enough data to compare the heating capacity and the power consumption of the heat pump. However, the energy meter for the heat pump includes the power consumption of the circulation pump for the evaporator and

condenser, and, in order to compare the power consumption, it was concluded that this should be taken into account. The simulations described in this chapter are therefore performed in order to compare these outputs.

The cooling capacity is not compared for this heat pump block either. This is because there is no volume flow sensor for the evaporator and no performance data for the evaporator.

6.4.1 Adaptation and configuration

For this heat pump, two things are adapted: the control signal and the power consumption of the circulation pumps.

6.4.1.1 Input data

As it can be seen in the matrix of Appendix II, the inputs into this block is the measured signal and the volume flow and temperatures of the fluids coming in and going out of the evaporator and condenser. No measurement sensor to measure the mass flow through the evaporator is found. It is however assumed that this value has a relatively small influence on the results, and the constant shown in the matrix is therefore regarded as adequate input for the volume flow.

6.4.1.2 Signal modification

Also for this heat pump block, the input signal is in adapted. This is because the control signal from the signal builder block in periods gives values that are between 0 and 1, which is the input signal to the heat pump.

The signal into the heat pump is modified in the same way that the signal coming into the SH-HP is modified, only that the control signal for this heat pump is 0 or 1. The blocks that are used in the transformation of the block are shown in Figure 27.

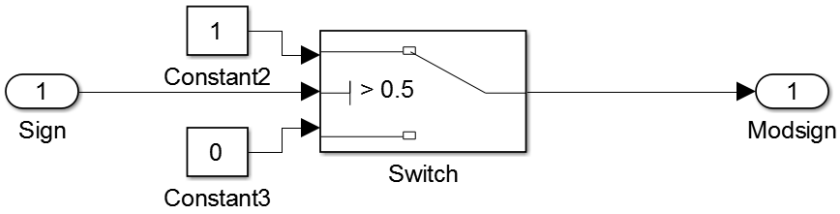

Figure 27 – Signal modification DHW-HP

6.4.1.3 Power consumption of circulation pumps

In the comparisons, 252 W is subtracted from the measured energy meter of the heat pump in order to account for the power consumption of the circulation pumps.

6.4.2 Simulations

Two simulations are performed for the DHW-HP, and these are specified in Table 13. The thermal capacity in the hot loop is the only parameter that is investigated in these simulations.

Table 13 – Simulations DHW-HP

Simulation	Description
1.	Original matrix
2.	Change in thermal capacity hot loop (the values of 40 000 J/K and 160 000 J/K is used in the simulations)

6.4.2.1 Simulation period

The longest running period for the heat pump is on the 09.04.2015 between 07:10 and 10:50. This period is therefore used for the comparison of this component.

6.4.2.2 Comparison data

As it is done for the SH-HP, the output temperature from the condenser and the simulated energy use of the heat pump is the outputs that are compared to the measured values.

6.5 Storage tanks for space heating

In the project work, it was concluded that the SH-ST has enough information to perform a comparison. It was however recommended that the comparison period should be in the summer, where the temperature differences in the storage tank is higher and the circulation of water between the storage tanks and the heat pump is not constant (Skjerve, 2016).

6.5.1 Adaptation and configuration

Three things are significant for the adaptation and configuration of the simulation for this component:

1. In the simulations, one storage tank is used (instead of two), because there is no point in investigating two identical storage tanks and to minimise simulation time. The mass flows into the storage tank are therefore halved.
2. A difference between the real component and the simulation component is that the real has two combined inlets and outlets while the simulation component has two inputs and two outputs. The consequence of this is that the simulated storage tank is coupled differently. This is illustrated in Figure 28, where the real storage tank is illustrated to the left and the simulated storage tank is illustrated to the right. In this case, charge

represents the heat pump and discharge represents the space and ventilation heating circuits.

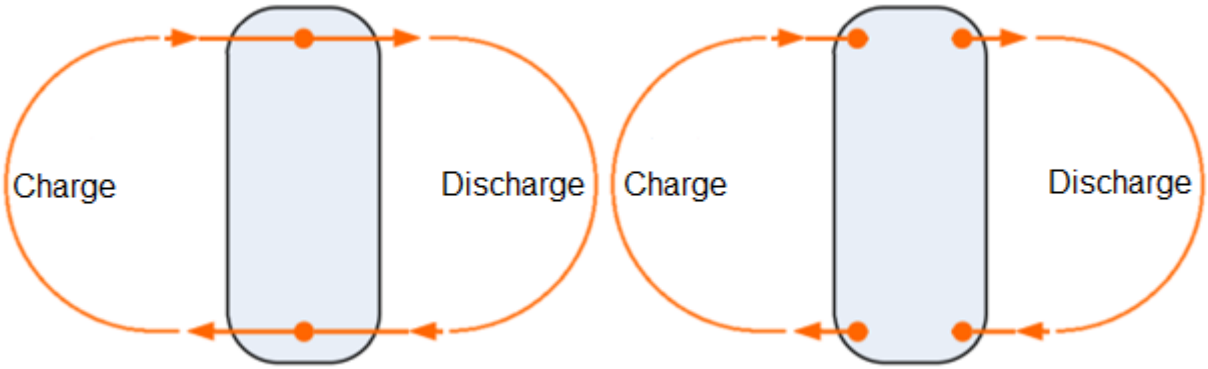

Figure 28 – Illustration of different coupling

For the real component, this makes the fluids mix before they go into the storage tank, which results in different temperatures and flow patterns in the tanks.

3. There is no single volume flow sensor measuring the circulation or temperature returning from the discharge circuit. The volume flow and returning temperature therefore must be found from the energy meters in the space heating and ventilation heating circuits in the system.

6.5.1.1 Input data

As it can be seen from Appendix III, the inputs into the storage tank block are the temperature and mass flows of the water from the heat pump and the water returning from the space heating system. There are sensors for temperature and flow from the heat pump, in addition to the energy meters from the space and ventilation heating system.

6.5.1.2 Mass flow in discharge circuit

It can be seen from Figure 22 that the volume flow and temperature from the ventilation heating circuits (OE003, OE005 and OE007) can be taken directly, but the volume flows and temperatures from the radiator circuits (OE004 and OE006) are found by performing an energy balance. The volume flow from the radiator circuits is found using equation 5.

$$\dot{V}_1 = \frac{\dot{V}_2 \cdot \Delta t_2}{\Delta t_1} \qquad 5$$

In situations where Δt_1 is less than one, $\dot{V}_1$ is set to be equal to $\dot{V}_2$ in order to avoid peaks in $\dot{V}_1$. The total volume flow is then found by adding the volume flows from each circuit.

The return temperatures is then multiplied by the volume flow for each circuit, and then added together. This is then divided by the total volume flow, which gives the total return temperature to the storage tanks.

The energy meters OE003, OE004 and OE006 is placed in the technical room, while the energy meters OE005 and OE007 is placed in the place of the ventilation units. The heat loss in the circulation pipes is therefore fully included for energy meter OE003, OE004 and OE006, but not for OE005 and OE007.

6.5.2 Simulations

Four simulations are performed for the SH-ST, and these simulations are presented in Table 14. As given in the table, parameters that are investigated in the simulations are the U-value, the EVC and the nodes.

Table 14 – Simulations SH-ST

Simulation	Description
1.	Original matrix
2.	Change in the U-value (the values 1 W/m^{2}K, 1.3 W/m^{2}K and 2.5 W/m^{2}K is used in the simulations)
3.	Change in the vertical heat conductivity (the values 0.5 W/mK, 1 W/mK and 1.5 W/mK is used in the simulations)
4.	Change in the nodes (the numbers of 2, 5 and 15 is used in the simulations)

6.5.2.1 Simulation period

The period for the comparison is decided to be 01.08.2015 to 11.08.2015, since it shows the longest charge/discharge cycle for the storage tank that could be found. The simulations are however performed between 15.07.2015 and 11.08.2015 in order to give the temperatures in the tank time to develop from the initial temperature.

6.5.2.2 Comparison data

As it can be seen in Appendix III, there are sensors for the temperature in the storage tank, temperature of the fluid going to the heat pump and temperature of the fluid going to the space and ventilation heating. The measured and simulated temperature in the storage tank, temperature out to the heat pump and temperature out to the space heating and ventilation heating circuit is the values compared in these simulations.

6.6 GSHE

From the project work, it was concluded that there is enough information to perform a comparison between the borehole at Powerhouse Kjørbo and the ground heat exchanger block in NZEP. Two different simulations are performed for the borehole:

1. Simulation to investigate the characteristics of the GSHE block. This is done for a chosen period, which is divided into an initialization period and a comparison period. The comparison is performed between the measured and simulated energy taken from or given to the borehole.
2. Simulation to investigate the temperature development in the ground for a long-term use. The purpose of this simulation is therefore not to perform a comparison, but to investigate whether the temperature development in the boreholes is realistic.

6.6.1 Simulation 1

As mentioned, the simulation period is divided into an initialization period and a comparison period. In the initialization period, input parameters with an upper and lower tolerance are changed in order to adapt the simulation to the measured data. These parameters and their tolerances are given in Table 15. The rest of the input parameters are from the original matrix of Appendix V.

Table 15 – Input parameters for simulation 1

Input parameter	**Value**
Thermal conductivity ground in W/m/K	1.9-4.4 (Skjerve, 2016)
Heat capacity of the ground in J/(kgK)	2100 ± 200 (Skjerve, 2016)
Density of the ground in kg/m^3	2650 ± 50 (Skjerve, 2016)
Field geometry	2x8 probes B/H=0.05 2x8 probes B/H=0.10 1x1 probes 5x12 probes B/H=0.05

6.6.1.1 Comparison period

Appendix IX shows a timeline that is made for the boreholes. This timeline is made with information gathered from measurements in the CC-system. The timeline goes from 01.03.2014 to 10.11.2015 because it is considered that this is the best period comparing the ground heat exchanger block and the real boreholes. This is because of three reasons:

1. At the end of the period, there is a 10-day period and several shorter periods where the measurements are missing, and it is therefore assumed that the least complicated and most accurate are to exclude these parts from the simulations. This therefore becomes a natural point of separation, where simulations should be performed either before or after this period.

2. In Chapter 3, it is written that the building was inaugurated in April 2014. The first measurement is taken the 27.03.2014, and it is therefore assumed that this measurement is from the borehole was first used. This is therefore considered a good place to start the simulations since the ground temperatures should be unchanged.
3. It is mentioned in Chapter 4.4.3 that the ground heat exchanger block does not have the ability to change the mass flow circulating in the block. It is therefore assumed that the block should be simulated both with and without a constant mass flow in order to investigate the magnitude of this design flaw. This is the only period with both constant and variable mass flow.

The comparison period for the ground heat exchanger is therefore 01.03.2014 07:50 to 11.11.2015 00:10, and the initialization period from 01.03.2014 07:50 to 31.07.2014 23:55.

6.6.1.2 Missing measurements within the period

There are periods of missing measurements the 02.06.2014 between 09:00 and 12:55 and 28.08.2014 between 21:10 and 23:00. In the first period, there are 48 missing measurements, and there are 22 missing measurements in the second period. Since these are two relatively short periods, it is assumed that they just affect the temperatures in the filling and the ground close to the filling, and that it therefore does not influence the overall simulation noticeably. Substitute values are therefore produced by performing linear regression between the last given and first reappearing measurement in this period. Graphs showing these periods are given in Appendix X.

6.6.1.3 Design mass flow rate

As mentioned, the ground heat exchanger block does not have the ability to change the mass flow in the simulations. It is therefore assumed that the mass flow circulated in the boreholes has a large impact on the results of the comparisons. A graph showing the measured volume flow for the simulation period is shown in Appendix XI. From this graph, it is possible to see that the volume flow circulating in the borehole is controlled to be constant in the period 27.03.2014 to 01.12.2014, and that it is varying the rest of the period. Even though the volume flow is controlled to be constant in the first period, it can be seen that the constant volume flow have been changed several times.

It is assumed that the most accurate for the simulations is to use the design mass flow rate that is measured over the longest period, and then use this period to compare the real component and the simulation component. The average mass flow of 2.6 kg/s, found over the period 24.04.2014 08:05 to 01.12.2014 00:00, is therefore used as the design mass flow rate.

6.6.1.4 Inputs and outputs

As it is given in Appendix V, the inputs into the ground heat exchanger block are the measured brine temperature and mass flow into the boreholes. The method described in Chapter 6.2 is used to transform the volume flow into mass flow. The measured and simulated temperature coming out of the borehole is compared values.

6.6.2 Simulation 2

As mentioned, this simulation investigates the temperature development for a long-term use of the borehole.

6.6.2.1 Inputs

For this simulation, the measured supplied and ejected thermal energy for period 01.03.2014 07:50 to 11.11.2015 00:10 is used as an input. The measured thermal energy for the year 11.11.2014 to 11.11.2015 is then added to the timeline four times. In all, this makes a period of 5 years and 8 months with supplied and rejected heat in the boreholes.

The input parameters into these simulations are the input parameters that are found in the initialization process of simulation 1.

6.6.2.2 Outputs

In order to avoid too much fluctuation in the temperature of the outputs, the temperature of the ground in roughly one-meter distance from the borehole is investigated in this simulation. As mentioned in Chapter 2.4.4, the output Tn is giving the temperatures of the nodes in the ground. The nodes in the ground can be described as a grid of radial and axial nodes, where there at default are five axial nodes and nine radial nodes (Ytterhus, 2014). The distance between the radial nodes can be calculated with the help of equation 6.

$$r_h = r_{h-1} + (r_m - r_1) \cdot \frac{1-f}{1-f^{m-1}} \cdot f^{h-2} \qquad 6$$

The radiuses of the different nodes are calculated in Appendix VII, and it is found that r_8, with the value 0.85 m, is the closest to 1 meter. The nodes measured in r_8 are therefore the outputs from the simulations.

6.7 Storage tanks for DHW

From the matrix in Appendix IV and from the conclusion in the project work, it is possible to see that there are several measurement sensors missing in order to perform a comparison between the real and simulated component. In addition to this, the energy measurement sensors

for the DHW, as mentioned in Chapter 3.3.2, is giving a much lower measured energy consumption compared to the energy meter for the heat pump.

Because of these missing measurements and faulty energy meters, no simulations are performed for this component. This also means that there is not performed any simulations for the DHW system or for the whole system.

6.8 Space heating system

In order to compare a larger number of components interconnected together, a simulation model for the space heating system is made. The components used in this simulation are the heat pump, storage tank and the GSHE.

6.8.1 Adaptation and configuration

A figure showing the setup of the components can be found in Appendix XV. The GSHE block is connected to the evaporator of the heat pump while the condenser is connected to the charging port of the storage tank. The discharge port of the storage tank is connected to the load block.

6.8.1.1 Input data

The inputs into this simulation are energy meter OE002 to OE007 in addition to the measured outdoor temperature.

6.8.1.2 Control system

The measured outdoor temperature is used to find the set point for the heat pump from the outdoor compensation curve given in Figure 13. The control system explained in Chapter 3.2.1.1 is replicated as closely as possible. An attempt to explain the control system is done in Figure 29.

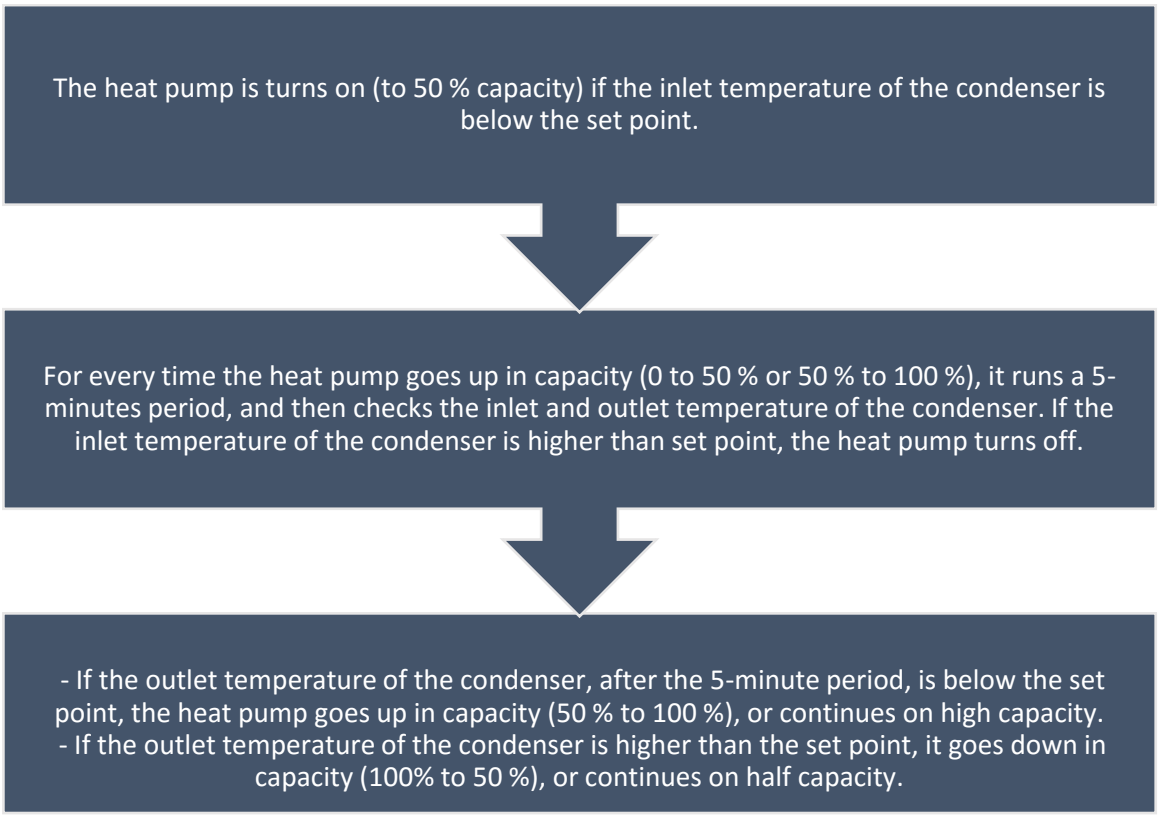

Figure 29 – Control system

A system for counting the amounts of starts/stops and regulating the on/off time of the heat pump is not implemented.

6.8.1.3 Load block

The load block uses the measured thermal energy from the energy meters OE002 to OE007 in order to calculate the returning temperature and the mass flow of the discharge circuit. As it can be seen from Figure 22, these energy meters measures the thermal energy ejected or supplied for the district heating, ventilation heating and the space heating circuits.

The returning temperature is found by assuming a 25℃ returning temperature from the ventilation heating and assuming a temperature difference (between supply and return), dependent on the outdoor temperature, for the radiator circuits. The temperature difference in the radiator circuit follows the curve given in Figure 30. These returning temperatures is based on the design temperature levels of 50/40℃ for the radiator circuit and 50/25℃ for the ventilation heating circuit (Nordang, 2014).

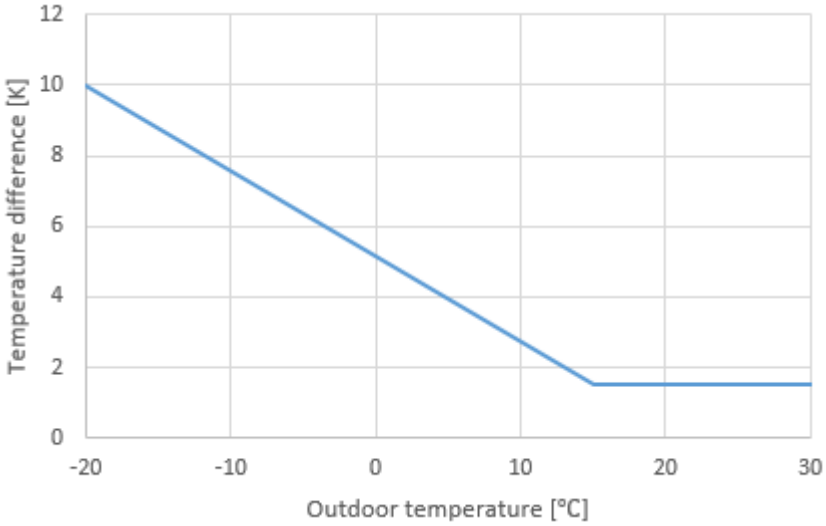

Figure 30 – Temperature difference radiator circuit

The mass flow is then found using equation 7, where $\dot{Q}$ is the sum of the thermal energy measurement sensors.

$$\dot{m} = \frac{\dot{Q}}{C_p \cdot \Delta t}\,[kg/s] \qquad 7$$

6.8.2 Simulation

One simulation is performed for this system.

6.8.2.1 Simulation period

The simulation period is 01.12.2014 to 11.11.2015. This period is chosen because it is the longest period of coherent measurements.

6.8.2.2 Input parameters

The input parameters into the storage tank and the heat pump block are the parameters from the original matrixes, while the input parameters into the GSHE is the ones found in the initialization of simulation 1 for the simulations described in Chapter 6.5.2.2.

The mass flow between the heat pump and the borehole is set to be 2.6 kg/s, and to be 2 kg/s between the heat pump and the storage tank.

7 Comparison

In this chapter, the results of the simulations described in Chapter 6 is compared to the measured values and then discussed in two levels. The first level discusses the comparisons for each simulation, while the second level discusses whether each component is functioning based on the comparisons and the first level discussions in this chapter. In order to keep the chapter as tidy as possible, the results of the simulations are first compared to the measured values, explained and then discussed.

7.1 Heat pump for space heating

As described in Chapter 6.3.2, four simulations are performed for the SH-HP. The figures of simulation 1, 2 and 3, for the SH-HP, are regarded to be where the effect of the processing of the control signal to the heat pump is easiest to spot. This is because the short simulation period makes the signal builders linear regression between each measurement more distinct. If there had not been a processing of the control signal to the heat pump, the simulated graphs would have started to rise or fall at the same spot as the measured graphs, and would have had a rise or fall that would be in about the same rate as the measured graph. Apart from this, the graphs would be the same.

7.1.1 Simulation 1

As it is given in Chapter 6.3.2, simulation 1 is a simulation of the original matrix of the SH-HP, and is a simulation performed in order to compare the simulated and real component.

7.1.1.1 Comparison

In Figure 31, *Pm* stands for "measured power consumption" and *Ps* stands for "simulated power consumption". The period between about 07:13 to 17:32 the simulated and the real heat pump runs in full capacity, while they run on half capacity for the period roughly between 17:32 and 17:43. From the figure, it can be seen that the simulated heat pump has a higher power consumption than the real one for the whole period.

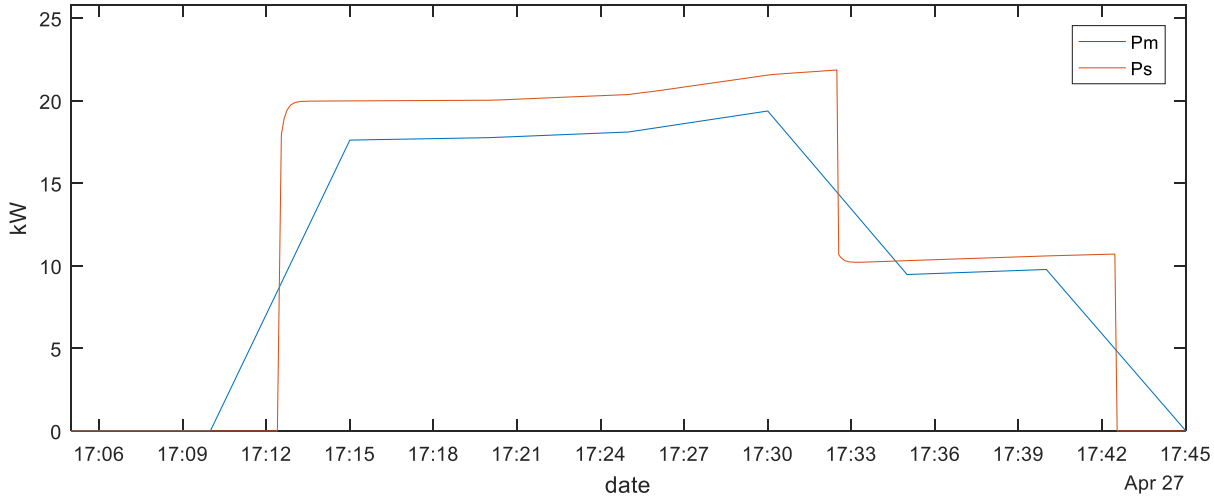

Figure 31 – Comparison SH-HP simulation 1: Power consumption

In Figure 32, *Tocm* stands for "measured temperature out of the condenser", *Tocs* stands for "simulated temperature out of the condenser" and *Tic* stands for "(measured) temperature into the condenser". As we can see, the simulated temperature out of the condenser is higher compared to the measured.

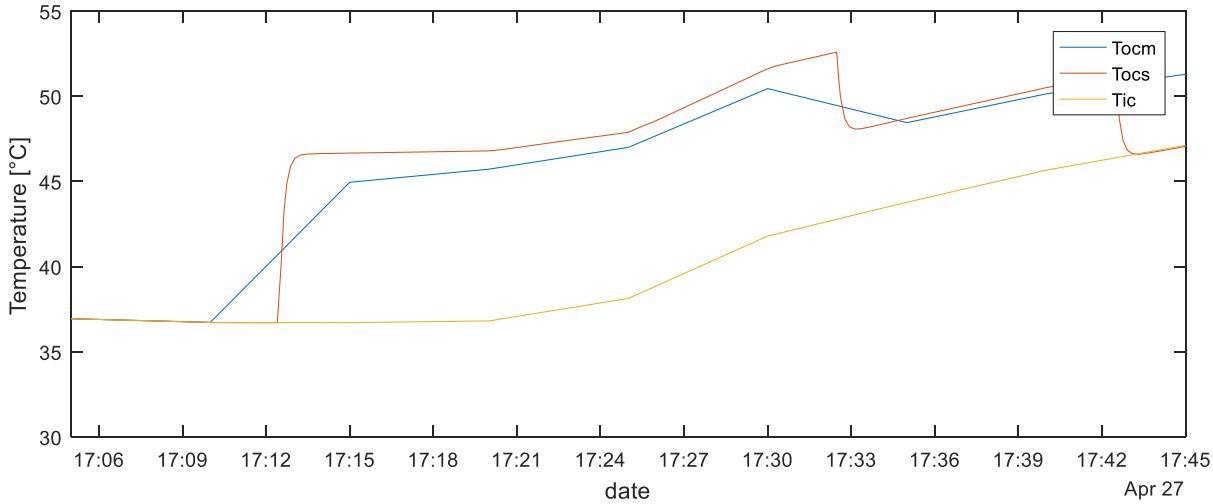

Figure 32 - Comparison SH-HP simulation 1: Temperature in and out of condenser

In Figure 33, *TdCm* stands for "measured temperature difference over the condenser", *TdCs* stands for "simulated temperature difference over the condenser" and *TdEm* stands for "measured temperature difference over the evaporator". For all "temperature differences over the …", it means the temperature difference between inlet and outlet fluid of the specified component. From the figure, it can be seen that the *TdCs* is higher than the *TdCm* in both full and half capacity.

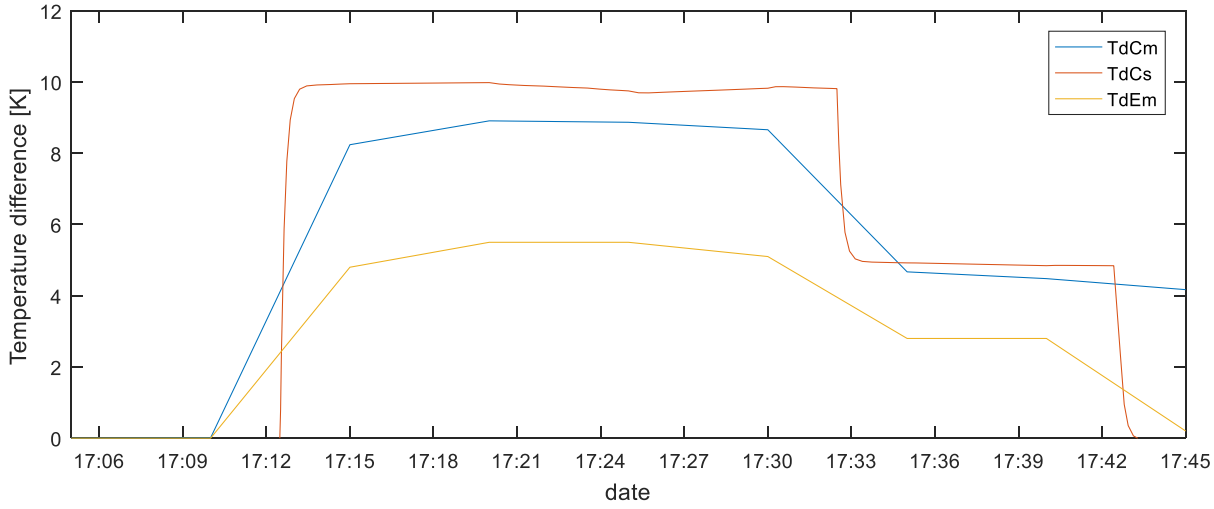

Figure 33 - Comparison SH-HP simulation 1: Temperature difference condenser and evaporator

7.1.1.2 High simulated values

Both the power consumption and the heating capacity (illustrated with the temperature of the fluid going out of the condenser) are higher for the simulated component.

An explanation might be that the temperature difference between the inlet and outlet fluids for the evaporator and condenser is not according to the temperature differences specified for the performance data, and that the simulated and real heat pump therefore does not have the same working conditions. The measured inlet brine temperature of the evaporator for the simulation period is 9.4℃ ±0.0, while the measured temperature returning from the condenser is in the range of 45℃ to 50℃. In Chapter 3.2.1.2, it is specified that the temperature difference in the evaporator should be 3K for the inlet temperatures of 0℃ and 10℃ to the evaporator. It is also specified that the temperature difference in the condenser should be 5K for 45℃ and 10K for 55℃ outlet temperature of the condenser. If linear interpolation is used, the temperature difference in the condenser should be 7.5K for 50℃.

In the period of 17:15 to 17:30, the measured temperature difference in the evaporator is about 5K, the measured temperature difference in the condenser is roughly 9K, and the simulated temperature difference in the condenser is roughly 10K. Compared to the temperature

differences specified for the standard rating condition, the measured temperature difference is 2K higher for the evaporator, and between 1.5K and 4K higher for the condenser.

This means a decrease in both condenser and evaporator temperature since the inlet temperature for the condenser and the outlet temperature for the evaporator is reduced. A reduced temperature in the evaporator increases the specific volume of the gas, and, since compressors have a set suction volume, the mass flow of circulated working fluid in the heat pump therefore decreases. A lower mass flow of circulated working fluid also means a lower heating capacity and power consumption of the condenser, which could explanation the results (Stene, 1997).

Another explanation however might be that the performance data gathered for the Carrier 61WG-070 without option 272 is not a good replacement.

Based on that the simulated and measured heat pumps does not have the same operating conditions and that the performance data is uncertain, it is concluded that it is impossible to pinpoint the reason for the deviations.

7.1.1.3 Low measured heating capacity in the start of the simulation

From Figure 31, the difference between the measured and simulated power consumption is as good as constant in the period of 17:15 to 17:30. The simulated temperature difference, shown in Figure 33, however shows that the simulated temperature difference is higher at 17:15, but becomes roughly constant in the period of 17:20 to 17:30. This might be explained by that the real heat pump uses a certain time to reach nominal operation (Ruschenburg et al., 2014).

7.1.2 Simulation 2

As it is given in Chapter 6.3.2, simulation 2 is a simulation of the performance data found by extrapolation. In this subchapter, the results of simulation 2 are compared to the results of simulation 1 and measured values.

7.1.2.1 Comparison

In Figure 34, *Pm* stands for "measured power consumption", *OrgPs* stands for "simulated power consumption with original matix" and *Ps* stands for "simulated power consumption". In this simulation, *Ps* is the simulation of the performance data found by extrapolation. As it can be seen from the figure, *Ps* is at all times higher than the *OrgPs*.

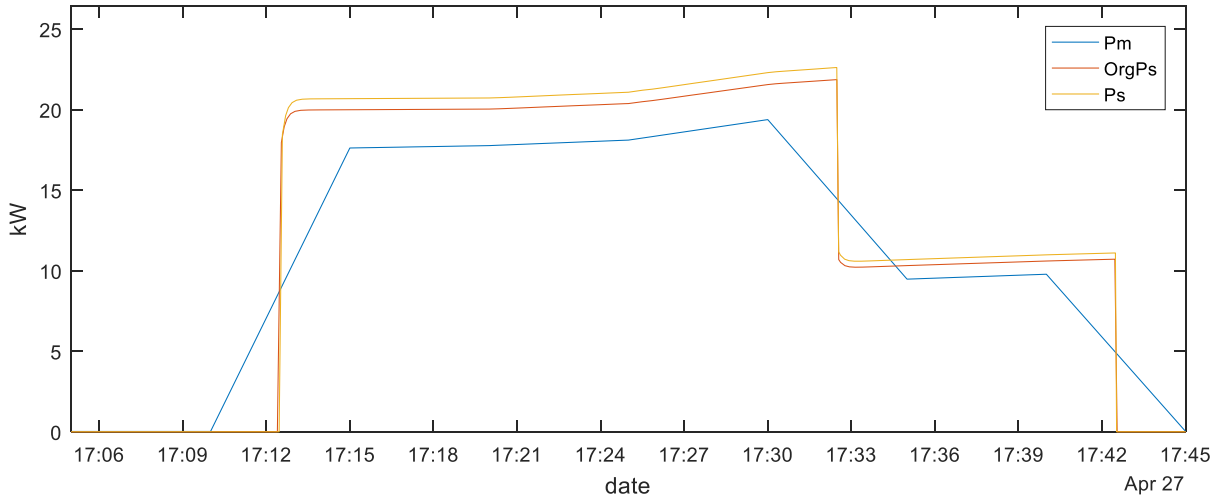

Figure 34 - Comparison SH-HP simulation 2: Power consumption

In Figure 35, *TdCm* stands for "measured temperature difference over the condenser", *TdCs* stands for "simulated temperature difference over the condenser" and Org*TdCs* stands for "simulated temperature difference over the condenser with original matrix". For all "temperature differences over the …", it means the temperature difference between inlet and outlet fluid of the specified component. In this simulation, *TdCs* is the simulation of the performance data found by extrapolation. As it can be seen from the figure, *TdCs* is at all times lower than Org*TdCs*.

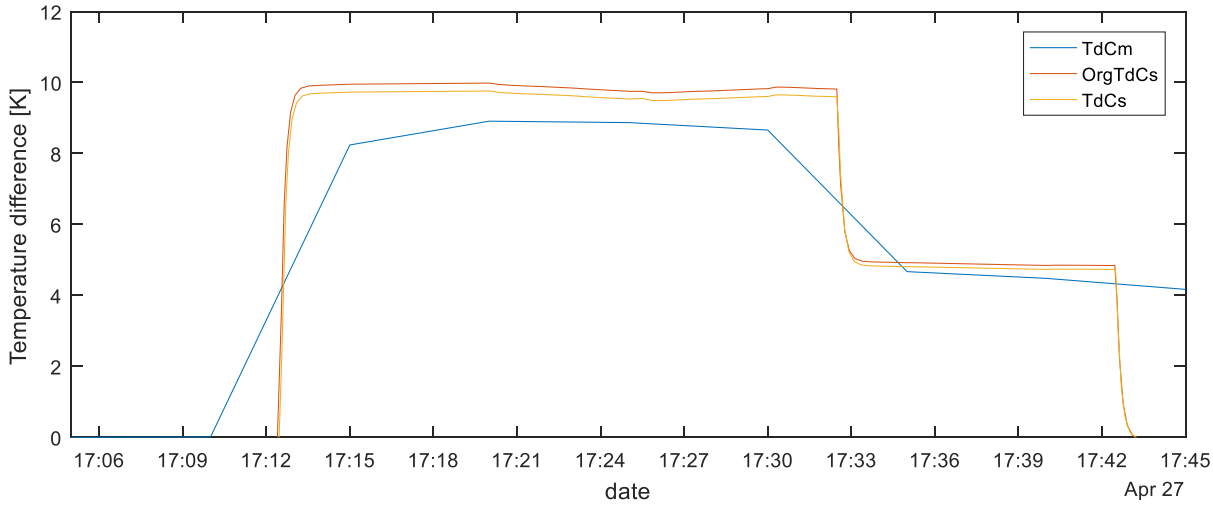

Figure 35 - Comparison SH-HP simulation 2: Temperature difference condenser

7.1.2.2 Discussion

From the comparison, it is possible to see that the performance data found with extrapolation has a higher power consumption and a lower heating capacity (illustrated with temperature difference over the condenser) compared to the simulation performed with performance data in the original matrix. As mentioned in Chapter 7.1.1.3, the temperature differences between the inlet and outlet fluids in the evaporator are not the same as the temperature differences for the performance data. It is therefore considered that it is impossible to make a conclusion to whether this extrapolated performance data is more accurate than the performance data given in the original matrix.

7.1.3 Simulation 3

As it is given in Chapter 6.3.2, simulation 3 is performed in order to investigate the blocks behaviour when changing thermal capacity in the hot loop. In this subchapter, the results of simulation 3 are compared to the results of simulation 1 and measured values.

7.1.3.1 Comparison

In Figure 36, *Pm* stands for "measured power consumption" and *Ps* stands for "simulated power consumption". *Ps* is simulated for different thermal capacity hot loop values, where the values are given within the bracket. As it can be seen from the figure, the simulated difference with changing the input parameter can best be seen in the start-up of the heat pump, where a high thermal capacity lengthens the time before the heat pump reaches nominal operation.

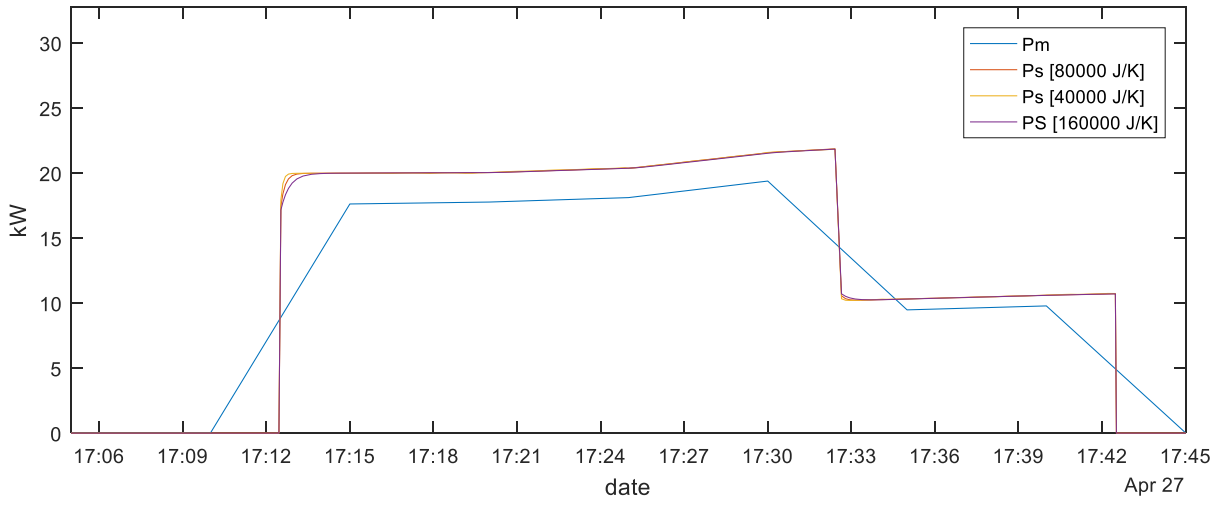

Figure 36 - Comparison SH-HP simulation 3: Power consumption

In Figure 37, *TdCm* stands for “measured temperature difference over the condenser”, *TdCs* stands for “simulated temperature difference over the condenser”. For all “temperature differences over the …”, it means the temperature difference between inlet and outlet fluid of the specified component. As it can be seen from the figure, the differences between the different simulations are most noticeable where the heat pump changes capacities.

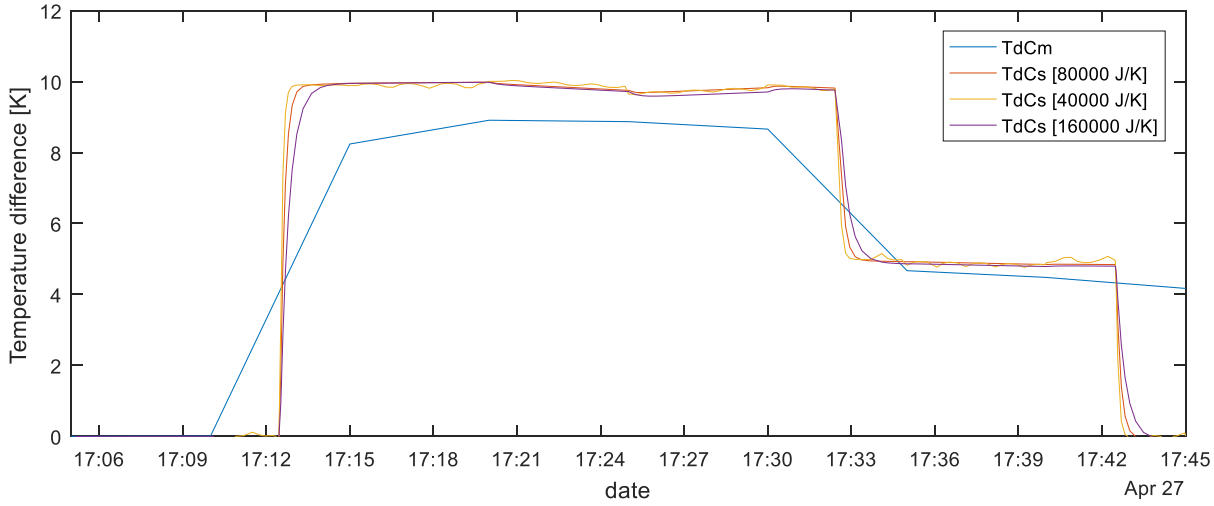

Figure 37 - Comparison SH-HP simulation 3: Temperature difference condenser

7.1.3.2 Discussion

From the figures of this subchapter, it is possible to see that the thermal capacity hot loop affects the time before the heat pump reaches a nominal operation. However, with the 5-minutes sample time for the measurements, it is considered impossible to draw any conclusions to whether the parameter has any realistic impact on the simulations.

7.1.4 Simulation 4

As it is given in Chapter 6.3.2, simulation 4 is performed in order to investigate the part load operation of the heat pump. In this subchapter, the results of simulation 4 are compared to measured values.

7.1.4.1 Comparison

In Figure 38, *Pm* stands for "measured power consumption" and *Ps* stands for "simulated power consumption". As it can be seen from the figure, the *Ps* is higher than the *Pm* for the whole period.

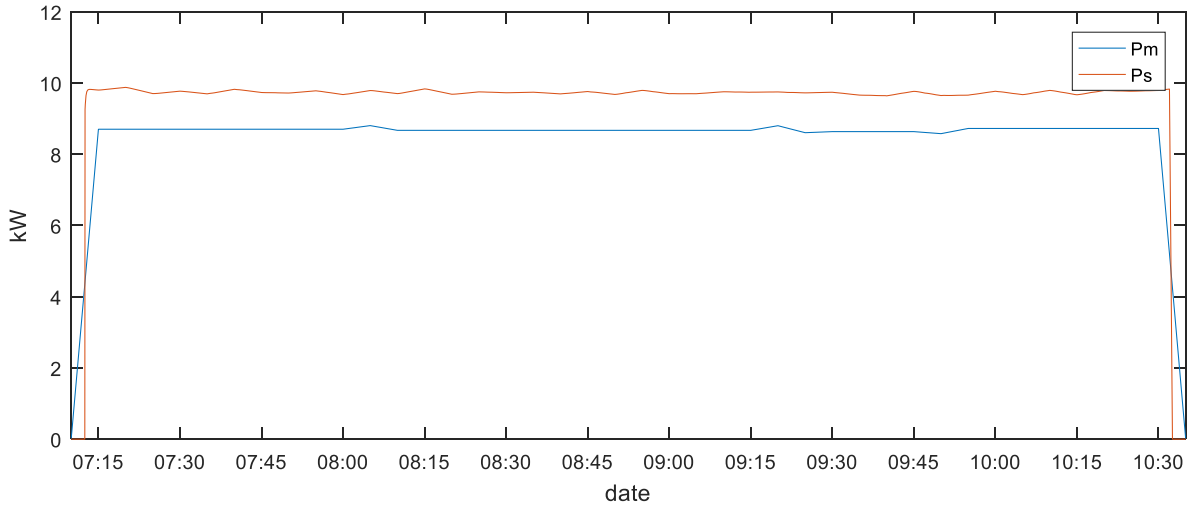

Figure 38 - Comparison SH-HP simulation 4: Power consumption

In Figure 39, *Tocm* stands for "measured temperature out of the condenser", *Tocs* stands for "simulated temperature out of the condenser" and *Tic* stands for "(measured) temperature into the condenser". As it can be seen from in the figure, the real and simulated heat pump gives very similar temperatures out of the condenser. It can also be seen that the temperatures out of the condenser in this period is also very stable at 45°C.

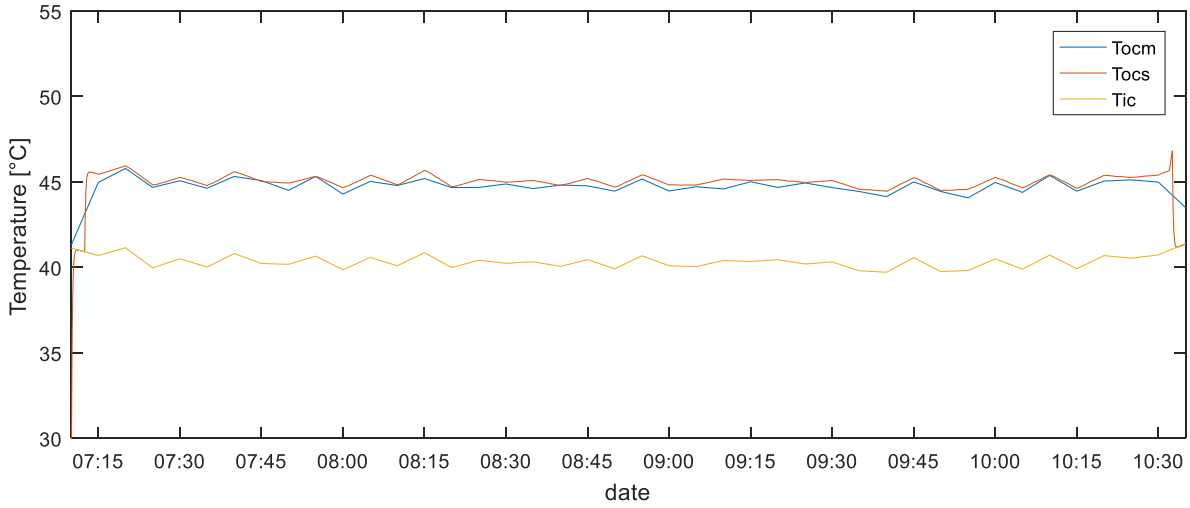

Figure 39 - Comparison SH-HP simulation 4: Temperature out of condenser

In Figure 40, *TdCm* stands for "measured temperature difference over the condenser", *TdCs* stands for "simulated temperature difference over the condenser" and *TdEm* stands for "measured temperature difference over the evaporator". For all "temperature differences over the …", it means the temperature difference between inlet and outlet fluid of the specified component. As mentioned for the previous figure, the measured and simulated condenser temperature is very similar for this simulation. Another thing that can be seen is that the measured temperature difference in the beginning of the simulation is rising slower than the simulated temperature difference.

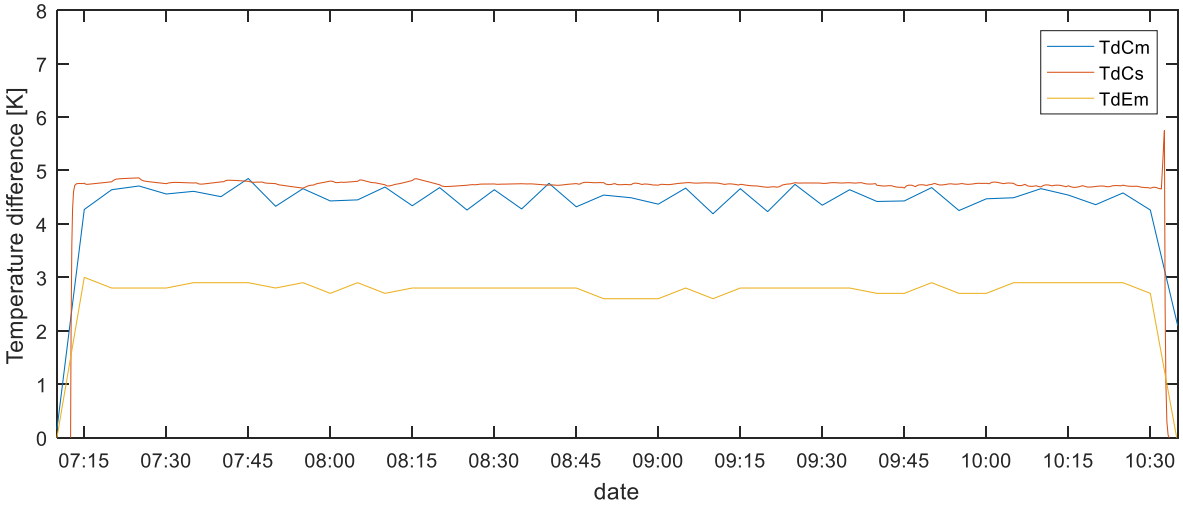

Figure 40 - Comparison SH-HP simulation 4: temperature difference condenser

7.1.4.2 High simulated power consumption

It can be seen that the simulated power consumption is clearly higher than the measured. The simulated and measured heating capacity (illustrated with the temperature difference over the condenser) however, has a relatively close fit, where the simulated is slightly higher. For the heating capacity, this makes an improvement compared to the comparison presented in Chapter 7.1.1. This might be explained by the fact that that the temperature difference in the evaporator and condenser now is very close to the ones for the measured performance data given for the heat pump. However, another possible explanation is that the part load efficiency for the real heat pump is better than for the simulated heat pump, and that the measured heating capacity therefore are closer to the simulated.

It is concluded that it is impossible to, with the information available, pinpoint the exact reason for the deviations.

7.1.4.3 Low measured heating capacity in the start of the simulation

One can see that the first measurement for the heating capacity (illustrated with the temperature difference in the condenser), is a bit lower. As mentioned in Chapter 7.1.1.3, this might be explained with that the real heat pump uses some time to reach nominal operation.

7.2 Heat pump for DHW

This subchapter shows and discusses the results of the two simulations performed for the DHW-HP.

7.2.1 Simulation 1

As it is given in Chapter 6.4.2, simulation 1 compares the result of the simulations performed with the original matrix against measured values of the real component.

7.2.1.1 Comparison

In Figure 31, *Pm* stands for "measured power consumption" and *Ps* stands for "simulated power consumption". As it can be seen from the figure, the measured and simulated power consumption is very similar. It can also be seen that there are some fluctuations for both the simulated and measured power consumption at about 07:22, 08: 22, 08:38 and 10:45.

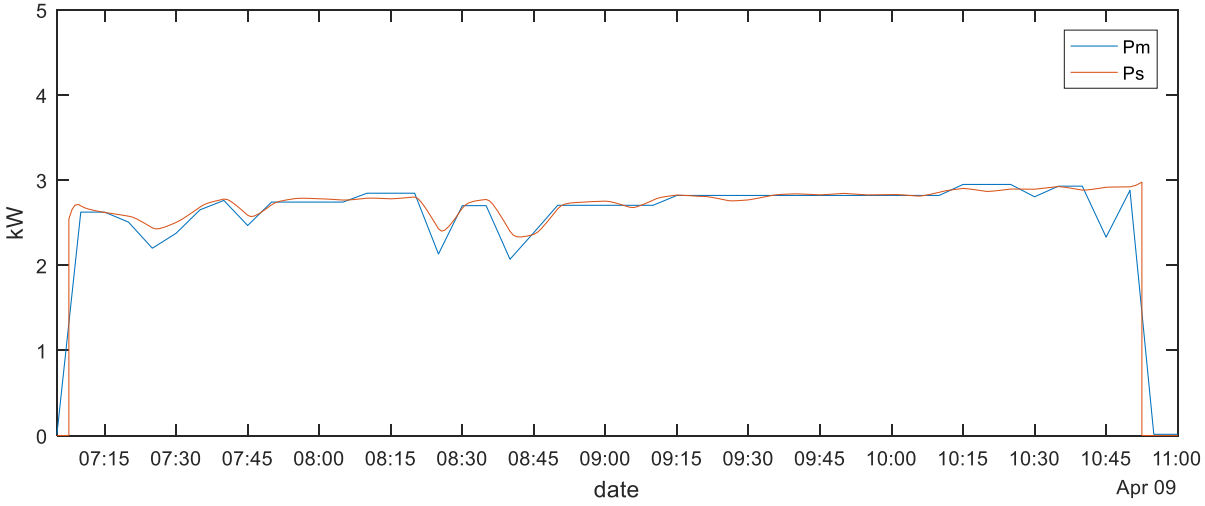

Figure 41 - Comparison DHW-HP simulation 1: Power consumption

In Figure 42, *Tocm* stands for “measured temperature out of the condenser”, *Tocs* stands for “simulated temperature out of the condenser” and *Tic* stands for “(measured) temperature into the condenser”. From this figure, it can be seen that the simulated and measured temperatures are very similar. However, *Tocm* stands out at the measurement measured at 08:45.

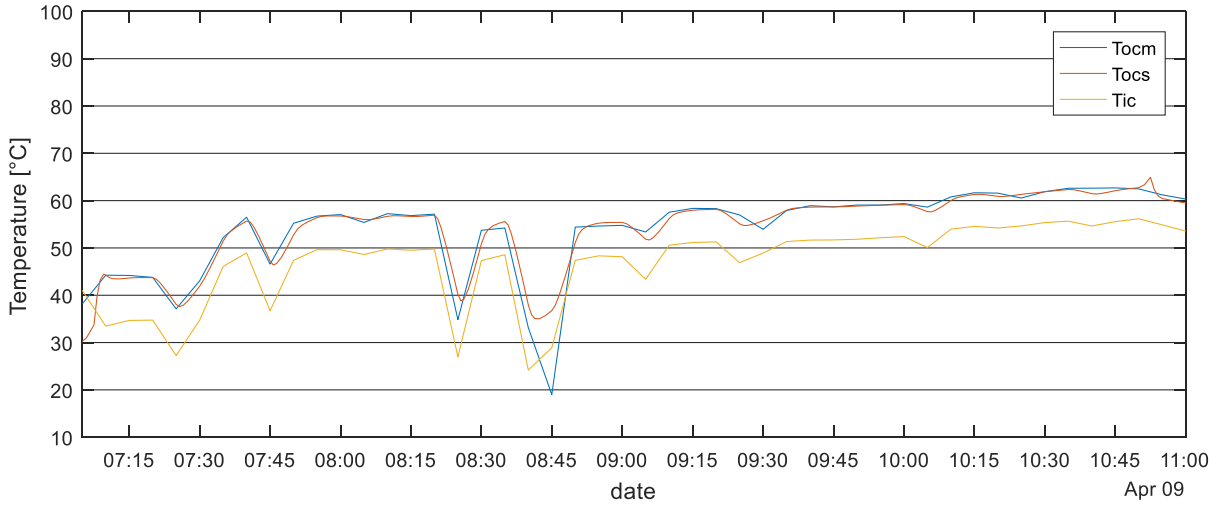

Figure 42 - Comparison DHW-HP simulation 1: Temperature out of condenser

In Figure 43, *TdCm* stands for “measured temperature difference over the condenser” and *TdCs* stands for “simulated temperature difference over the condenser”. For all “temperature differences over the …”, it means the temperature difference between inlet and outlet fluid of the specified component. From this figure, it can be seen that the simulated and measured temperature difference is close to identical in certain periods, while there are some deviations in others.

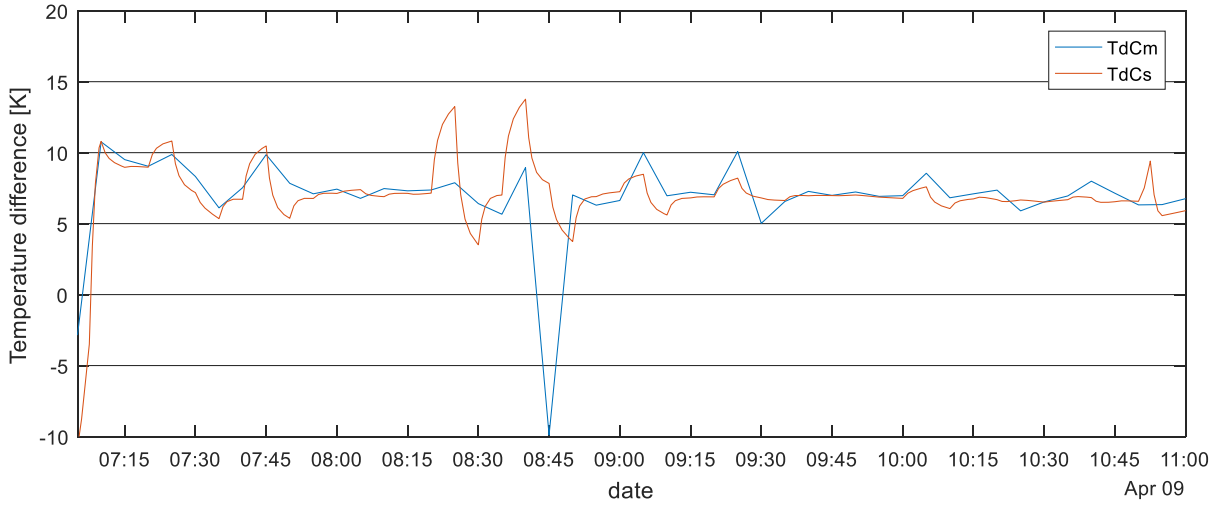

Figure 43 - Comparison DHW-HP simulation 1: Temperature difference condenser

In Figure 44, *TdEm* stands for “measured temperature difference over the evaporator” and *TdEs* stands for “simulated temperature difference over the evaporator”. For all “temperature differences over the …”, it means the temperature difference between inlet and outlet fluid of the specified component. From this figure, it can be seen that the simulated and measured temperature difference is close to identical in certain periods, while there are some deviations in others. As it can be seen from the figure, the measured and simulated temperature difference over the evaporator is very similar.

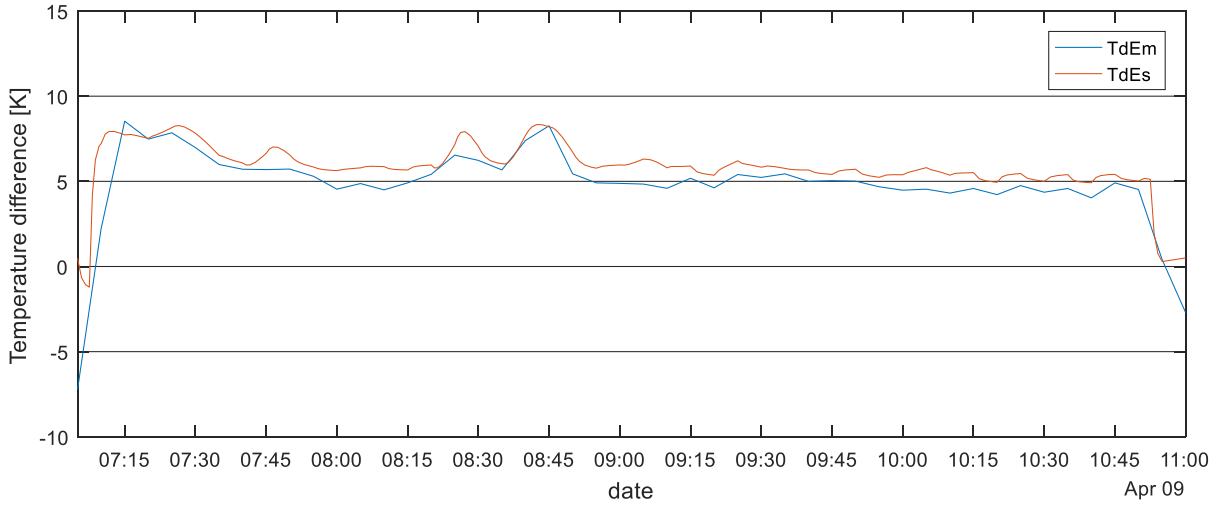

Figure 44 - Comparison DHW-HP simulation 1: Temperature difference evaporator

In Figure 45, *MdotE* stands for “mass flow in evaporator” and *MdotC* stands for “mass flow in condenser”. From the figure, it can be seen that the mass flow in the evaporator is constant and that the mass flow in the condenser is varying.

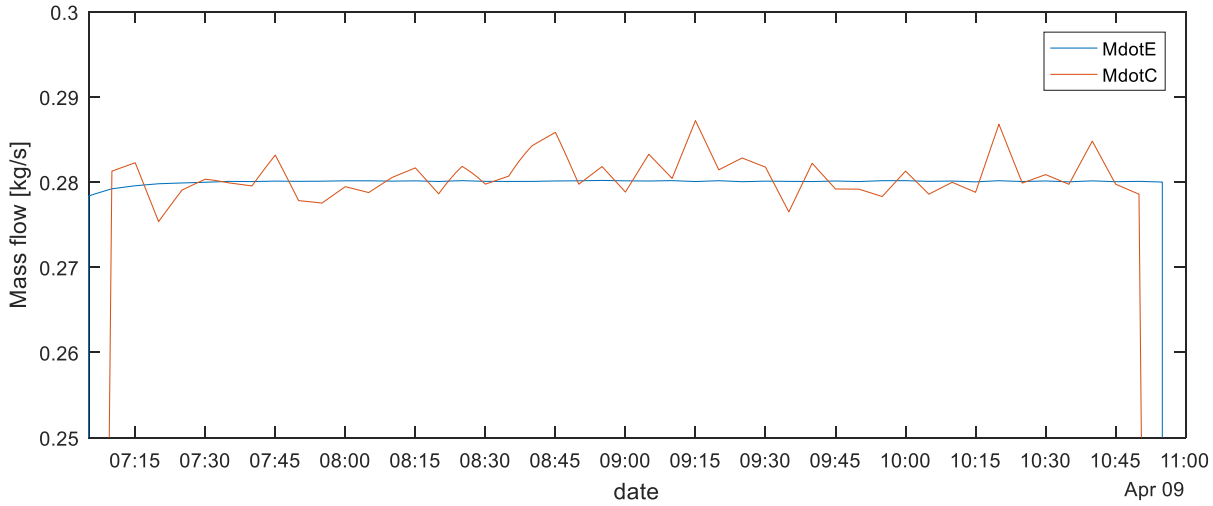

Figure 45 - Comparison DHW-HP simulation 1: Mass flow evaporator and condenser

7.2.1.2 Alike

The measured and simulated is very close when it comes to the power consumption and the heating capacity (illustrated with the temperature difference for the condenser). From the temperature differences between the inlet and outlet of the evaporator and the condenser, it can be seen that there are some differences compared to the temperature differences specified in the standard rating condition of NS-EN 14511-2:2013. The standard rating conditions specifies that the temperature difference for the evaporator should be 3K, and that the temperature difference for the condenser should be 5K, 8K and 10K for 45℃, 55℃ and 65℃ outlet condenser temperature respectively. The lowest measured temperature difference for the evaporator is about 4K and the temperature difference for the condenser is roughly 7K for temperatures above 55℃. The working condition for the simulated and the measured components are therefore not exactly the same.

However, the power consumption and heating capacity is very close, even when the temperature differences in the evaporator and in the condenser is varying or are not according to the standard rating conditions specified in NS-EN 14511-2:2013. It is therefore concluded that the heat pump block works god in this simulation.

7.2.1.3 Fluctuations in the temperature difference

As it can be seen in Figure 43, there are some fluctuations in the simulated temperature difference. If the time for the fluctuations is compared to the timing of changes for the mass flow in the condenser in Figure 45, it can be seen that there is a correlation. An explanation is that when the mass flow changes, the condenser temperature changes, and that when there are changes in the condenser temperature, the thermal capacity of the condenser takes some time to adjust to the new temperature.

7.2.2 Simulation 2

As it is given in Chapter 6.4.2, simulation 2 is performed in order to investigate the blocks behaviour when changing the thermal capacity hot loop parameter. In this subchapter, the results of simulation 3 are compared to the results of simulation 1 and measured values.

7.2.2.1 Comparison

In Figure 46, *Pm* stands for "measured power consumption" and *Ps* stands for "simulated power consumption". *Ps* is simulated for different thermal capacity hot loop values, where the values are given within the bracket. As it can be seen in the figure, the differences between the simulated power consumption are visible in the start-up of the heat pump and where there are changes in the power consumption.

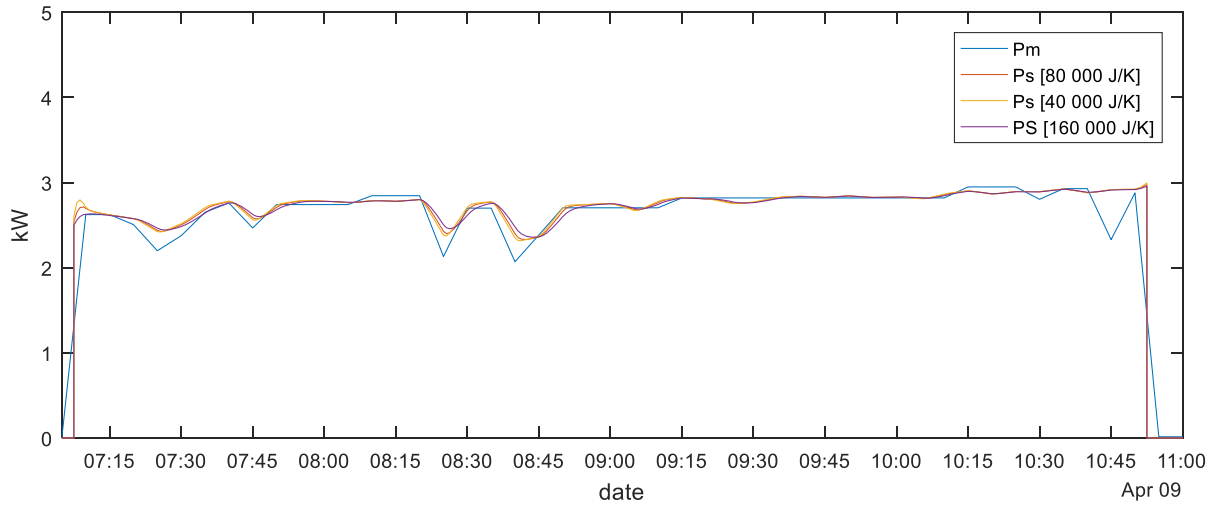

Figure 46 - Comparison DHW-HP simulation 2: Power consumption

In Figure 47, *TdCm* stands for "measured temperature difference over the condenser", *TdCs* stands for "simulated temperature difference over the condenser". For all "temperature differences over the …", it means the temperature difference between inlet and outlet fluid of the specified component. As mentioned for the previous figure, the differences between the simulations is visible where there are visible in the start-up of the heat pump, and in changes of the temperature difference.

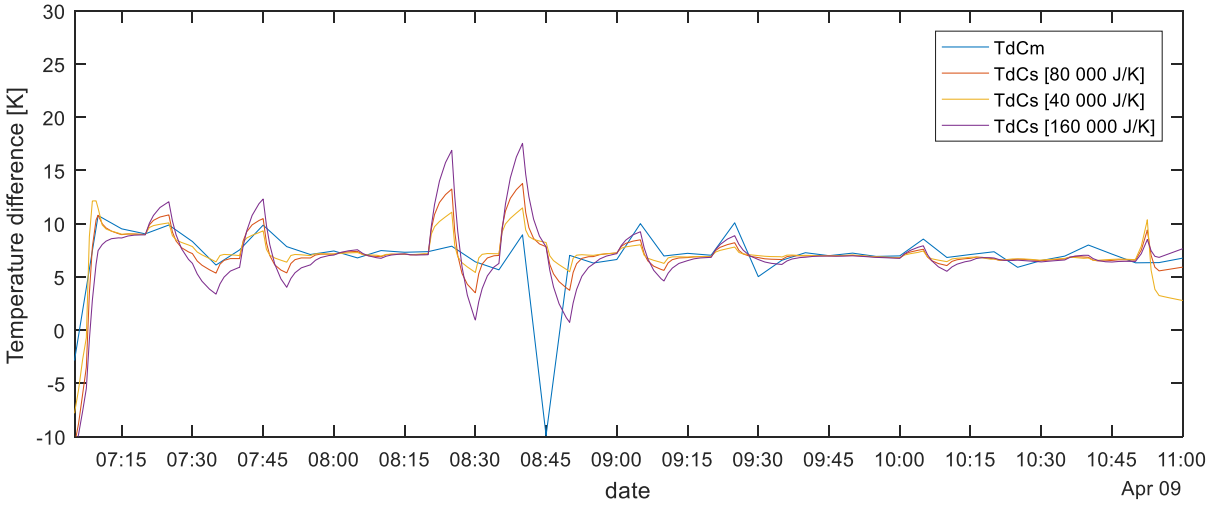

Figure 47 - Comparison DHW-HP simulation 2: Temperature difference condenser

7.2.2.2 Discussion

As it is discussed in Chapter 7.2.1.3, the thermal capacity for the condenser creates fluctuations in the temperature difference in the condenser. From Figure 47, it can be seen that the size of the fluctuations is differing when different thermal capacity in the hot loop is used. This therefore supports the explanation that is presented in Chapter 7.2.1.3.

From Figure 47, it also can be seen that the measured and simulated temperature difference for the condenser has fluctuations at the same places, but that the size of the fluctuations is varying. It is considered that the fluctuations could have been matched better if the sample time of the measurements had been shorter.

7.3 Storage tanks for space heating

This subchapter shows and discusses the results of the four simulations performed for the SH-ST.

7.3.1 Simulation 1

As it is given in Chapter 6.5.2, simulation 1 is a simulation of the original matrix of the SH-ST, and is a simulation performed in order to compare the simulated and real component.

7.3.1.1 Comparison

In Figure 48, *Ttm* stands for "measured temperature in the tank" and *TtsXX* stands for "simulated temperature in the tank at node XX". Node 10 and 1 is the nodes placed highest and lowest in the tank respectively.

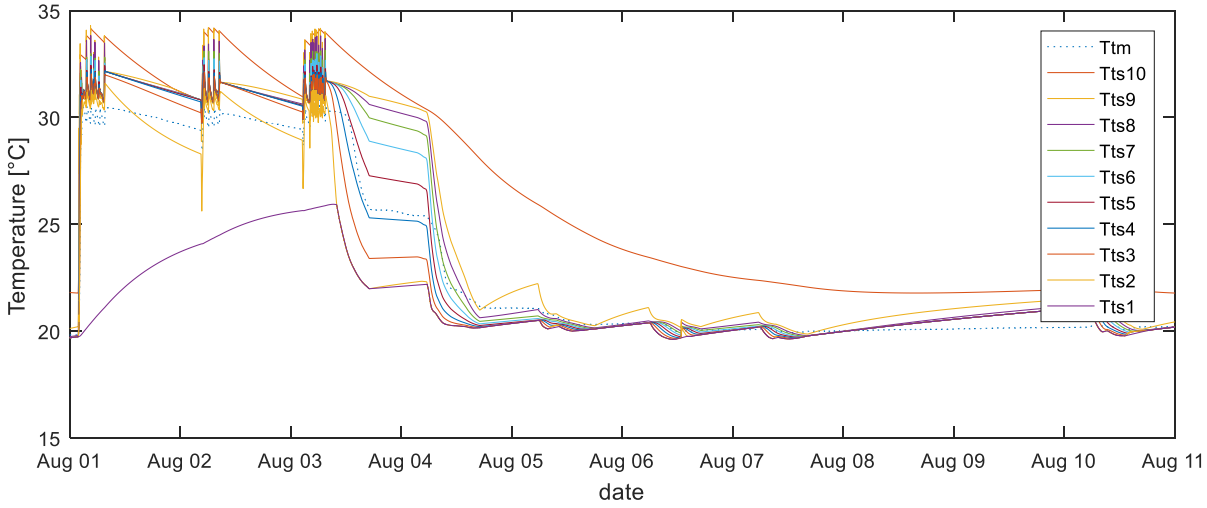

Figure 48 - Comparison SH-ST simulation 1: Tank temperature

In Figure 49, *ToHP* stands for "(measured) outlet temperature to the heat pump" and *ToHPs* stands for "simulated outlet temperature to the heat pump". As it can be seen, the measured and simulated temperatures are very similar the periods about 08.00 the first, second and third august, but are varying very much in other periods.

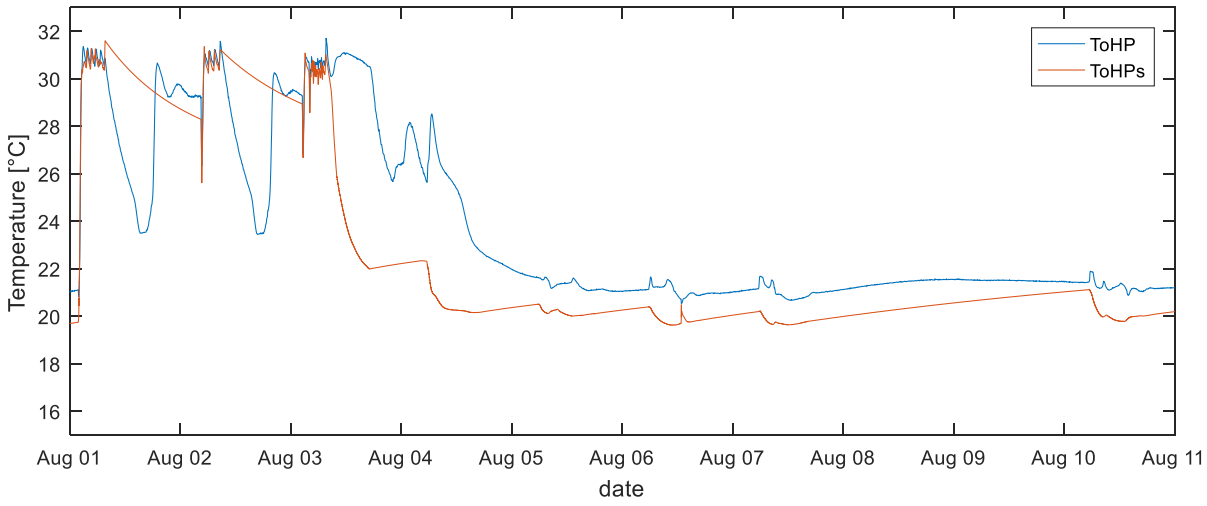

Figure 49 - Comparison SH-ST simulation 1: Temperature to heat pump

In Figure 50, *ToSH* stands for "(measured) outlet temperature to the space heating system" and *ToSHs* stands for "simulated outlet temperature to the space heating system". It is not as strong trend that it is for the previous figure, but the measured and simulated temperatures have a similar trend the periods about 08.00 the first, second and third august, but are varying very much in other periods.

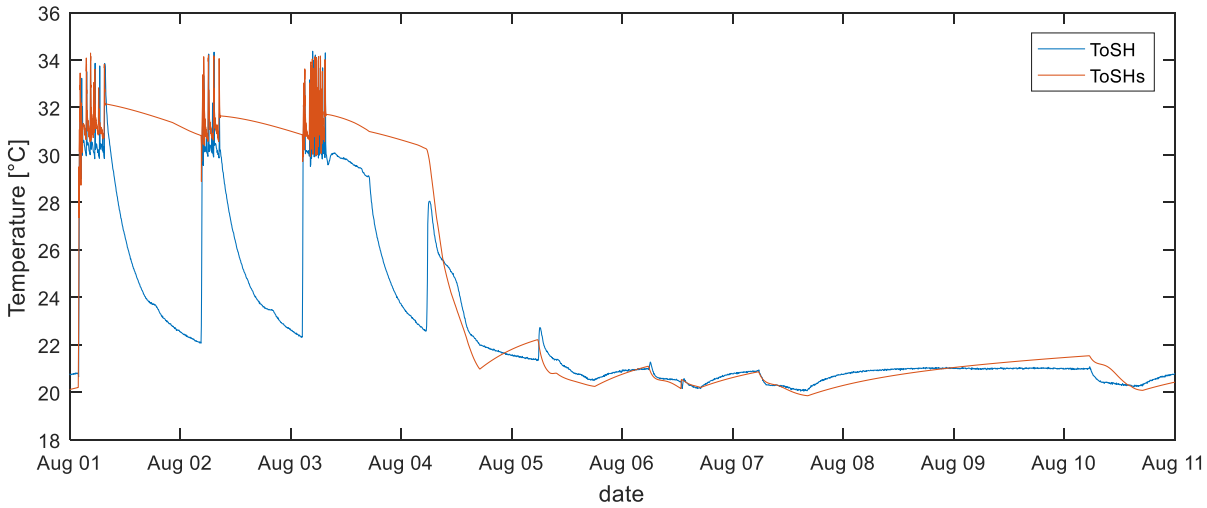

Figure 50 - Comparison SH-ST simulation 1: Temperature to SH

7.3.1.2 Outlet temperatures

As it can be seen from Figure 49, the measured and simulated temperature that is going to the heat pump is very similar in certain periods, while it can be seen from Figure 50, that the temperature going to the space and ventilation heating circuits is simulated a bit higher for the same periods. It can also be seen that the outlet temperatures outside of these periods is not so similar.

As it is given in Chapter 6.5.1, the mass flow for the charge circuit is found from the flow sensor of the heat pump, while the mass flow for the discharge circuit is calculated from energy meter OE002 to OE007. An explanation for the similar temperatures going to the heat pump and the higher temperatures going to the space and ventilation heating system might be that the heat loss in the discharge circuit for the simulation is lower than the real one. For this period, this is assumed a likely explanation since there is little heat demand (in the middle of the summer). This leads to a lower mass flow of water being circulated in the supply pipelines, which again leads to that the temperature of the water in the pipes has more time to cool down because of the heat loss to the ambient air.

The dissimilar temperatures outside of the periods previously discussed, can be explained with that the real temperature sensors is placed on the pipes outside of the storage tank, and that they therefore is cooled down by the ambient air.

7.3.1.3 High simulated temperature in the storage tank

As it can be seen from Figure 48, the temperature of the nodes is a bit high compared to the measurements from the temperature sensors in the storage tank. Ideally, the measured temperature should be between the simulated temperatures of *Tts5* and *Tts6* since they are the nodes in the centre of the storage tank. A possible explanation is that also this is caused by the lower heat loss for the discharge circuit of the simulated storage tank, which certainly would heighten the temperature of the lower nodes of the storage tank.

7.3.2 Simulation 2

As it is given in Chapter 6.5.2, simulation 2 is performed in order to investigate the blocks behaviour when changing the U-values of the storage tank. In this subchapter, the results of simulation 2 are compared to measured values.

7.3.2.1 Comparison

In Figure 51, *Ttm* stands for "measured temperature in the tank" and *TtsXX* stands for "simulated temperature in the tank at node XX". Node 10 and 1 is the nodes placed highest and lowest in the tank respectively. In this figure, the U-values of the storage tank are 1 W/m^{2}K.

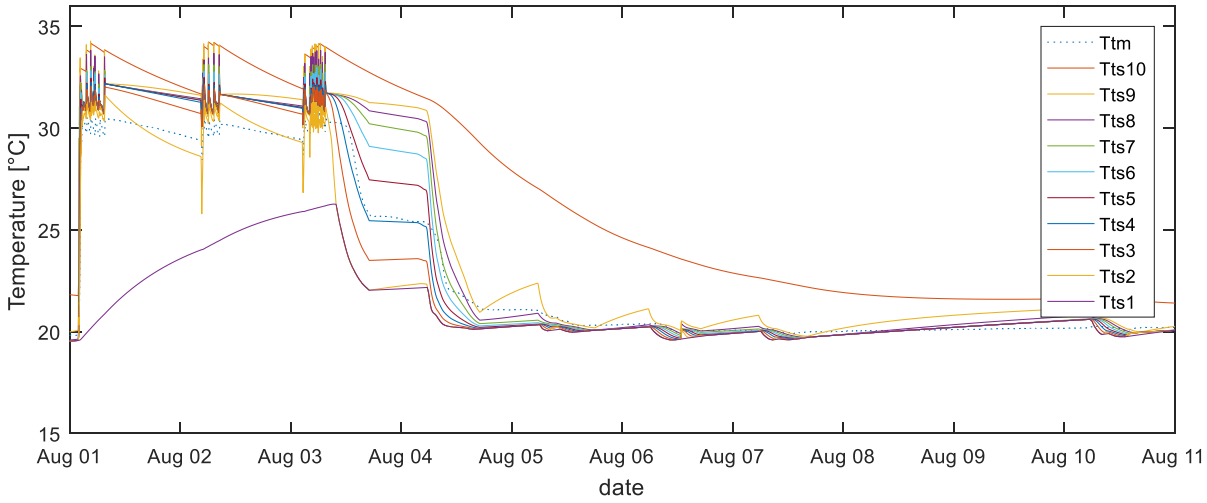

Figure 51 - Comparison SH-ST simulation 2: U=1 W/m^{2}K

In Figure 52, *Ttm* stands for "measured temperature in the tank" and *TtsXX* stands for "simulated temperature in the tank at node XX". Node 10 and 1 is the nodes placed highest and lowest in the tank respectively. In this figure, the U-values of the storage tank are 1.3 W/m^{2}K.

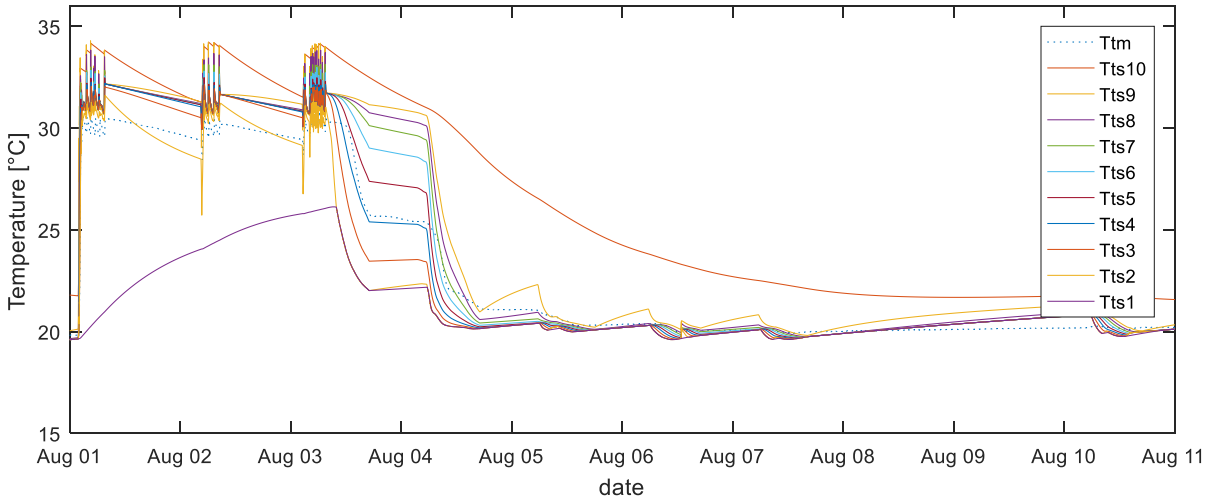

Figure 52 - Comparison SH-ST simulation 2: U=1.3 W/m^{2}K

In Figure 53, *Ttm* stands for "measured temperature in the tank" and *TtsXX* stands for "simulated temperature in the tank at node XX". Node 10 and 1 is the nodes placed highest and lowest in the tank respectively. In this figure, the U-values of the storage tank are 2.5 W/m^{2}K.

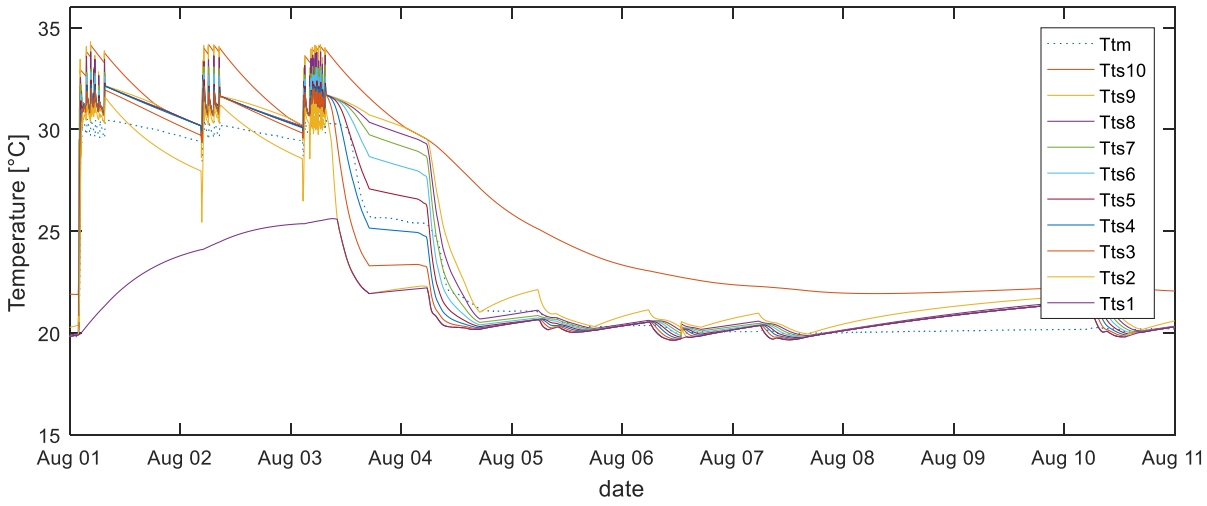

Figure 53 - Comparison SH-ST simulation 2: U=2.5 W/m^{2}K

In Figure 54, *ToHP* stands for "(measured) outlet temperature to the heat pump" and *ToHPs* stands for "simulated outlet temperature to the heat pump". *ToHPs* is simulated for different U- values, where the value for each simulation is given in the bracket.

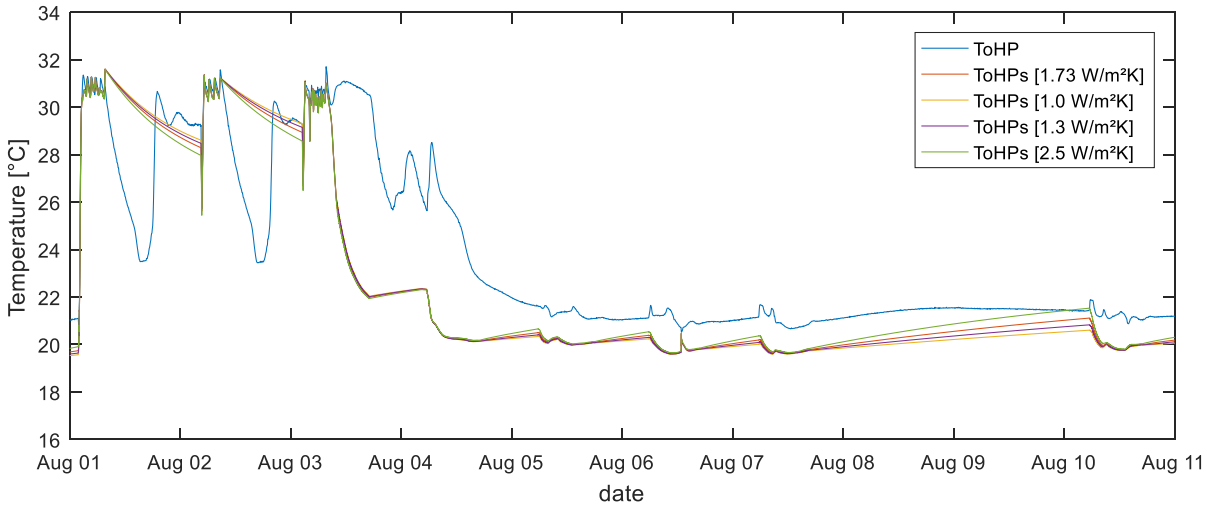

Figure 54 - Comparison SH-ST simulation 2: Temperature to heat pump

In Figure 55, *ToSH* stands for "(measured) outlet temperature to the space heating system" and *ToSHs* stands for "simulated outlet temperature to the space heating system". *ToSHs* is simulated for different U- values, where the value for each simulation is given in the bracket.

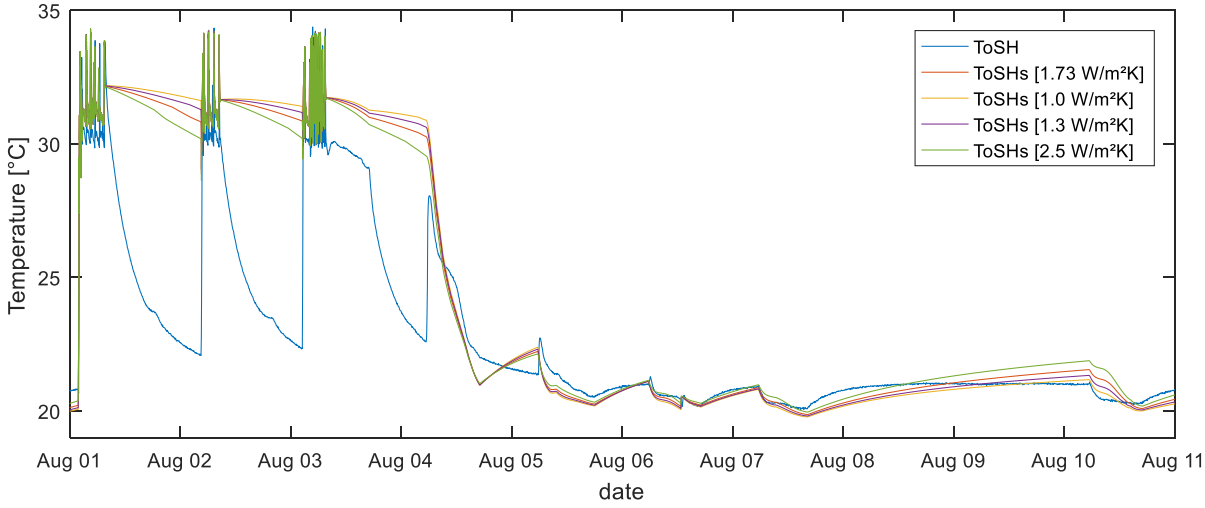

Figure 55 - Comparison SH-ST simulation 2: Temperature to SH

7.3.2.2 Discussion

It is possible to see that the temperature of node 10 is sinking more rapidly for higher U-values. Apart from this, it cannot be seen any marked improvement on the temperatures inside the tank or the ones on the outlets.

7.3.3 Simulation 3

As it is given in Chapter 6.5.2, simulation 3 is performed in order to investigate the blocks behaviour when changing the EVC of the storage tank. In this subchapter, the results of simulation 3 are compared to measured values.

7.3.3.1 Comparison

In Figure 56, *Ttm* stands for "measured temperature in the tank" and *TtsXX* stands for "simulated temperature in the tank at node XX". Node 10 and 1 is the nodes placed highest and lowest in the tank respectively. In this figure, the EVC value for the storage tank is 0.5 W/mK.

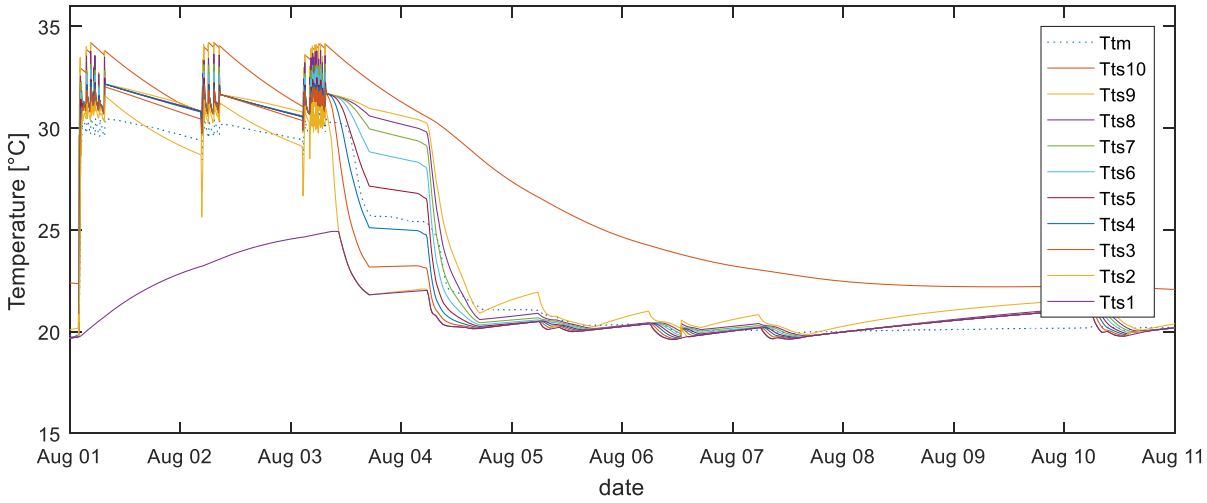

Figure 56 - Comparison SH-ST simulation 3: EVC=0.5W/mK

In Figure 57, *Ttm* stands for "measured temperature in the tank" and *TtsXX* stands for "simulated temperature in the tank at node XX". Node 10 and 1 is the nodes placed highest and lowest in the tank respectively. In this figure, the EVC value for the storage tank is 1 W/mK.

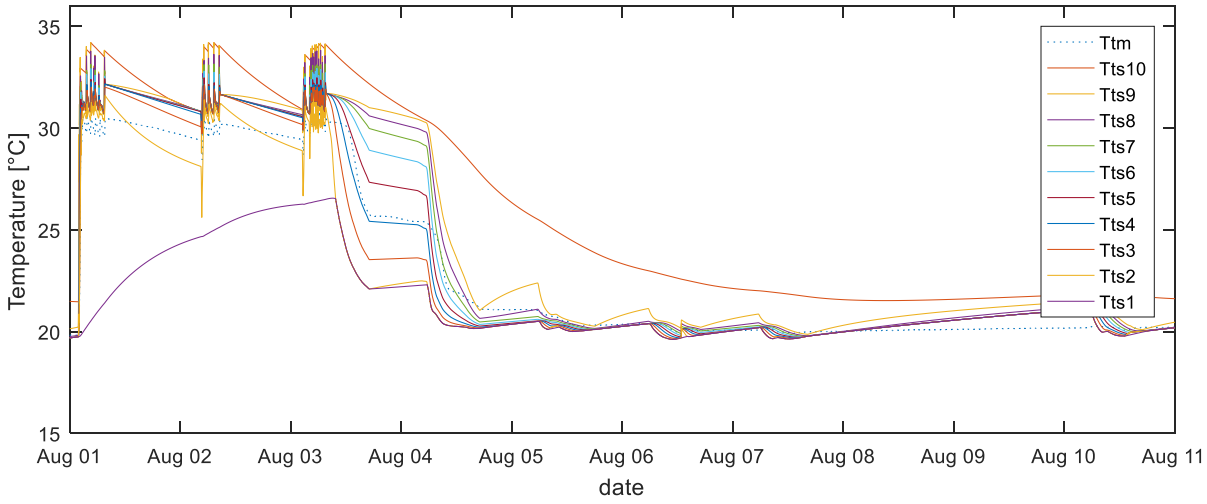

Figure 57 - Comparison SH-ST simulation 3: EVC=1.0W/mK

In Figure 58, *Ttm* stands for "measured temperature in the tank" and *TtsXX* stands for "simulated temperature in the tank at node XX". Node 10 and 1 is the nodes placed highest and lowest in the tank respectively. In this figure, the EVC value for the storage tank is 1.5 W/mK.

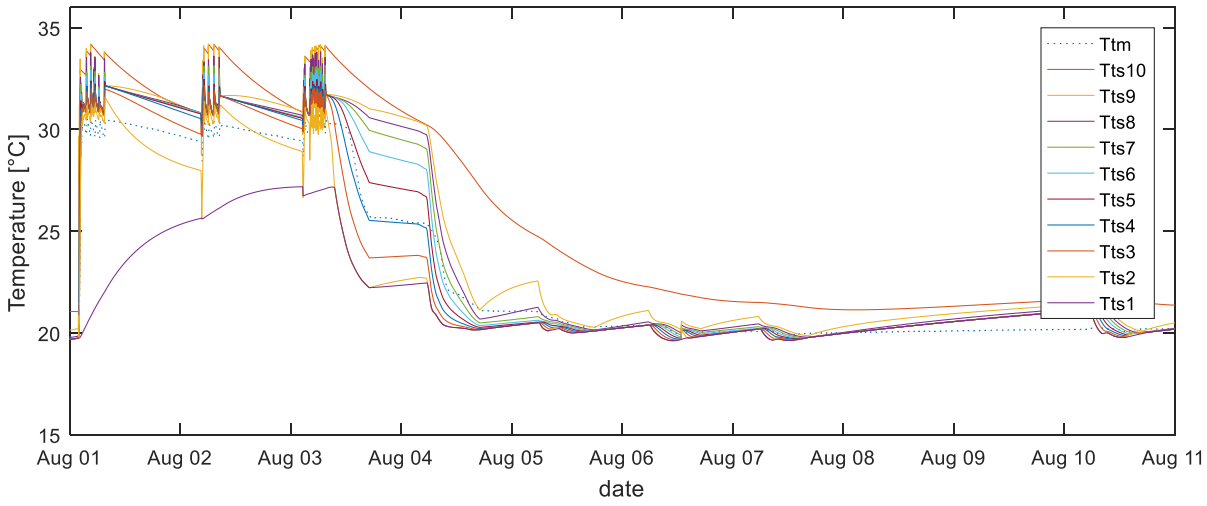

Figure 58 - Comparison SH-ST simulation 3: EVC=1.5W/mK

In Figure 59, *ToHP* stands for "(measured) outlet temperature to the heat pump" and *ToHPs* stands for "simulated outlet temperature to the heat pump". *ToHPs* is simulated for different EVC values, where the value for each simulation is given in the bracket.

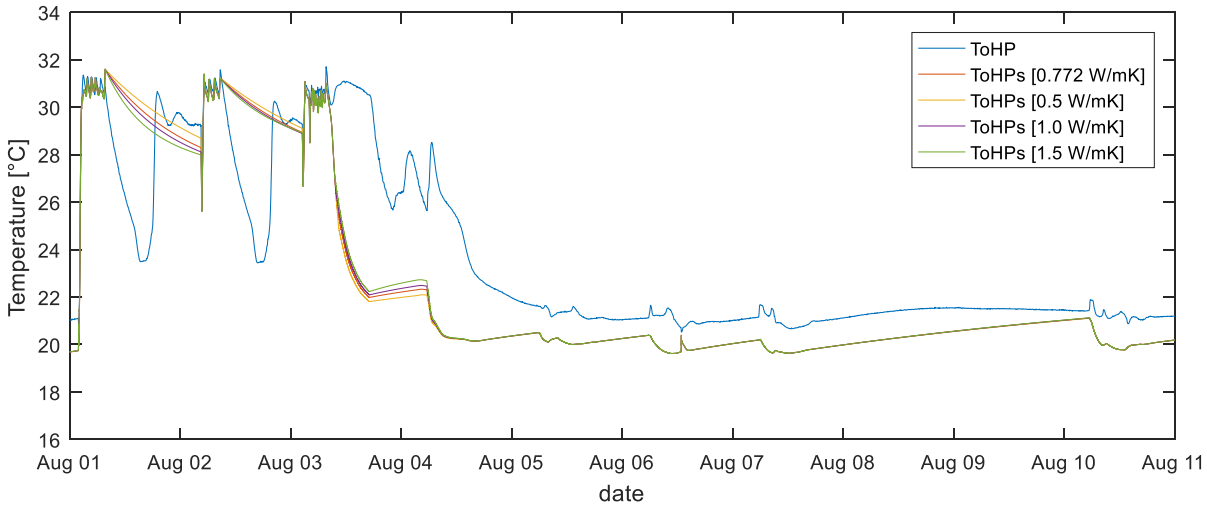

Figure 59 - Comparison SH-ST simulation 3: Temperature to heat pump

In Figure 60, *ToSH* stands for "(measured) outlet temperature to the space heating system" and *ToSHs* stands for "simulated outlet temperature to the space heating system". *ToSHs* is simulated for different EVC values, where the value for each simulation is given in the bracket.

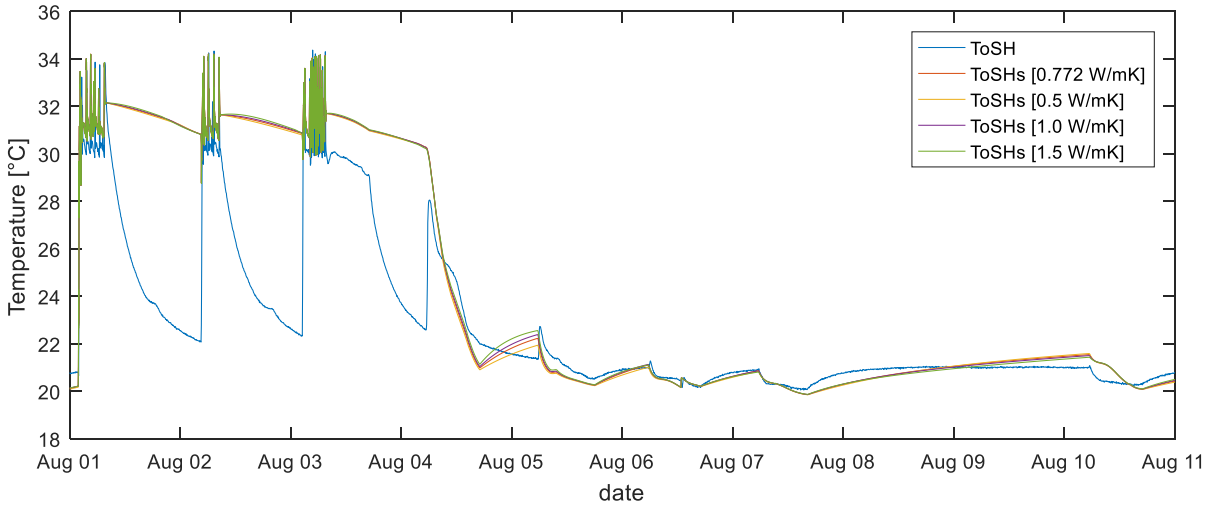

Figure 60 - Comparison SH-ST simulation 3: Temperature to SH

7.3.3.2 Discussion

It is possible to see that the temperature of node 10 is sinking more rapidly for higher EVC values. Apart from this, it cannot be seen any marked improvement on the temperatures inside the tank or the ones on the outlets.

7.3.4 Simulation 4

As it is given in Chapter 6.5.2, simulation 4 is performed in order to investigate the blocks behaviour when changing the number of nodes for the storage tank. In this subchapter, the results of simulation 4 are compared to measured values.

7.3.4.1 Comparison

In Figure 61, *Ttm* stands for "measured temperature in the tank" and *TtsXX* stands for "simulated temperature in the tank at node XX". In this simulation, 2 nodes are simulated for the storage tank. Node 2 and 1 is the nodes placed highest and lowest in the tank respectively.

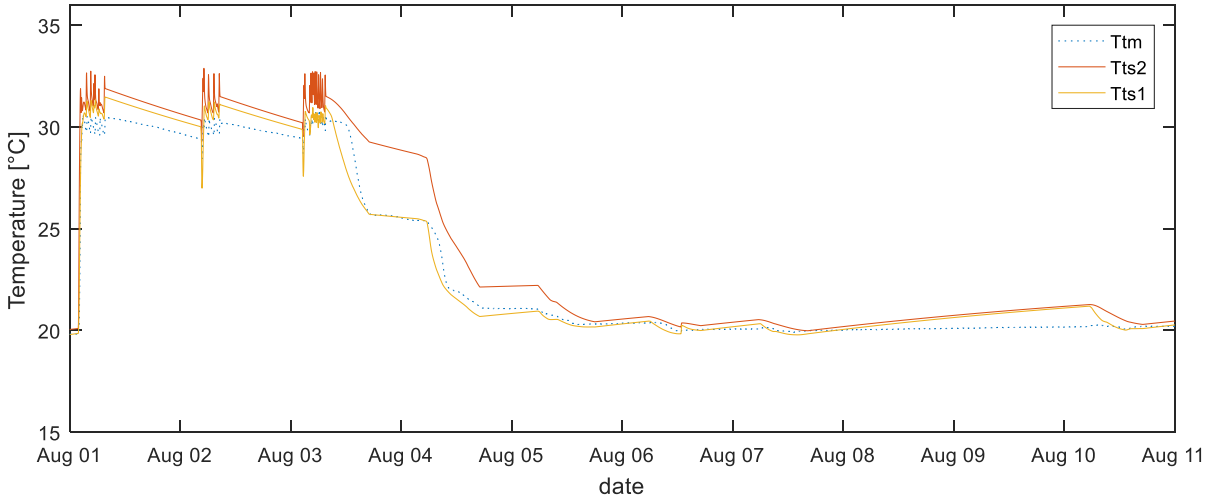

Figure 61 - Comparison SH-ST simulation 4: 2 nodes

In Figure 62, Ttm stands for "measured temperature in the tank" and TtsXX stands for "simulated temperature in the tank at node XX". In this simulation, 5 nodes are simulated for the storage tank. Node 5 and 1 is the nodes placed highest and lowest in the tank respectively.

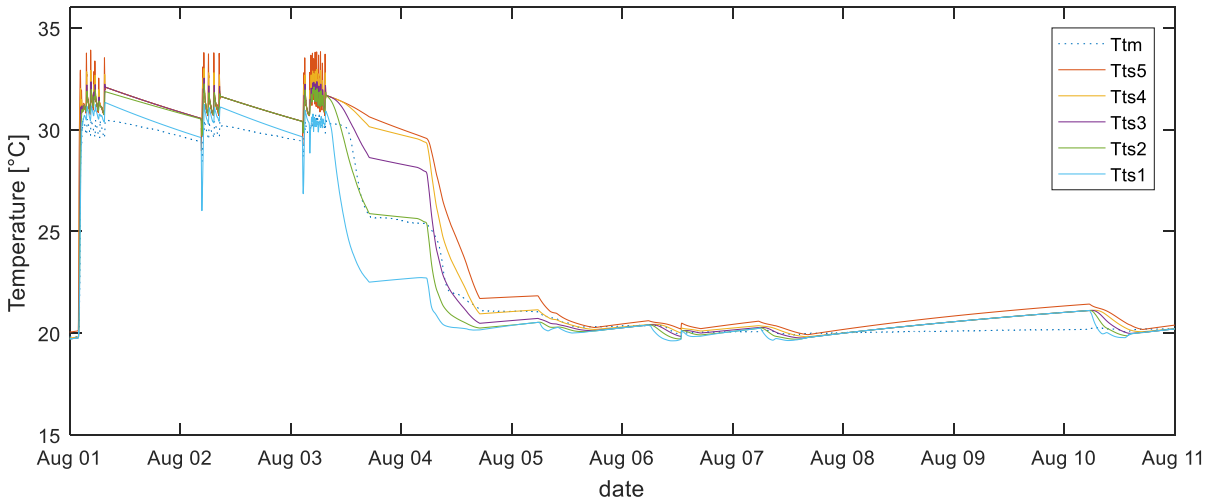

Figure 62 - Comparison SH-ST simulation 4: 5 nodes

In Figure 61, Ttm stands for “measured temperature in the tank” and TtsXX stands for “simulated temperature in the tank at node XX”. In this simulation, 15 nodes are simulated for the storage tank. Node 15 and 1 is the nodes placed highest and lowest in the tank respectively.

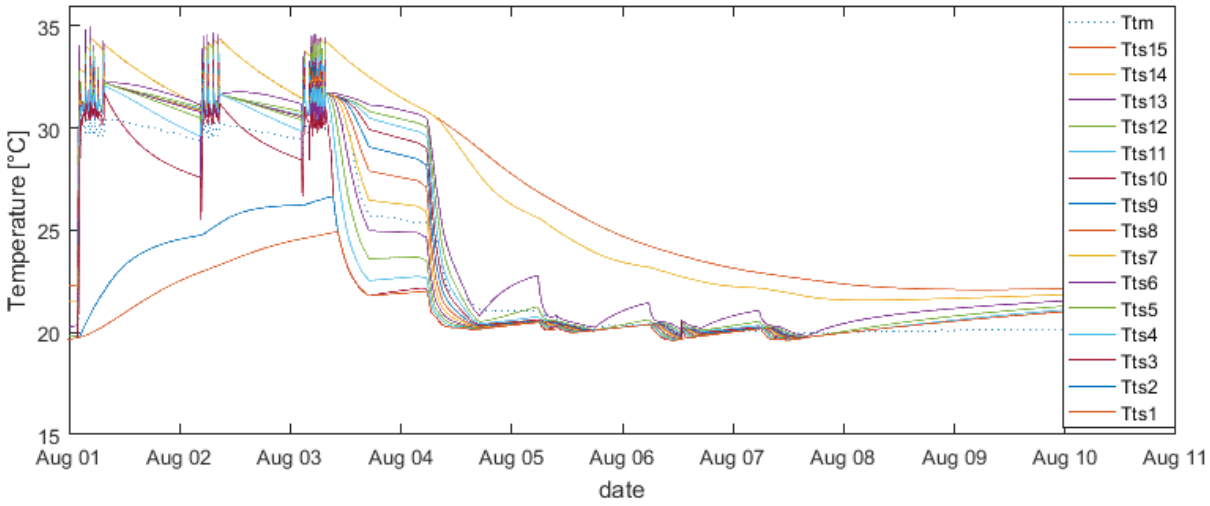

Figure 63 - Comparison SH-ST simulation 4: 15 nodes

In Figure 64, *ToHP* stands for “(measured) outlet temperature to the heat pump” and *ToHPs* stands for “simulated outlet temperature to the heat pump”. *ToHPs* is simulated with different amount of nodes, where the number of nodes for each simulation is given in the bracket.

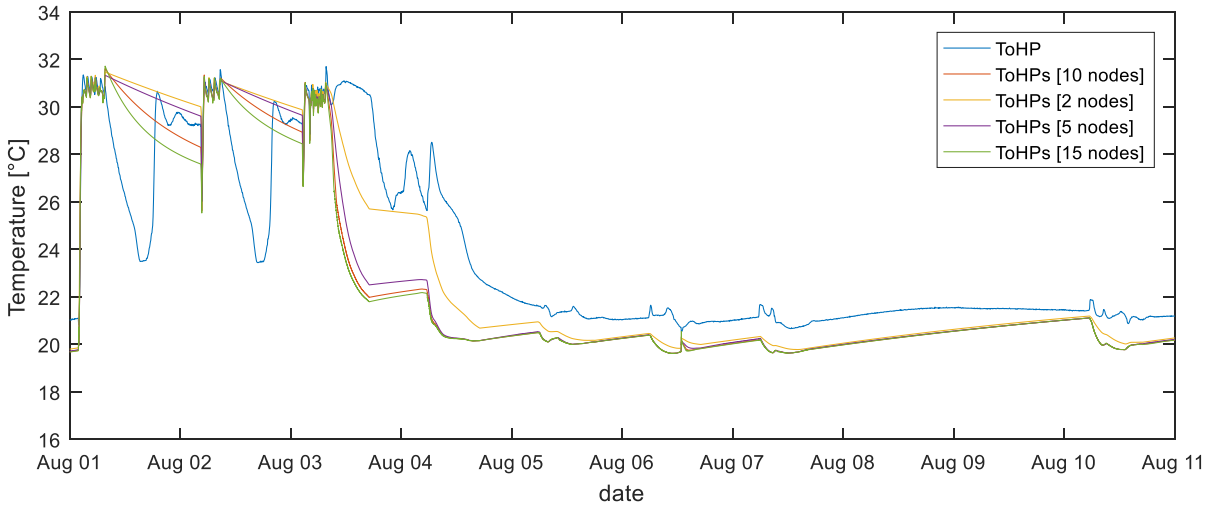

Figure 64 - Comparison SH-ST simulation 4: Temperature to heat pump

In Figure 60, *ToSH* stands for "(measured) outlet temperature to the space heating system" and *ToSHs* stands for "simulated outlet temperature to the space heating system". *ToSHs* is simulated with different amount of nodes, where the number of nodes for each simulation is given in the bracket.

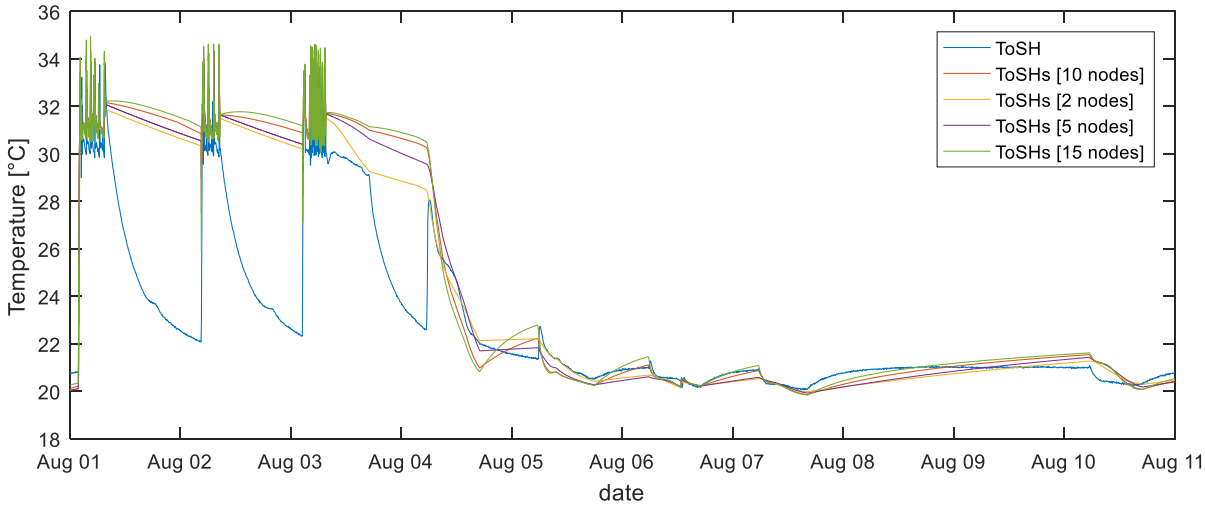

Figure 65 - Comparison SH-ST simulation 4: Temperature to SH

7.3.4.2 Discussion

It is hard to see any marked improvement or worsening of the results. However, this might be a useful conclusion since it shows that there is not much difference in the results if the block is simulated with 2 or 15 nodes. One thing is for certain, the simulation time is much higher if 15 nodes are used, compared to if 2 nodes are simulated.

7.4 Boreholes

This subchapter shows and discusses the results of the simulations performed for the ground source heat exchanger block.

7.4.1 Initialization period simulation 1

In Chapter 6.6.1, is given that the simulation 1 is divided into one initialization period and one comparison period. In this subchapter, the different simulations in the initialization period is showed and discussed.

7.4.1.1 Comparison

When performing the simulations for the initialization period, it became apparent that changing the thermal conductivity from the value in the original matrix to 1.9 W/mK gave the most authentic results for the GSHE block.

In Figure 66, *Toutm* stands for "measured outlet temperature for the borehole" and *Touts* stands for "simulated outlet temperature for the borehole". As it can be seen, the

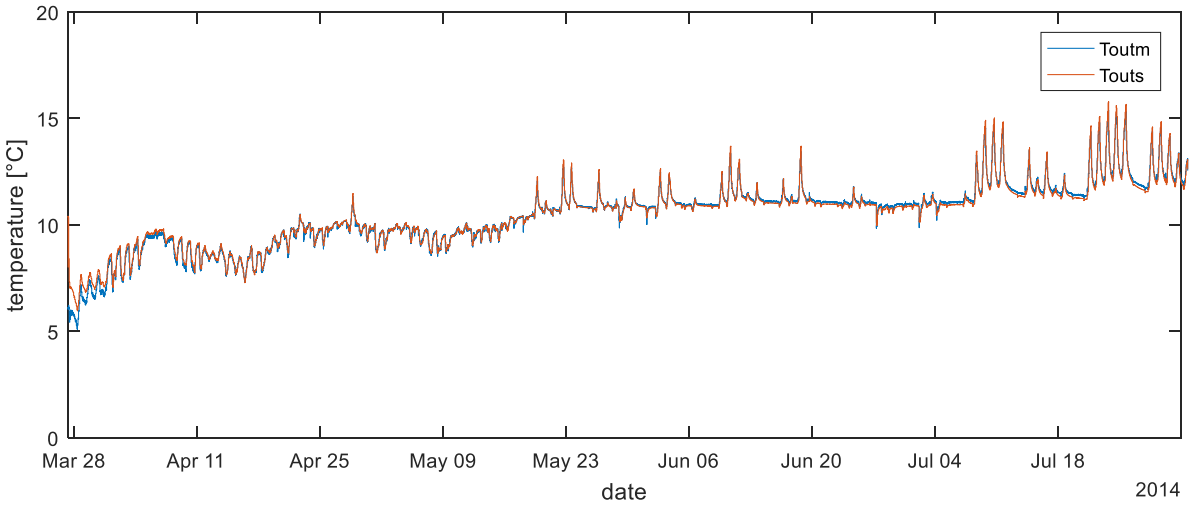

Figure 66 – Comparison GSHE initialization simulation 1: Outgoing temperature

In Figure 67, the measured supplied and ejected thermal power for the borehole is presented.

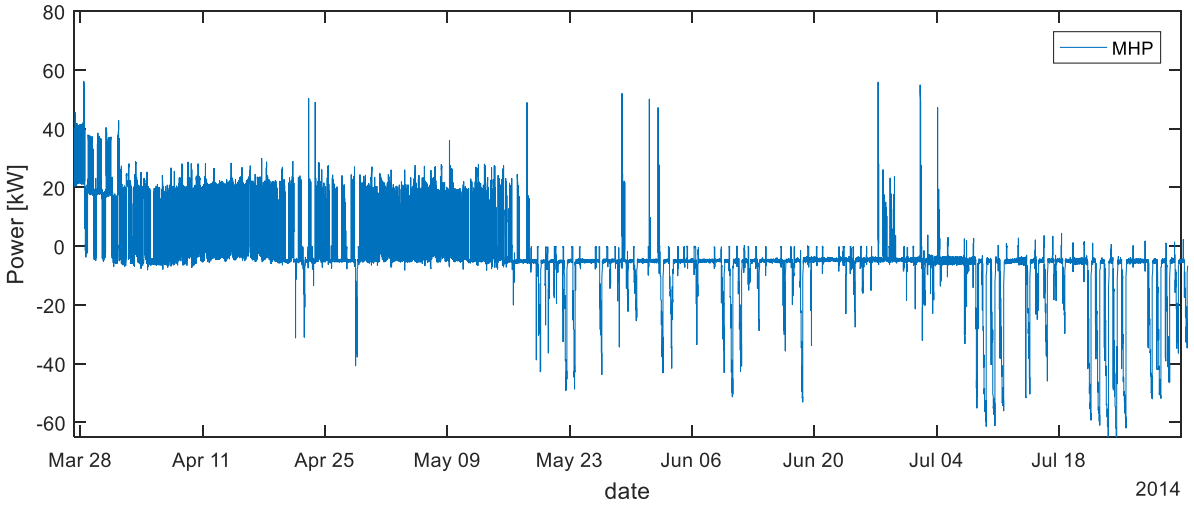

Figure 67 – Initialization: Measured supplied and ejected thermal power for the borehole

In Figure 68, the simulated supplied and ejected thermal power for the borehole is presented.

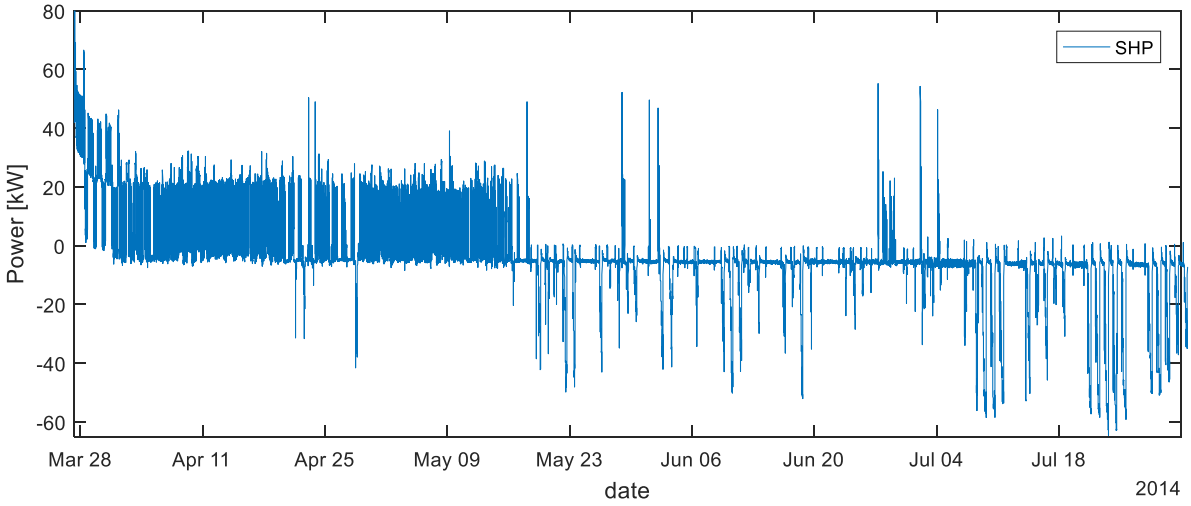

Figure 68 – Initialization: Simulated supplied and ejected thermal power for the GSHE

In Figure 69, the difference between the simulated and the measured supplied and ejected thermal power is presented.

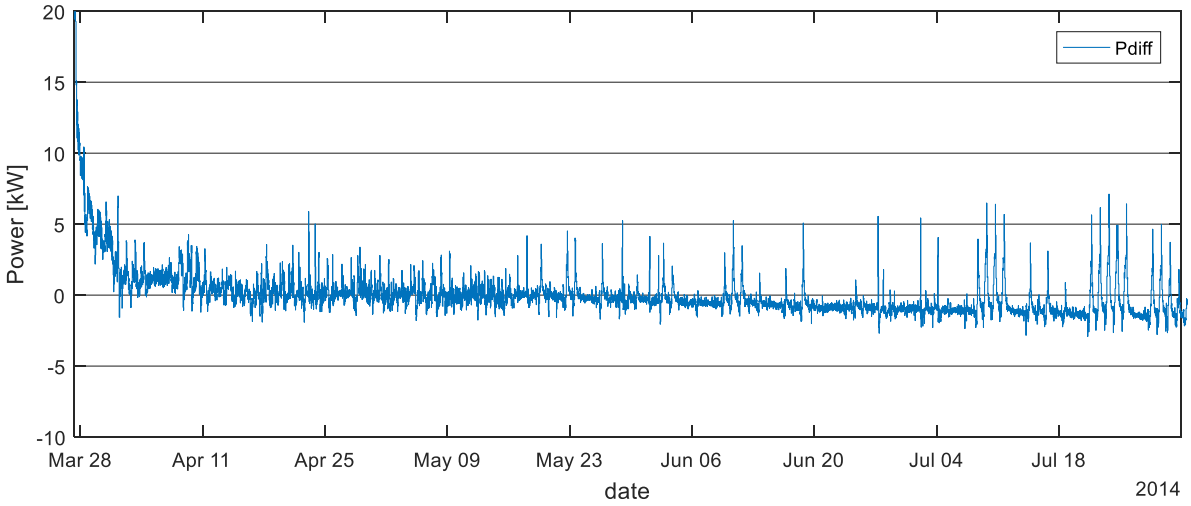

Figure 69 – Initialization: Difference between simulated and measured thermal power

In Figure 70, the measured mass flow for the initialization period is presented.

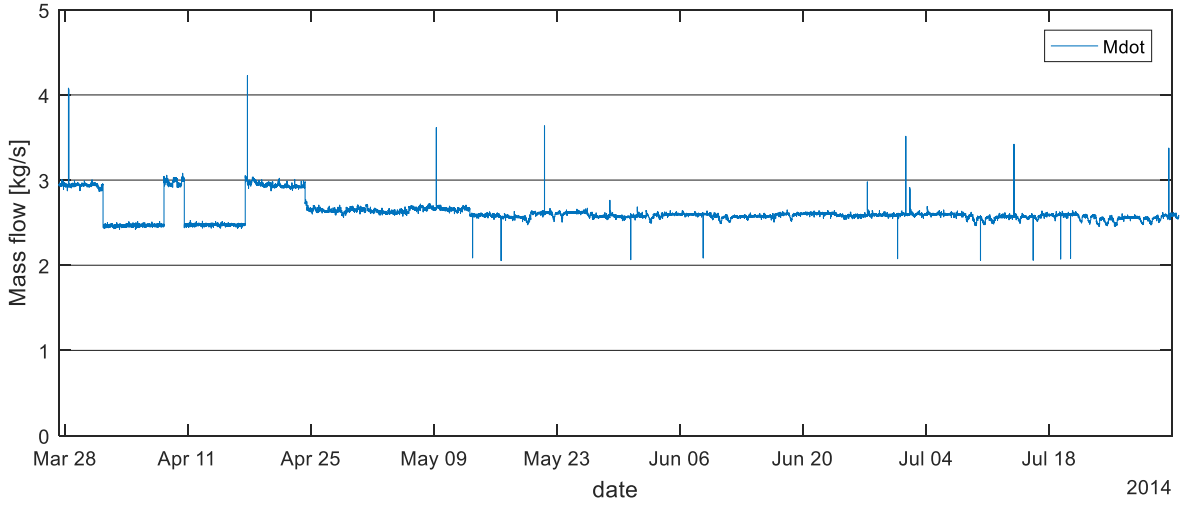

Figure 70 – Initialization: Measured mass flow in the borehole

7.4.1.2 Discussion

From Figure 66 and Figure 69, that the simulated and measured temperature and supplied and ejected thermal power is very similar. The differences in both temperature and supplied and ejected thermal power are however getting larger at the end of the initialization period.

As it is given in Chapter 3.2.5, a flow of ground water at the depth 170-190 meters was found in the thermal response test of borehole 10. A flow of ground water might heat up parts of the collector tube, which could explain the higher temperature and the supplied and ejected thermal power delivered from the real borehole compared to the simulated.

7.4.2 Comparison period

As mentioned in Chapter 7.4.1, simulation 1 is divided into one initialization period and one comparison period. In this subchapter, the results from the simulation performed with the input parameters established in the initialization period are presented and discussed.

7.4.2.1 Comparison period

In Figure 71, the measured and simulated outlet temperature is compared. *Toutm* is the measured value, and *Touts* is the simulated value.

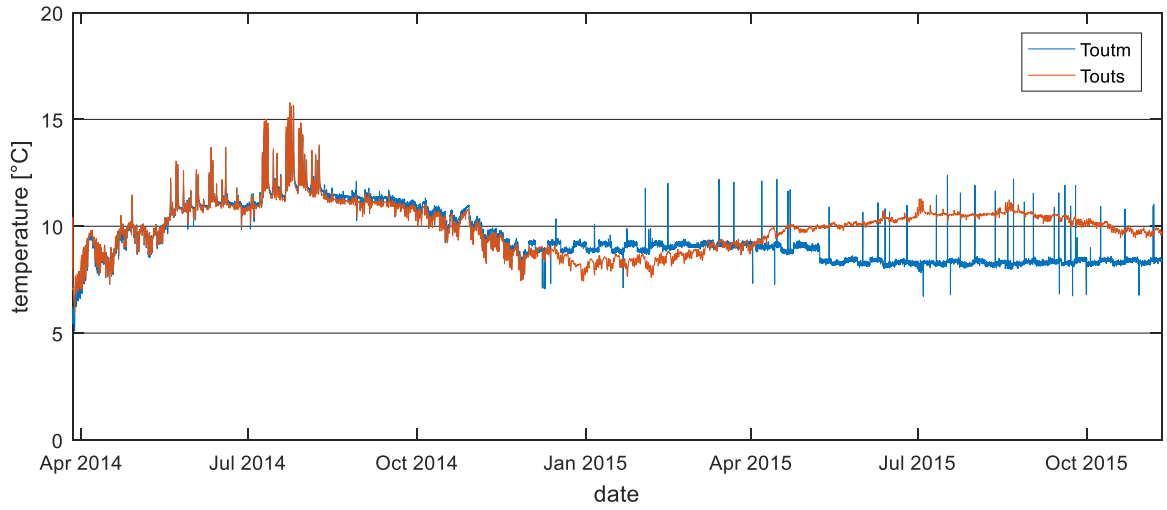

Figure 71 – Comparison GSHE simulation 1: Outgoing temperature

In Figure 72, the measured supplied and ejected thermal power for the borehole is illustrated.

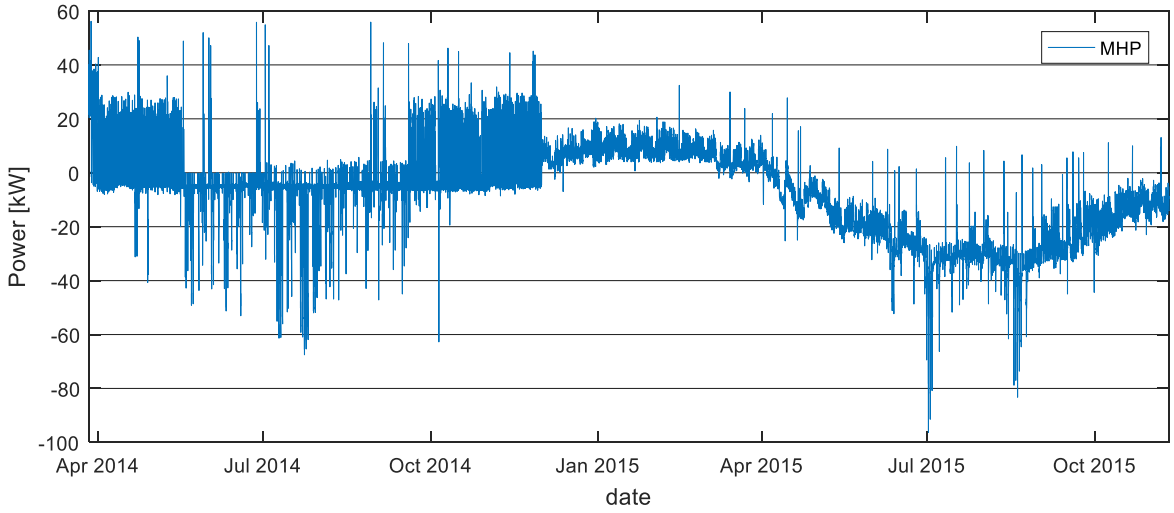

Figure 72 – Measured supplied and ejected thermal power for the borehole

In Figure 73, the simulated supplied and ejected thermal power for the GSHE is illustrated.

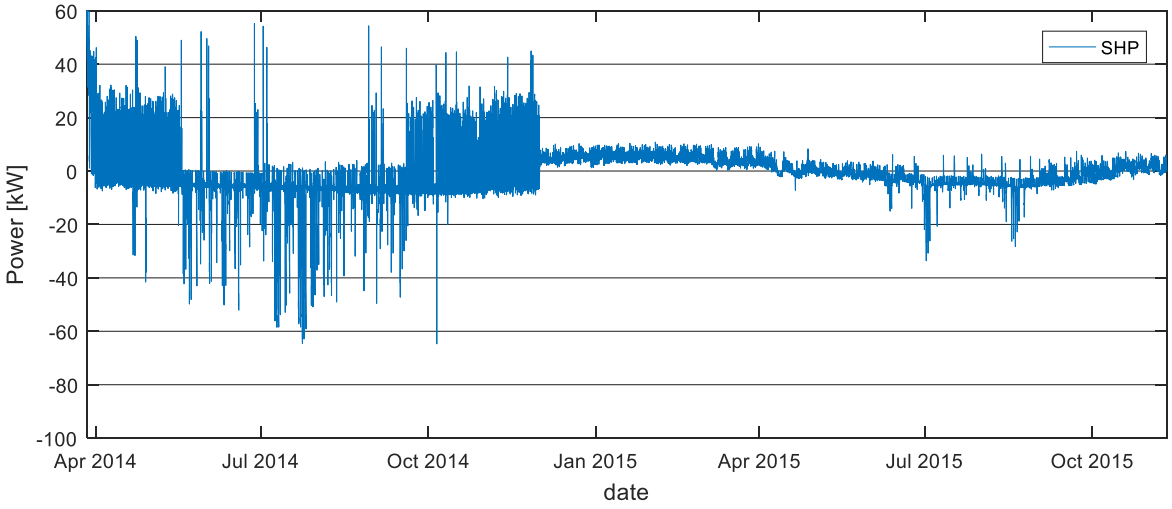

Figure 73 – Simulated supplied and ejected thermal power for the GSHE

In Figure 74, the difference between the simulated and the measured supplied and ejected thermal power for the GSHE is illustrated.

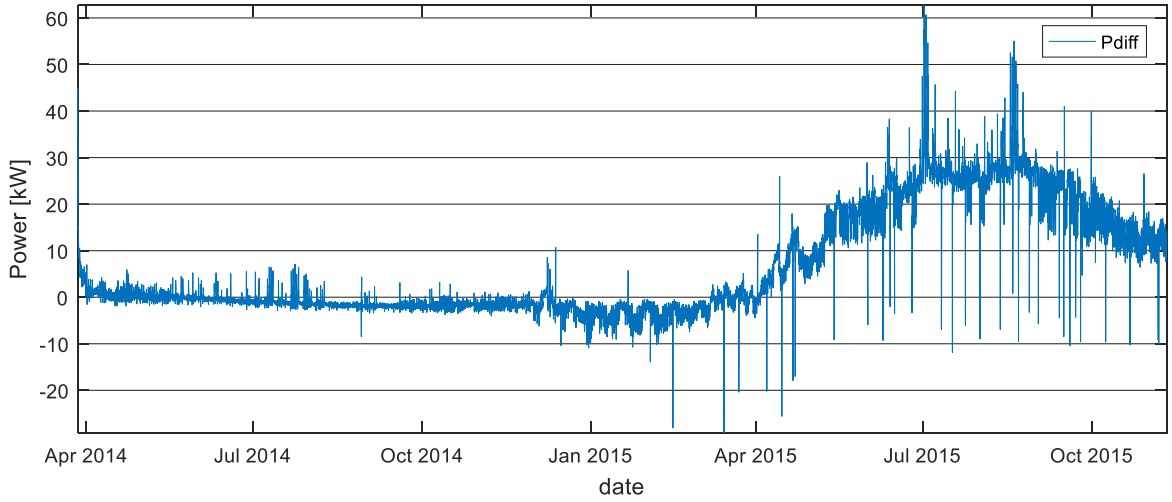

Figure 74 - Difference between simulated and measured thermal power

In Figure 75, the measured mass flow for the borehole is visualised.

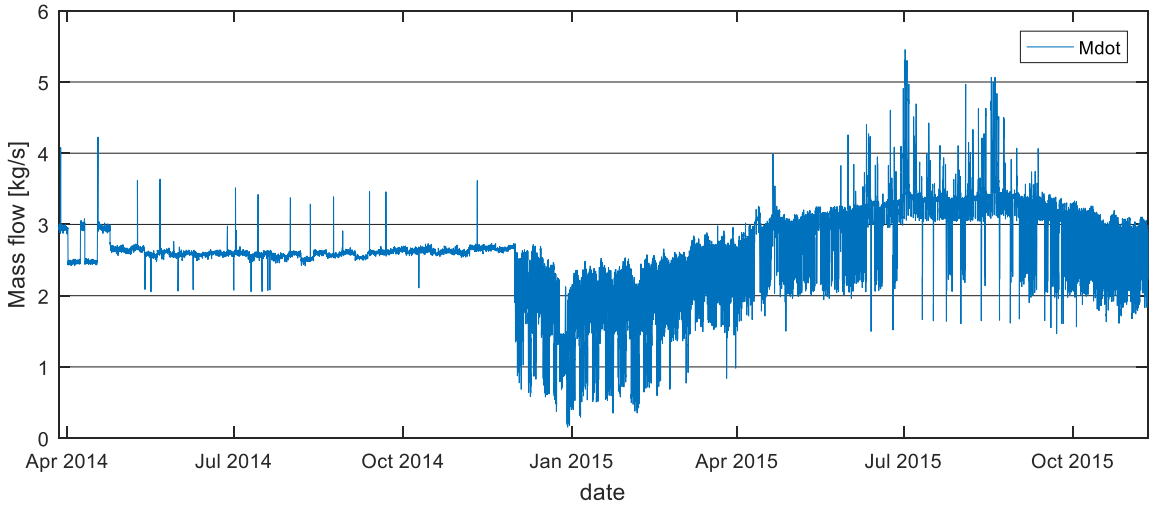

Figure 75 - Measured mass flow in the borehole

7.4.2.2 Changing similarities with changing mass flow

As can be seen, the simulated and measured outlet temperature from the borehole is almost identical when the design mass flow is set to the same constant mass flow as it is in the borehole. It can also be seen that the similarities between the simulated and measured mass flow becomes almost non-existent when the mass flow in the borehole is changed from constant mass flow to varying mass flow. Based on what is written in Chapter 4.4.3, this is considered an expected outcome since the measured and simulated component has different working conditions. The conclusion is therefore that the simulated component performs well for the period up to December 2014.

7.4.3 Simulation 2

As it is given in Chapter 6.6.1, simulation 2 is a long-term simulation performed on order to investigate the temperature development in the ground 0.84 m from GSHE block.

7.4.3.1 Results

Figure 76 to Figure 80 gives the temperatures for the 5 axial nodes of the borehole. Temperature 1 is the highest node and temperature 5 is the lowest one.

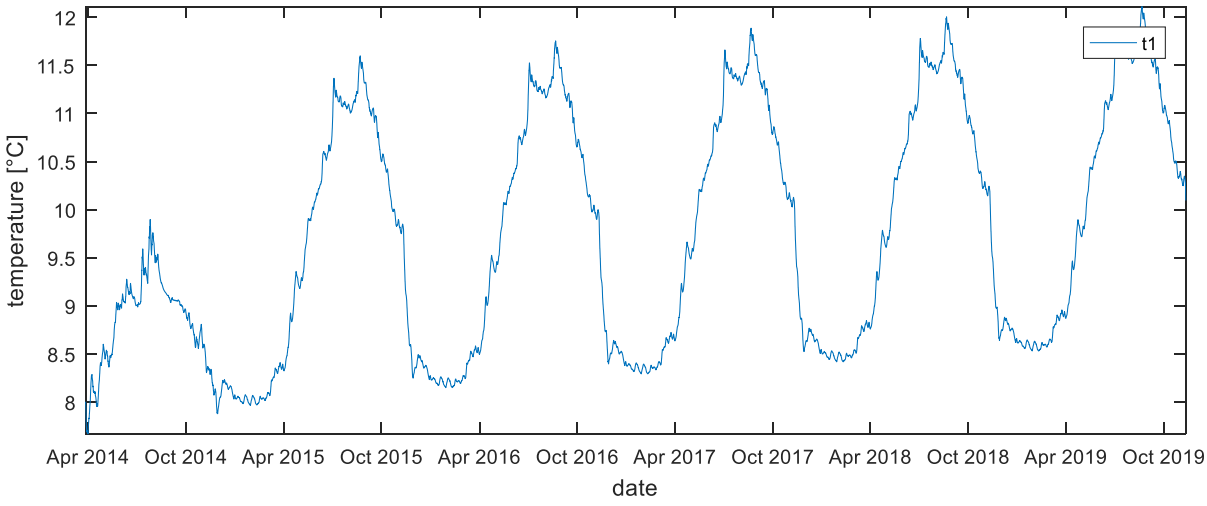

Figure 76 – Boreholes simulation 2: Temperature in the ground nr.1

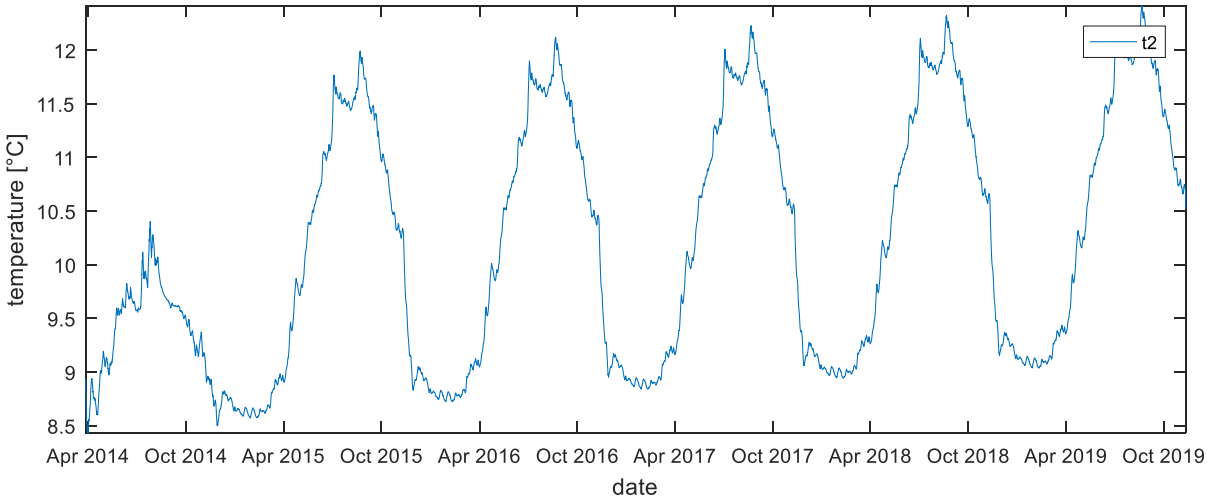

Figure 77 – Boreholes simulation 2: Temperature in the ground nr.2

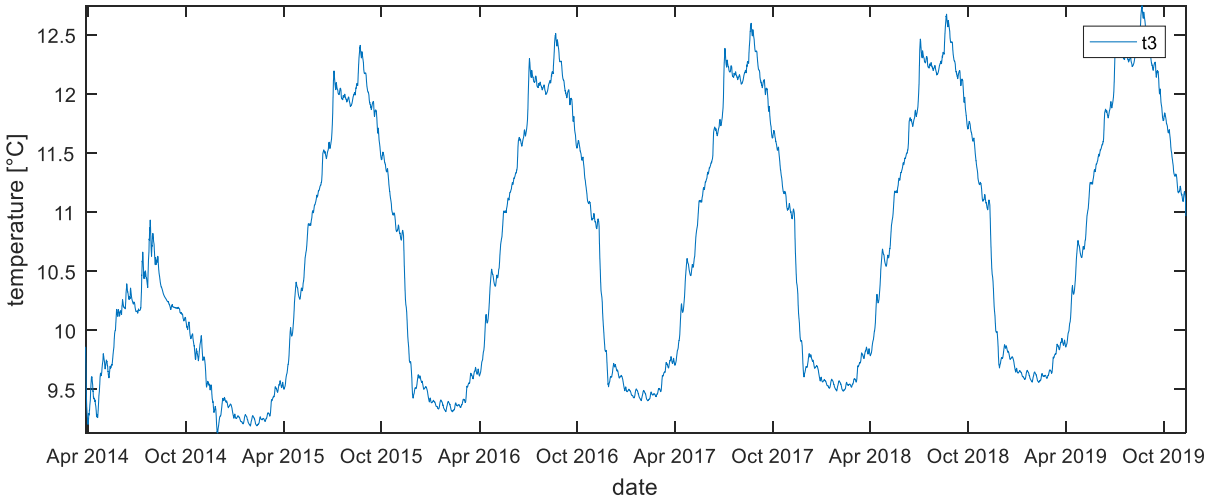

Figure 78 – Boreholes simulation 2: Temperature in the ground nr.3

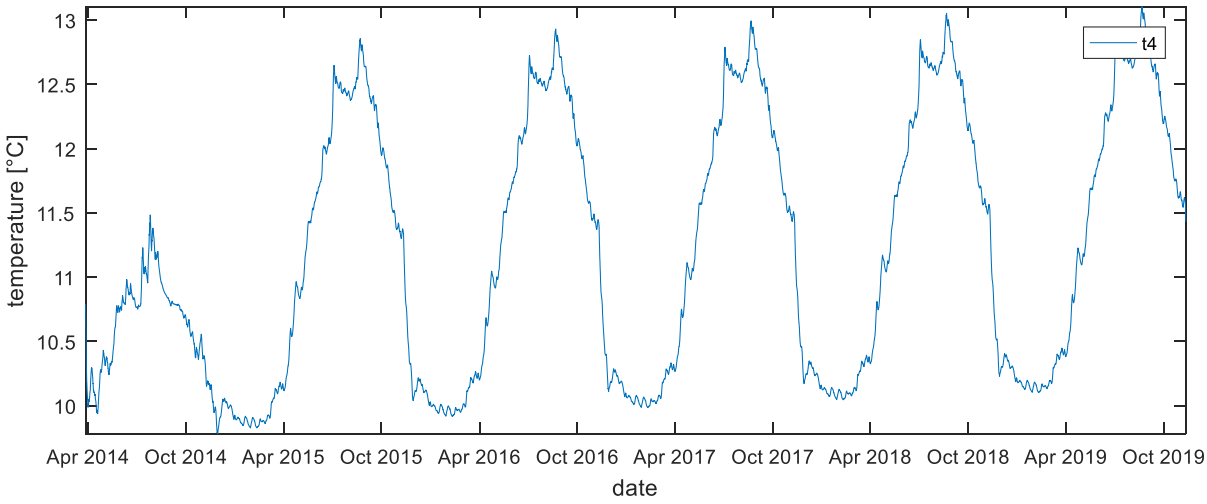

Figure 79 – Boreholes simulation 2: Temperature in the ground nr.4

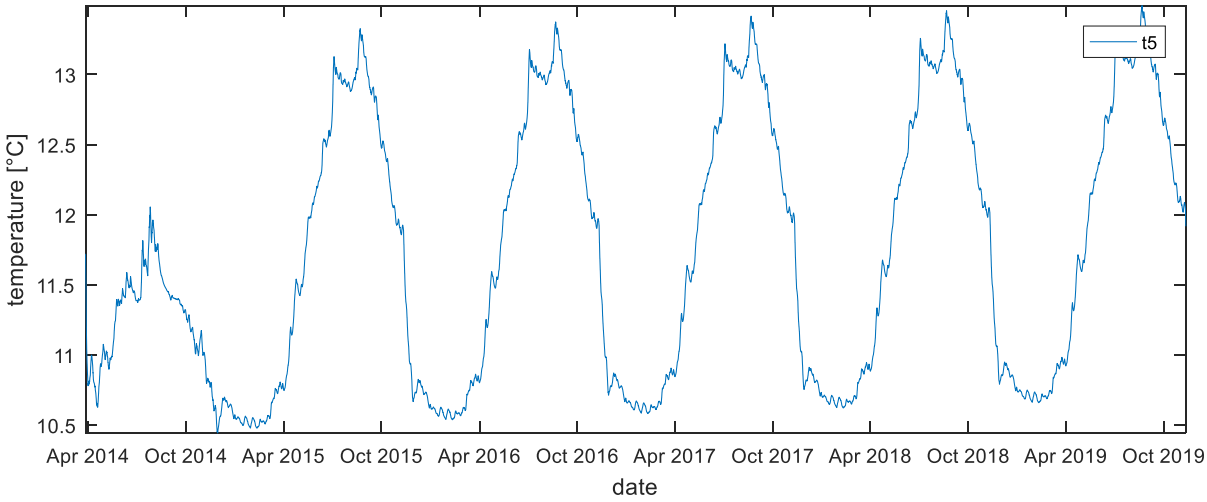

Figure 80 – Boreholes simulation 2: Temperature in the ground nr.5

In Figure 81, the simulated accumulated supplied and ejected thermal energy in the ground is presented. In this figure, a positive trend means that the heat is stored in the borehole and a negative one means that heat is taken from the borehole. In other words, if the trend is positive, the borehole is used for cooling, and if the trend is negative, the borehole is used for heating.

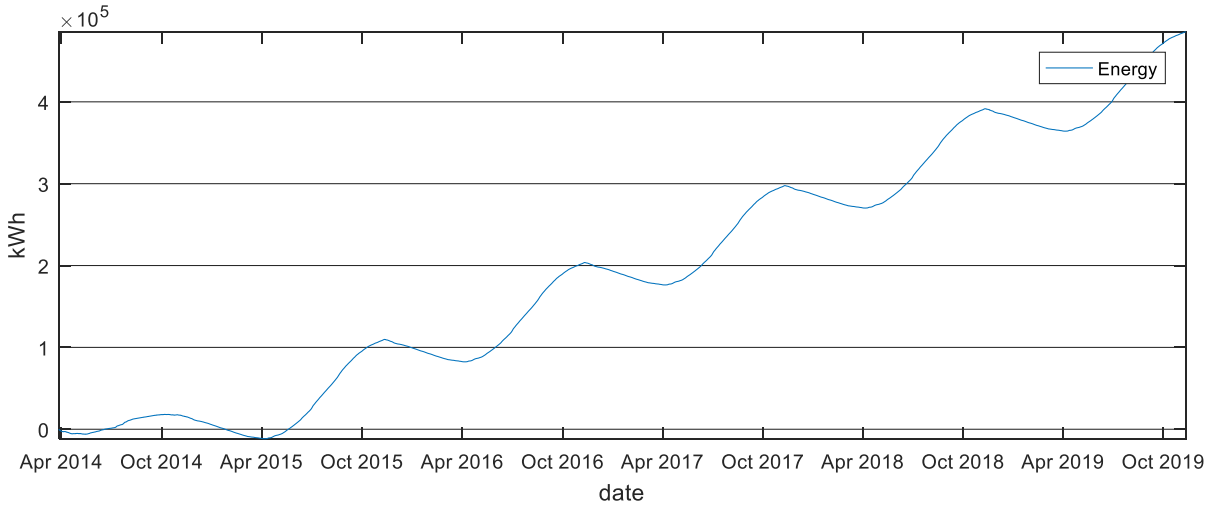

Figure 81 – Boreholes simulation 2: Accumulated thermal energy in the ground

7.4.3.2 Discussion

As it can be seen from Figure 76 to Figure 80, the temperature in the ground 1 meter from the borehole is going up with about 0.7℃ from the peak in October 2015 to the peak in October 2019. According to Figure 81, this is logical since the accumulated thermal energy in the boreholes is going up, which means that heat is being stored in the borehole.

From Figure 81, it can be seen that the total heat stored in the boreholes is about 500 000 kWh, which makes an annual average thermal energy stored in the borehole of 40.68 kWh/m. It is hard to find reference numbers concerning recommended annual thermal energy stored in the borehole. However, if one compares the average thermal energy stored in the borehole to the recommended thermal energy ejected from the borehole, which is 70-100 kWh/m (Borgnes and Ramstad, 2015), the value is considered low.

From this, it can be concluded that the temperature in the ground for the ground source heat exchanger is evolving based on the accumulated supplied and ejected thermal energy to the borehole.

7.5 Space heating system

This subchapter shows and discusses the results of the simulations performed for the space heating system.

7.5.1 Comparison

In Figure 82, the measured temperature from the storage tank to the space and ventilation circuits is illustrated.

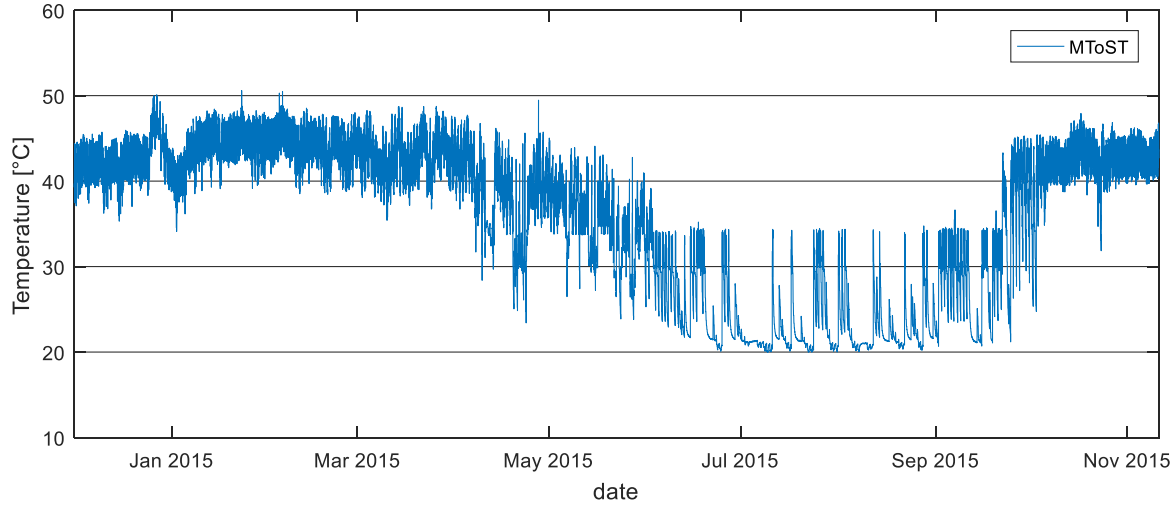

Figure 82 – Comparison SH-system simulation 1: Measured temp. to SH

Figure 83 shows the simulated temperature from the storage tank to the space and ventilation circuits.

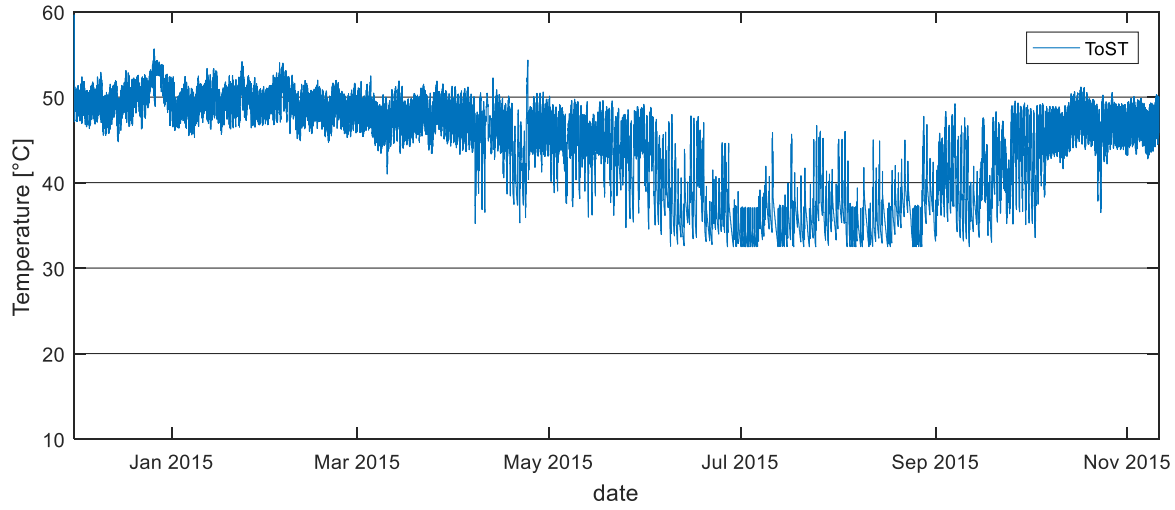

Figure 83 - Comparison SH-system simulation 1: Simulated temp. to SH

In Figure 84, the simulated set point for the heat pump is given.

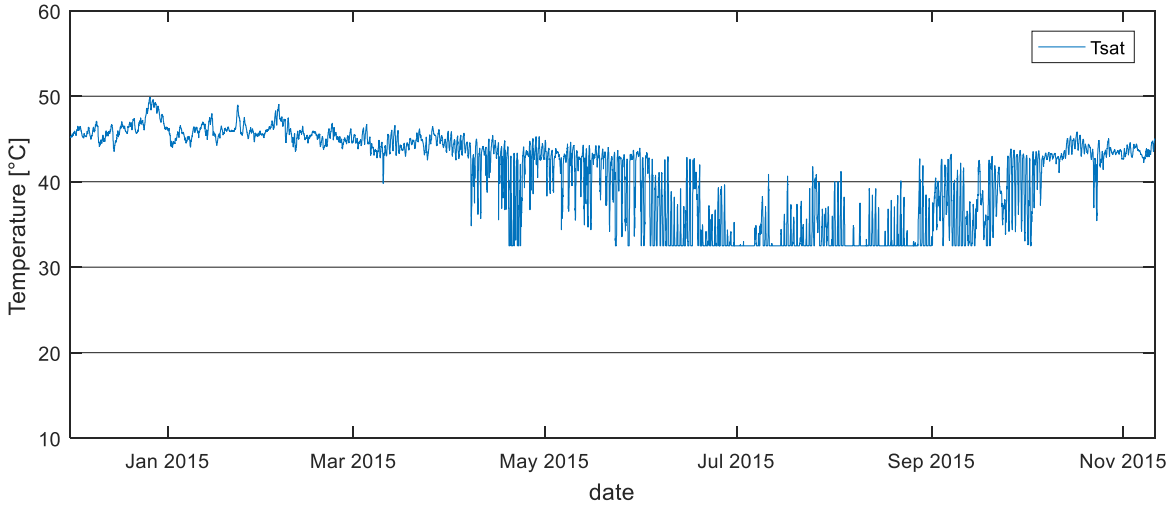

Figure 84 – Comparison SH-system simulation 1: Simulated set-temp

In Figure 85, the measured and simulated energy consumption of the heat pump is illustrated.

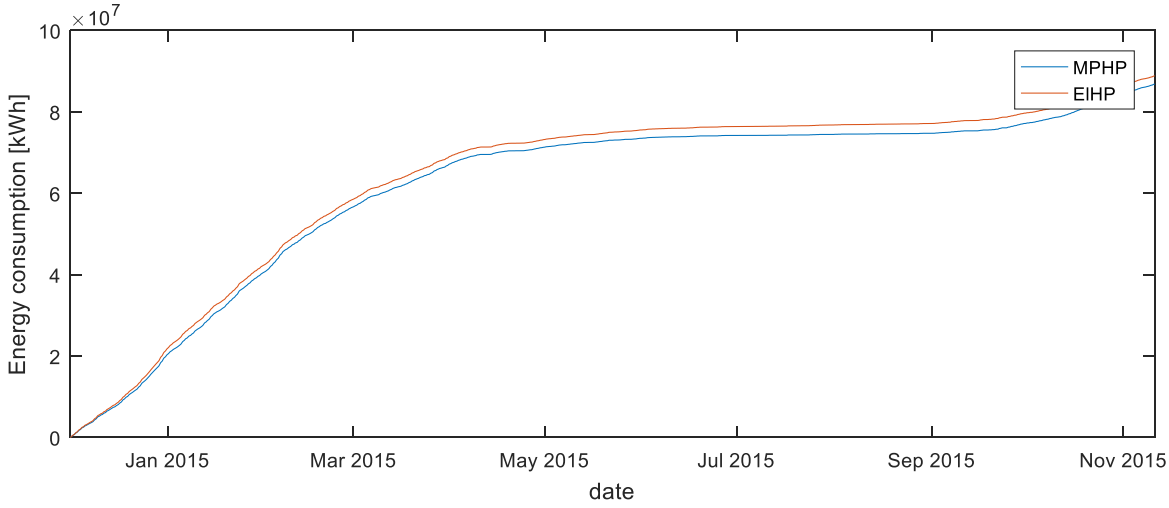

Figure 85 Comparison SH-system simulation 1: Energy consumption heat pump

7.5.2 Discussion

7.5.2.1 Higher simulated outlet temperature

As it can be seen from Figure 82 and Figure 83, the simulated outlet temperature from the storage tank to the space and ventilation heating system is higher than the measured value. If Figure 82 and Figure 83 are compared to Figure 84, it can seem like the measured outlet temperatures from the storage tank in most cases are lower than the set point temperature, while the simulated outlet temperature is above. An explanation to this might be that the control system of the heat pump has to long fixed operation time, which heats the water more than necessary.

7.5.2.2 Energy consumption for the system

The compared energy consumption of the two systems is very similar, where the simulated energy consumption of the system for the comparison period is 88 852 376 kWh and the measured energy consumption is 86 846 286 kWh. The simulated energy consumption is hence 2.3 % higher than the simulated, which is considered a very low deviation. This might be explained with the higher simulated outlet temperature of the storage tank to the space and ventilation heating system is higher for the simulated system, which is mentioned in the previous subchapter.

Another explanation might however be that the performance factor for the simulated heat pump is not the same as for the real component. From Chapter 7.1.4.1 it can seem like the relationship between the simulated and measured power consumption of the heat pump in part load is higher than the relationship of the heating capacity (illustrated with the temperature difference over the condenser). Since the heat pump, in the simulation of the space heating system, mostly is run in part load capacity, this can be an explanation of the higher energy use of the simulated system.

7.6 Discussion

In this subchapter, it is, based on what is presented up to this point of the chapter, discusses whether the simulation components works and what measures that should be taken in order to calibrate the simulations properly.

7.6.1 Heat pump

7.6.1.1 Nominal operation

Two single component simulations are performed for this block: the simulation of the SH-HP and the simulation of the DHW-HP. For the simulation of the SH-HP, the power consumption and the heating capacity is simulated higher than the measured values, but it is however considered impossible to pinpoint whether this is caused by different working conditions for the comparison or bad input data.

The simulation performed for the DHW-HP however, simulates power consumption and heating capacity very comparable to the measured values all though the working conditions is varying. Keeping in mind that the performance data gathered for the DHW-HP also is more credible, because it is measured for the correct heat pump, the result for the simulations performed on this heat pump is considered more trustworthy than the simulations for the SH-

HP. It is therefore concluded that the heat pump block simulates the power consumption and heating capacity very precisely in nominal operation.

7.6.1.2 Start-up

As it is discussed in Chapter 7.1.1.3 and in Chapter 7.1.4.3, the real heat pump uses some time to reach nominal operation. The simulated heat pump also has the capability to influence the time to reach nominal operation trough adjusting the thermal capacity of the hot loop (condenser) or in the cold loop (evaporator). It is however concluded that the high sample time of the measurements makes it impossible to investigate whether this parameter makes the start-up of the heat pump more realistic.

7.6.1.3 Sample time of measurements

The single component simulations in this thesis are performed with the intent of investigating the characteristics of the simulated component against measured data from the real component. Based on the comparisons that are performed in this chapter, it is considered that the heat pumps at Powerhouse Kjørbo should have shorter sample for the measurements in order to investigate the characteristics of the heat pumps properly. A 5-minute time step between each measurement makes it hard to exactly know when the heat pump starts/stops and makes an investigation of characteristics such as time to reach nominal operation impossible.

Of course, the shorter sample period that is used, the more details it is possible to get from the measurements. A shorter sample time however leads to more data being stored, and therefore a need for more storage space. It is also assumed that measuring equipment becomes more costly as the needed sample time decreases. It is therefore considered that an estimate sample time should be proposed.

A research into the topic of the sample time for measurements used for validation is performed, and no clear method to find the desired logging time is found. Some information is however found within the topic of sampling rates for measurement of signals. In that topic the Nyquist theorem states that one should have at least twice the sample rate as the frequency of the measured signal in order to digitally reproduce the signal (Candè and Wakin, 2008).

It is considered that the values measured at Powerhouse Kjørbo can be viewed as waves with differing frequency, and that it therefore is possible to use this theory to decide the sample rate for the measurements.

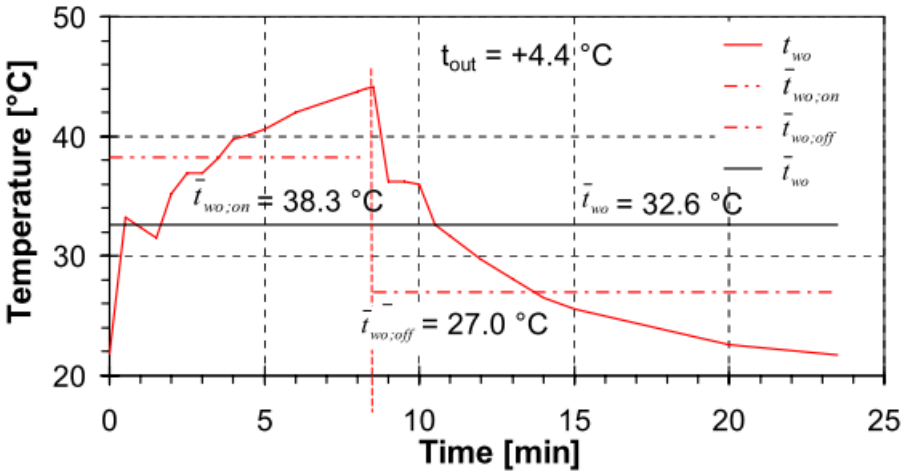

Figure 86 – Heat pump cycle (Karlsson and Fahlén, 2007)

Figure 86 shows the temperature coming out of the condenser during one heat pump cycle. It can seem like the graph is made out of measurements with a 30-second sampling time. It is assumed that this graph is not representable for all heat pumps and it is impossible to know how much information that is missing because the sample time that is used in the figure. It is however considered that a sampling time of 30 seconds in this case gives a decent view into the temperature development of the outlet fluid from the condenser.

All though a sample time of 30 seconds would give much information about the heat pump cycle, the uncertainty concerning the exact start and stop time for the heat pump. It is therefore considered that an event-based measuring system would be a good solution for logging the control signals. This system would log the time of the change in addition the value of the signal. It is believed that this would be a good solution because it is precise and would not need much storage space.

From this, it is concluded that event-based measurements should be used to measure the control signals of the heat pump, and that measurements with 30-second sample rate or less should be used to measure other values for the heat pump, such as temperatures, flow and energy consumption.

7.6.2 Storage tank

In the comparisons performed for the storage tank block in this chapter, one thing became apparent: the simulated outlet temperature to the space and ventilation heating system and the simulated temperatures for the nodes in the storage tank are higher than the measured temperatures. It is considered that both the high simulated node temperatures and the outlet temperature supports the suspicion that the real heat loss for the discharge circuit of the storage tank is higher than what is measured in energy meter OE002 to OE007.

However, all though the temperatures for the nodes and for the outlet to the space and ventilation heating is high compared to the measured values, the trends for the temperatures is very similar. It most also not be disregarded that the simulated and measured outlet temperature to the heat pump is almost identical.

Based on this, it is concluded that the storage tank block simulates temperatures that has very similar trends compared to the measured values, but that an energy measurement sensor should be placed on the discharge circuit of the storage tanks in order to calibrate the simulations properly.

7.6.3 GSHE

From the comparison presented in this chapter, it becomes apparent that the GSHE block performs very similar results to the real component when the mass flow of the real component is constant. It also shows that the temperature in the borehole evolves based on the accumulated thermal energy supplied and ejected into the borehole. It is however considered that another comparison should be performed between the GSHE block and field measurements. In this comparison, the mass flow circulating in the measured borehole need to be constant, and measurement data should be available for at least one year.

7.6.4 Space heating system

In the comparison between the real and the simulated space heating system, there is simulated a 2.3 % higher energy consumption, which is considered a very good result. However, the outlet temperature from the storage tank to the space and ventilation heating system showed generally higher simulated temperatures than measured ones. All though there are differences, the trends of the measured and simulated outlet temperatures are very similar. It is however considered that differences in the control system of the heat pump might be an explanation to the deviations, since the simulated outlet temperature is above the set point and that the measured outlet temperature is below.

Based on this, it is concluded that the multiple component simulation of the space heating system works very well, all though there are additional complications in implementing a control strategy for the system.

8 Conclusion

In this chapter, the conclusions from the discussion in Chapter 6.8.2.2 are summed up according to the goals set in Chapter 1.1.

8.1 Heat pump block

From the comparisons performed for the heat pump block, discussed in Chapter 7.6.1, it is concluded that the heat pump block simulates nominal power consumption and heating capacity very good. However, the measured heat pump uses longer time to reach nominal operation of the heating capacity, and it is considered that this should be investigated more closely.

In order to investigate the characteristics of the start-up for the real heat pump, it is proposed event-based measuring of the control signals and 30 second or less sample time for measuring the other values.

8.2 Storage tank block

Based on the comparisons and the discussions presented in Chapter 7.2, it is concluded that the trends of the temperatures simulated by the storage tank block is very similar to the measured values, but that an energy measurement sensor should be placed on the discharge circuit of the storage tanks in order to calibrate the simulations properly.

8.3 Ground source heat exchanger block

For the comparison between the block and the field measurements in this thesis, it is concluded that the block performs very similar results when the mass flow for the real component is constant. It is also concluded that the block simulates ground temperatures realistically according to the accumulated supplied and ejected thermal energy in the borehole. However, since the GSHE block only can simulate a constant circulated brine mass flow, it considered that a new comparison should be performed, where the GSHE block is compared to a borehole where the circulated brine mass flow is constant and there are measurement data for at least one year.

8.4 System level

In the comparison between the real and the simulated space heating system, there is simulated a 2.3 % higher energy consumption, which is considered a very good result. However, the outlet temperature from the storage tank to the space and ventilation heating system shows generally higher simulated temperatures than measured ones. All though there

are differences, the trends of the measured and simulated outlet temperatures are very similar. Based on this, it is concluded that the multiple component simulation of the space heating system works very well, all though there are additional complications in implementing a control strategy for the system.

9 Proposals for future work

Compare the GSHE block to a new borehole

It is considered that a new comparison should be performed, where the GSHE block is compared to a borehole where the circulated mass flow is constant and there are measurement data for at least one year.

Improve the measurement sensors and perform more comparisons

Install measurement sensors or change the sample time for the existing measurement sensors and perform a new comparison.

Tidying the model and develop new blocks

Make one place for inputs of external data. In the model developed by Mikkel Ytterhus, signal builder blocks, which contribute necessary information to the model, can be found in various locations of the model. It is considered that it would be most convenient to have the signal builder blocks at one location in order to have a better overview of the inputs in the model.

Capacity control of the heat pumps

Make a system where the user can chose a solution for capacity control of the heat pump, and integrate a system that corrects the performance of the heat pump.

Heat pump cycle

Make a system that corrects the heat pump cycle in the way that it is using time constants to set the time before the specific heat pump reaches nominal operation and so on.

Bibliography

ALDEBERT, S. 2015. *Implementation of a reversible air-source heat pump in Simulink for a nZEB Design Tool.* Project thesis at the University of Science and Technology (NTNU). EPT-P-2015-.

ALONSO, M. J., STENE, J., BANTLE, M. & GEORGES, L. 2015. Simulations of Heat Pumps for Nearly Zero Energy Buildings. *Annex 40.* Sintef, Cowi, NTNU.

BEIER, R. A., ACUÑA, J., MOGENSEN, P. & PALM, B. 2012. Vertical temperature profiles and borehole resistance in a U-tube borehole heat exchanger. *Geothermics,* 44**,** 23-32.

BORGNES, B. G. & RAMSTAD, R. K. 2015. Erfaringstall fra Futurum Energi AS og Asplan Viak AS.

CANDÈ, E. J. & WAKIN, M. B. 2008. An introduction to compressive sampling. *Signal Processing Magazine, IEEE,* 25**,** 21-30.

CARNOT 2010. *Extension to Simulink/Matlab.* 6.0 beta ed.: © Solar-Institut Jülich. Available for free at University of Applied Sciences Düsseldorf.

CARRIER SCS. 2012. *Water-Sourced Liquid Chillers/Heat Pumps with or without Integrated Hydronic Module* [Online]. Available: http://carrierab.se/media/49347/16121_psd_02_2012_61wg_30wg_lr.pdf [Accessed 24.10.2015 2015].

CARRIER SCS 2014. CONTROL SERVICE GUIDE FOR 30WG/61WG/30WGA SERIES Pro-Dialog Plus Control

HAFNER, B., PLETTNER, J., WEMHÖNER, C., WENZEL, T. 1999. *Carnot Blockset. User's Guide.* Solar-Institut Juelich.

KARLSSON, F. & FAHLÉN, P. 2007. Capacity-controlled ground source heat pumps in hydronic heating systems. *International Journal of Refrigeration,* 30**,** 221-229.

MURER, T. M. 2014. *Analysis of change in design procedures for heat pump systems in nZEB.* Master thesis at the University of Science and Technology (NTNU). EPT-M-2014-159.

NIBE. -. *Installatørhåndbok Nibe F1145* [Online]. Nibe. Available: http://www.nibe.no/nibedocuments/15195/231693-3.pdf [Accessed 09.03 2016].

NORDANG, I. F. 2014. *Analysis of the Thermal Energy Supply System at Powerhouse Kjørbo, Sandvika.* Project thesis at the University of Science and Technology (NTNU). EPT-P-2014-78.

NORDANG, I. F. 2015. *Analyse av varme- kjølesystemet ved Powerhouse Kjørbo.* Master thesis at the University of Science and Technology (NTNU). EPT-M-2015-65.

OSO HOTWATER. 2011. *Storberedere* [Online]. Available: http://osohotwater.no/files/OSO_Brosjyrer_Industriprodukter.pdf [Accessed].

OSO HOTWATER. 2016a. *Produktdatablad Maxi Standard 17RE* [Online]. Available: http://osohotwater.no/images/stories/oso-files/pdf/Spesifikk_Produktinformasjon/Produktdatablader/Industriprodukter__direkte_elektrisk/OSO_Produktdatablad__Maxi_Standard__17RE.pdf [Accessed 07.03 2016].

OSO HOTWATER. 2016b. *Produktdatablad Maxi Standard 51R* [Online]. Available: http://osohotwater.no/images/stories/oso-files/pdf/Spesifikk_Produktinformasjon/Produktdatablader/Industriprodukter__indirekte_oppvarmet/oso_produktdatablad__maxi_accu__51r.pdf [Accessed 07.03 2016].

PACHAURI, R. K., ALLEN, M., BARROS, V., BROOME, J., CRAMER, W., CHRIST, R., CHURCH, J., CLARKE, L., DAHE, Q. & DASGUPTA, P. 2014. Climate Change 2014: Synthesis Report. Contribution of Working Groups I, II and III to the Fifth Assessment Report of the Intergovernmental Panel on Climate Change.

RAMSTAD, R. K. 2013. Kjørbo - resultater fra termisk responstest Asplan Viak AS.

RUSCHENBURG, J., ĆUTIĆ, T. & HERKEL, S. 2014. Validation of a black-box heat pump simulation model by means of field test results from five installations. *Energy & Buildings,* 84**,** 506-515.

SKJERVE, P. M. 2016. *Adapting the design procedure of heat pump systems to nZEB.* Project thesis at the University of Science and Technology (NTNU). EPT-P-2015-84.

SMÅLAND, L. 2013. *Modelling and Analysis of Heat Pumps for Zero Emission Buildings.* Master thesis at the University of Science and Technology (NTNU). EPT-M-2013-109.

SOLAR INSTITUTE JUELICH. 2014. *Carnot manual for MATLAB Simulink R2010b (R).*

STANDARD NORGE 2006. Water supply - Specification for indirectly heated unvented (closed) storage water heaters. *NS-EN 12897:2006.* Standard Norge.

STANDARD NORGE 2013. Air conditioners, liquid chilling packages and heat pumps with electrically driven compressors for space heating and cooling - Part 2: Test conditions. *NS-EN 14511-2:2013* Standard Norge.

STENE, J. 1997. *Varmepumper : grunnleggende varmepumpeteknikk,* Trondheim, SINTEF Energi, Klima- og kuldeteknikk.

THE MATHWORKS INC. 2016a. *Signal builder* [Online]. Available: http://se.mathworks.com/help/simulink/slref/signalbuilder.html [Accessed 10.05 2016].

THE MATHWORKS INC. 2016b. *Signal builder* [Online]. Available: http://se.mathworks.com/help/simulink/slref/signalbuilder_cmd.html [Accessed 23.06 2016].

UGINE & ALZ. 2005. *Niobium-titanium stabilized molybdenum containing 18 % chromium ferritic stainless steel* [Online]. Available: http://www.metallvertrieb.com/uploads/katalog/WDB/ferritische/1.4521-Englisch.pdf [Accessed 07.03 2016].

YTTERHUS, M. 2014. *Modelling the ground during the early-phase design of heat pump systems in nZEB.* Project thesis at the University of Science and Technology (NTNU). EPT-P-2014-116.

YTTERHUS, M. 2015. *Adapting the Design Procedures of Heat Pump Systems to nZEB.* Master thesis at the University of Science and Technology (NTNU). EPT-M-2015-104.

ZIJDEMANS, D. 2012. *Vannbaserte oppvarmings- og kjølesystemer*, Skarland Press.

Appendix I- Matrix SH-HP

Inputs/outputs in NZEP

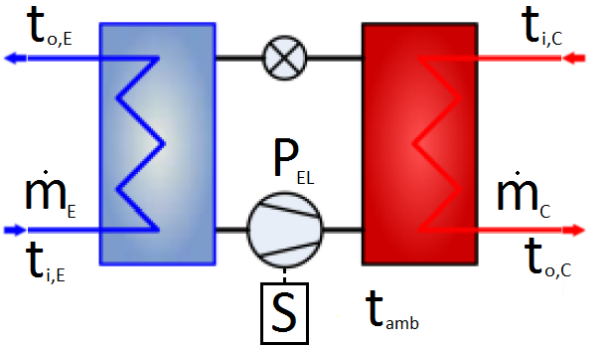

Measured inputs/outputs

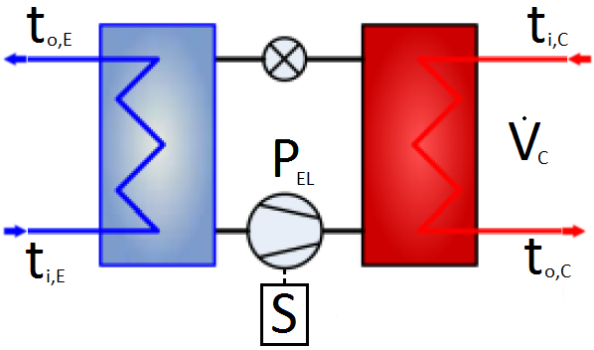

Input	**Sensor**	**Resolution**	**Accuracy**
$t_{i,E}$ [°C]	RT1501	5 minutes	-
$t_{i,C}$ [°C]	RT1500	5 minutes	-
S [−]		5 minutes	
Output	**Sensor**	**Resolution**	**Accuracy**
$t_{o,E}$ [°C]	RT1401	5 minutes	-
$t_{o,C}$ [°C]	RT1400	5 minutes	-
P_{EL} [W]	EL1	5 minutes	-

Alternative measurements	**Sensor**	**Resolution**	**Accuracy**	**Transformation equation**
$\dot{V}_C$ [l/h]	OE016	5 minutes	-	$\dot{m}_C = \frac{0.001}{3600} \cdot \dot{V}_C \cdot \rho(t) \left[\frac{kg}{s}\right]$
$\dot{V}_{bh}$[m^3/h]	OE015	5 minutes	-	$\dot{m}_E = \frac{1}{3600} \cdot \dot{V}_{bh} \cdot \rho(t) \left[\frac{kg}{s}\right]$

Missing measurements	**Additional information**
t_{amb} [°C]	Not found. A measured temperature of 23.4°C is used.
$\dot{m}_E$ [l/h]	

Input parameter	Default value	Base value
Inlet source temperature vector [℃]		[-5 0 5 10]
Outlet load temperature vector [℃]		[25 35 45 55 65]
Source power matrix [W]		[53300 47600 41600 36900 29800;62700 56500 49700 44600 37800;73300 67400 60300 54600 47800;85300 78600 71200 65100 56900]
Heating power matrix [W]		[65900 63100 60800 59300 56600;76000 72700 69300 67100 64700;86800 83400 79500 76400 72400;99700 95100 90800 87000 82300]
Electric power matrix [W]		[12600 15500 19200 22400 26800;13300 16200 19600 22500 26900;13500 16000 19200 21800 25600;14400 16500 19600 21900 25400]
Thermal capacity hot loop [J/K]	80000	
Thermal capacity cold loop [J/K]	50000	
Heat loss coefficient [W/K]	7	
Pressure drop parameters for the condenser and the evaporator	(default)	
Fluid information evaporator side		$F_{type,C}$: Water-ethanol $F_{Mix,C}$: 0.35
Fluid information condenser side		$F_{type,E}$: Water $F_{mix,C}$:-

Appendix II - Matrix DHW-HP

Inputs/outputs in NZEP

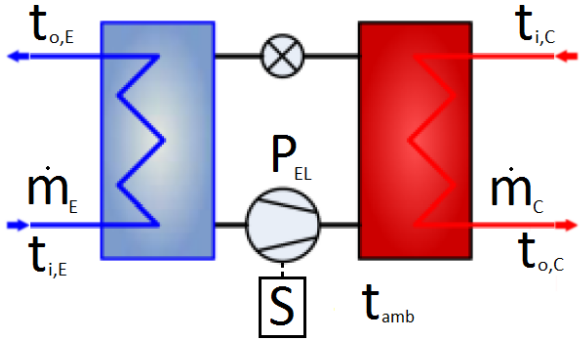

Measured inputs/outputs

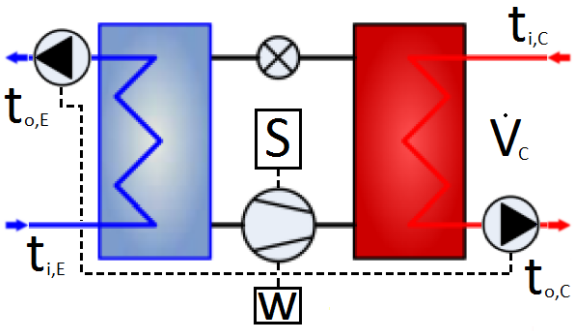

Input	**Sensor**	**Resolution**	**Accuracy**	
$t_{i,E}$ [°C]	RT4030	5 minutes	±0.5°C	
$t_{i,C}$ [°C]	RT1400	5 minutes	-	
S [−]		5 minutes		
Output	**Sensor**	**Resolution**	**Accuracy**	
$t_{o,E}$ [°C]	RT1510	5 minutes	-	
$t_{o,C}$ [°C]	RT1500		-	
Alternative values	**Sensor**	**Resolution**	**Accuracy**	**Transformation equation**
$\dot{V}_C$ $[l/h]$	EO16	5 minutes	-	$\dot{m}_C = \dot{V}_C \cdot \frac{0.001}{3600} \cdot \rho(t) \left[\frac{kg}{s}\right]$
P_{EL} $[kW]$	EL2	5 minutes	+0.1%	$P_{EL} = W - P_{pumps}\ [kW]$
Missing measurements	**Additional information**			
t_{amb} [°C]	Not found. A measured temperature of 23.4°C is used.			
$\dot{m}_E$ $[kg/s]$	Found to have a volume flow of 960 l/h and to have same input signal as HP			

Input parameter	Default value	Base value
Inlet source temperature vector [℃]		[0 10]
Outlet load temperature vector [℃]		[35 45 55 65]
Source power matrix [W]		[7650 6280 5200 4010;10630 9250 8150 6640]
Heating power matrix [W]		[9660 8550 7580 6490;12820 11800 10940 9650]
Electric power matrix [W]		[2010 2270 2380 2480;2190 2550 2790 3010]
Thermal capacity hot loop [J/K]	80000	
Thermal capacity cold loop [J/K]	50000	
Heat loss coefficient [W/K]	7	
Pressure drop parameters for the condenser and the evaporator	(default)	(Default)
Fluid information evaporator side		$F_{type,C}$: Water-ethanol $F_{Mix,C}$: 0.35
Fluid information condenser side		$F_{type,E}$: Water $F_{mix,C}$:-

Appendix III - Matrix SH-ST

Inputs/outputs in NZEP

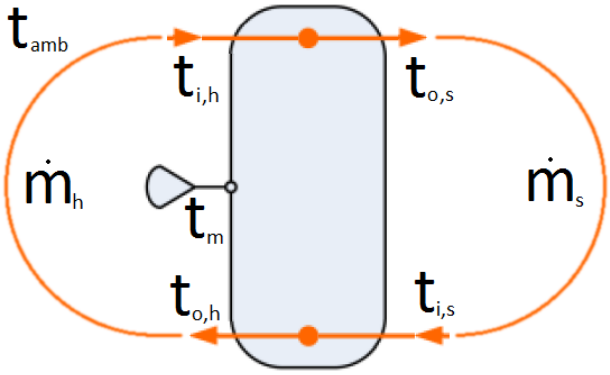

Measured inputs/outputs

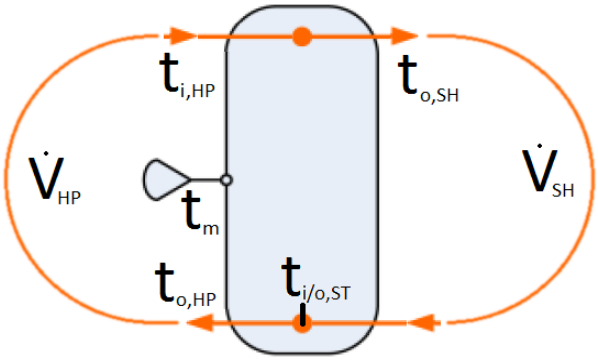

Input	**Sensor**	**Resolution**	**Accuracy**	
$t_{i,HP}$ [°C]	RT1400	5 minutes	-	
$t_{i/o,ST}$ [°C]	RT5010	5 minutes	±0.5°C	
Output	**Sensor**	**Resolution**	**Accuracy**	
$t_{O,HP}$ [°C]	RT1500	5 minutes	-	
$t_{o,SH}$ [°C]	RT4010	5 minutes	±0.5°C	
$t_{i/o,ST}$ [°C]	RT5010	5 minutes	±0.5°C	
t_m [°C]	RT4070	5 minutes	±0.5°C	
Alternative values	**Sensor**	**Resolution**	**Accuracy**	**Transformation equation**
$\dot{V}_{HP}$ $[m^3/h]$	OE001 (flow)	5 minutes	-	$\dot{m}_{HP} = \frac{1}{3600} \cdot \dot{V}_{HP} \cdot \rho(t) \left[\frac{kg}{s}\right]$
$\dot{V}_{SH}$ $[m^3/h]$	Both flow and temperature OE003 OE004 OE005 OE006 OE007	5 minutes	-	$\dot{m}_{SH} = \frac{1}{3600} \cdot \dot{V}_{SH} \cdot \rho(t) \left[\frac{kg}{s}\right]$ For finding the total mass flow:
Missing measurements	**Additional information**			
t_{amb} [°C]	Not found. A measured temperature of 23.4°C is used.			

Input parameter	Default value	Base value
Heat loss coefficient cylinder wall in W/(m²K)	1	1.73
Heat loss coefficient bottom in W/(m²K)	1	1.73
Heat loss coefficient top cover in W/(m²K)	1	1.73
Effective vertical conductivity in W/(m*K)	1	0.772
Initial temperature (vector or scalar) in℃	[10:5:55]	35
Volume in m³	-	0.9
Diameter in m	-	0.8
Position	Standing	Standing
Number of connections	2	2
Number of nodes	10	10
Number of measurement points	10	10
Fluid information		$F_{type,C}$: Water $F_{Mix,C}$:-
Relative height of highest inlet/outlet	1	0.813
Relative height of lowest inlet/outlet	0	0.187

Appendix IV - Matrix DHW-ST

Inputs/outputs in NZEP

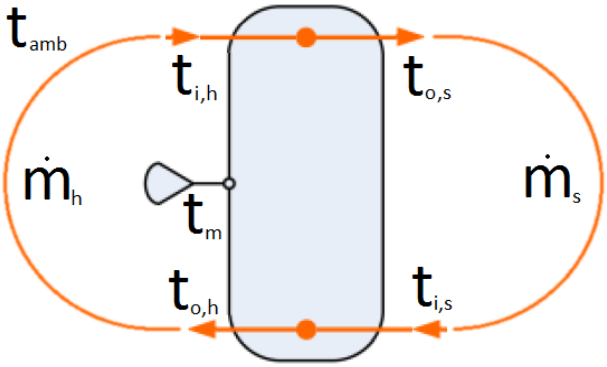

Measured inputs/outputs

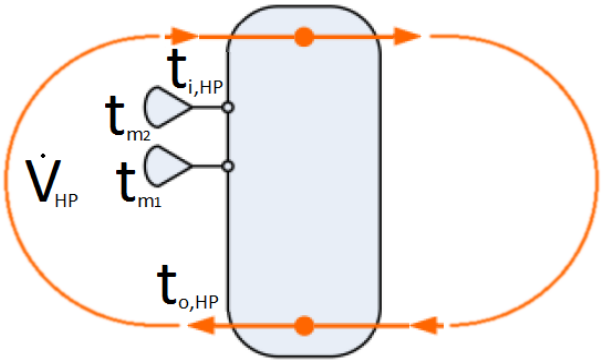

Input	**Sensor**	**Resolution**	**Accuracy**	
$t_{i,HP}$ [°C]	RT1516	5 minutes	-	
Output	**Sensor**	**Resolution**	**Accuracy**	
t_{m1} [°C]	RT4010	5 minutes	±0.5°C	
t_{m2} [°C]	RT4020	5 minutes	±0.5°C	
$t_{o,HP}$ [°C]	RT1416	5 minutes	-	
Alternative values	**Sensor**	**Resolution**	**Accuracy**	**Transformation equation**
$\dot{V}_{HP}$ $[l/h]$	OE016 (flow)	5 minutes	-	$\dot{m}_{HP} = \frac{0.001}{3600} \cdot \dot{V}_C \cdot \rho(t) \left[\frac{kg}{s}\right]$
Missing measurements	**Additional information**			
t_{amb} [°C]	Not found			
$t_{i,DHW}$ [°C]	Not found			
$t_{o,DHW}$ [°C]	Not found			
$\dot{m}_{DHW}$ $[kg/s]$	Not found			

Input parameter	Default value	Base value
Heat loss coefficient cylinder wall in W/(m²K)	1	1.58
Heat loss coefficient bottom in W/(m²K)	1	1.58
Heat loss coefficient top cover in W/(m²K)	1	1.58
Effective vertical conductivity in W/(m*K)	1	0.741
Initial temperature (vector or scalar) in℃	[10:5:55]	
Volume in m³	-	0.55
Diameter in m	-	0.65
Position	Standing	Standing
Number of connections	2	1
Number of nodes	10	10
Number of measurement points	10	10
Fluid information		$F_{type,C}$: Water $F_{Mix,C}$:-
Relative height of highest inlet/outlet	1	1
Relative height of lowest inlet/outlet	0	0

Appendix V - Matrix GHE

Inputs/outputs in NZEP

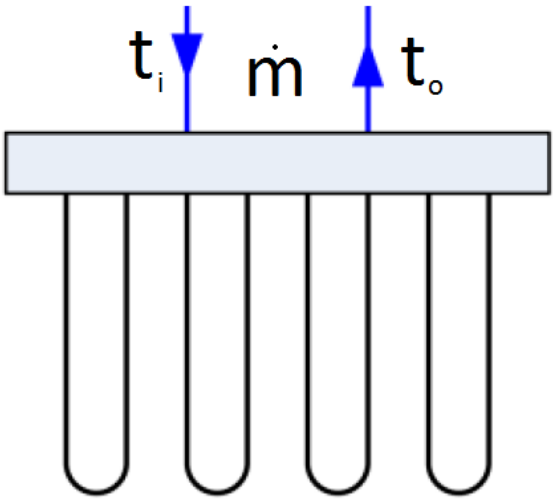

Measured inputs/outputs

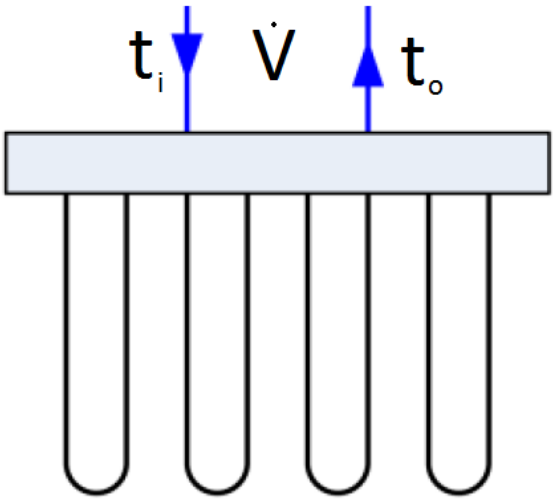

Input	**Sensor**	**Accuracy**	**Resolution**
t_i [°C]	OE015 (RT1415)	-	5 min
Input	Sensor	Resolution	Accuracy
t_o [°C]	OE015 (RT1515)	-	5 min

Alternative values	**Sensor**	**Accuracy**	**Resolution**	**Transformation equation**
$\dot{V}$ $[m^3/h]$	OE015 (flow)	-	5 min	$\dot{m}_C = \frac{1}{3600} \cdot \dot{V}_C \cdot \rho(t) \left[\frac{kg}{s}\right]$

Input parameter	Default value	Base value
Average annual outdoor temperature in℃	6	7
Temperature gradient in K/m, typical 0.025..0.04	0.025	0.0173
Thermal conductivity ground in W/m/K	2.0	1.9-4.4
Heat capacity of the ground in J/(kgK)	800	2100
Density of the ground in kg/m^3	2500	2650
Thermal conductivity filling in W/m/K	1.0	0.58
Heat capacity of the filling in J/kg/K	1000	4192
Density of the filling in kg/m^3	2000	1000
H: Length of earth probe in m	200	215
B: probe distance in m	20	10
Diameter of tube in m	0.032	0.04
Diameter of drilled hole in m	0.18	0.115
Field geometry	2 probes B/H=0.1	2x8 probes B/H=0.05
Number of parallel tubes	3	10
No. of nodes in axial direction (typical 10)	10	10
No. of nodes in radial direction (typical 10)	10	10
Grid factor (typical 2.5)	2.5	2.5
Design mass flow rate [kg/s]		
Fluid type	5	5 (water-glycol mix)
Fluid mix	0.25	0.35 (35 % glycol)

Appendix VI – Equations

Nr.	Formula	Source
1	$\lambda_{eff} = \frac{4 \cdot A_{wall} \cdot \lambda_{wall}}{\pi \cdot D^2} + \lambda_{fluid} \left[\frac{W}{mK}\right]$ Where, $\lambda_{eff} \left[\frac{W}{mK}\right]$: is the EVC A_{wall} $[m^2]$: is the horizontal area of the wall λ_{wall} $\left[\frac{W}{mK}\right]$: is the conductivity of the wall D $[m]$: is the inner diameter of the tank λ_{fluid} $\left[\frac{W}{mK}\right]$: is the conductivity of the fluid in the tank	HAFNER, B., PLETTNER, J., WEMHÖNER, C., WENZEL, T. 1999. *Carnot Blockset. User's Guide.* Solar-Institut Juelich.
2	$T(z) = \overline{T_{amb}} + 1 + \frac{dT}{dz} \cdot z[℃]$ Where, z: is the depth in the ground $T(z)$: is the temperature in the ground at depth z $\frac{dT}{dz}$: is the temperature gradient	YTTERHUS, M. 2014. *Modelling the ground during the early-phase design of heat pump systems in nZEB.* Project thesis at the University of Science and Technology (NTNU). EPT-P-2014-116.
3	$\dot{m} = \frac{0.001}{3600} \cdot \dot{V} \cdot \rho(t) \left[\frac{kg}{s}\right]$ Where, $\dot{V}$ $[l/h]$: is the volume flow $0.001/3600 \left[h \cdot m^3/s \cdot l\right]$: is a transformation constant to correct the units $\rho(t)[kg/m^3]$: is the density of the fluid for a given temperature	ZIJDEMANS, D. 2012. *Vannbaserte oppvarmings- og kjølesystemer*, Skarland Press.
4	$\dot{m} = \frac{1}{3600} \cdot \dot{V} \cdot \rho(t) \left[\frac{kg}{s}\right]$ Where, $\dot{V}$ $[m^3/h]$: is the volume flow $1/3600 \left[h/s\right]$: is a transformation constant to correct the units $\rho(t)[kg/m^3]$: is the density of the fluid for a given temperature	ZIJDEMANS, D. 2012. *Vannbaserte oppvarmings- og kjølesystemer*, Skarland Press.

5	$$\dot{Q}_1 = C_{p1} \cdot \rho_1 \cdot \dot{V}_1 \cdot \Delta t_1$$ $$\dot{Q}_1 = \dot{Q}_2 => \dot{V}_1 = \frac{\dot{V}_2 \cdot \Delta t_2}{\Delta t_1}$$ This equation is assumed accurate enough in a mix between two equal fluid types, where the temperature differences is not to large.	ZIJDEMANS, D. 2012. *Vannbaserte oppvarmings- og kjølesystemer*, Skarland Press.
6	$$r_h = r_{h-1} + (r_m - r_1) \cdot \frac{1-f}{1-f^{m-1}} \cdot f^{h-2}$$ Where, $r_h[m]$: is the radius for node h $r_m[m]$: is the maximum radius $f\ [-]$: is the grid factor	WETTER, M. & HUBER, A. 1997. Vertical borehole heat exchanger EWS Model. *TRNSYS type*.
7	$$\dot{m} = \frac{\dot{Q}}{C_p \cdot \Delta t}\ [kg/s]$$ Where it is assumed that the reader of this thesis should know this equation.	ZIJDEMANS, D. 2012. *Vannbaserte oppvarmings- og kjølesystemer*, Skarland Press.
8	$$S = \frac{\pi}{\sqrt{a^2-c^2}}\left[2a^2\sqrt{a^2-c^2} + ac^2 \ln\left(\frac{a+\sqrt{a^2-c^2}}{a-\sqrt{a^2-c^2}}\right)\right]$$ Where, $S\ [m^2]$: is the surface area of the sphere $a\ [m]$: is the distance from origin to the edge of the sphere (x- and y-axis) $c\ [m]$: is the distance from origin to the top of the sphere (z-axis)	WOLFRAM ALPHA. 2016. *Oblate Spheroid* [Online]. Available: http://mathworld.wolfram.com/OblateSpheroid.html [Accessed 08.03 2016].

Appendix VII – Calculations

Chapter 4.3.1: Calculation of U-values for ST-SH

In order to find the U-value, the surface area of the storage tank needs to be known. To estimate a surface area of the top and bottom of the storage tank, the equation for calculating the surface area of an oblate spheroid is used. This is because it is assumed that the top and bottom of the storage tank have a similar shape to one.

$$S = \frac{\pi}{\sqrt{a^2 - c^2}}\left[2a^2\sqrt{a^2 - c^2} + ac^2 \ln\left(\frac{a + \sqrt{a^2 - c^2}}{a - \sqrt{a^2 - c^2}}\right)\right] \quad 8$$

$$= \frac{\pi}{\sqrt{0.4^2 - 0.215^2}}\left[2 \cdot 0.4^2\sqrt{0.4^2 - 0.215^2} + 0.4 \cdot 0.215^2 \cdot \ln\left(\frac{0.4 + \sqrt{0.4^2 - 0.215^2}}{0.4 - \sqrt{0.4^2 - 0.215^2}}\right)\right]$$

$$= 1.43\ [m^2]$$

The equation parameters are explained in Appendix VI, while the values used are presented in the table below.

Parameter	Value	Source
$\boldsymbol{a}$	$0.4\ m$	(Oso Hotwater 2016, pers. comm., 11. Feb.)
$\boldsymbol{c}$	$0.215\ m$	(Oso Hotwater 2016, pers. comm., 11. Feb.)

Now that the surface areas of the storage tank are estimated, the U-value can be calculated using equation:

$$U = \frac{E_{24\ hour\ energy\ loss}}{24\ h \cdot \Delta T \cdot A_{tot}} \cdot 1000 = \frac{9.7\ kWh}{24\ h \cdot 45\ K \cdot 5.2\ m^2} \cdot 1000\ {}^{1}/_{k} = 1.73\ W/m^2K$$

The equation parameters are explained in Appendix VI, while the values used are presented in the table below.

Parameter	Value	Source
$\boldsymbol{D_{cylinder}}$	$0.8\ m$	(Oso Hotwater 2016, pers. comm., 11. Feb.)
$\boldsymbol{H_{cylinder}}$	$1.5\ m$	(Oso Hotwater 2016, pers. comm., 11. Feb.)
$\boldsymbol{A_{cylinder}}$	$3.77\ m^2$	Calculated with the equation below $A_{sylinder} = D_{sylinder} \cdot H_{sylinder} \cdot \pi = 0.8m \cdot 1.5m \cdot \pi = 3.77m^2$
$\boldsymbol{A_{top\ and\ bottom}}$	$1.43\ m^2$	
$\boldsymbol{A_{tot}}$	$5.2\ m^2$	
$\boldsymbol{E_{24\ hour\ energy\ loss}}$	$9.7\ kWh$	(OSO Hotwater, 2016b)
$\boldsymbol{\Delta T}$	$45\ K$	(Standard Norge, 2006)

Chapter 4.3.1: Calculation of U-values for ST-SH

In order to find the U-value, the surface area of the storage tank needs to be known. To estimate a surface area of the top and bottom of the storage tank, equation __ is for calculating the surface area of an oblate spheroid is used. This is because it is assumed that the top and bottom of the storage tank have a similar shape to one.

$$S = \frac{\pi}{\sqrt{a^2 - c^2}}\left[2a^2\sqrt{a^2 - c^2} + ac^2 \ln\left(\frac{a + \sqrt{a^2 - c^2}}{a - \sqrt{a^2 - c^2}}\right)\right]$$

$$= \frac{\pi}{\sqrt{0.335^2 - 0.18^2}}\left[2 \cdot 0.335^2\sqrt{0.335^2 - 0.18^2} + 0.335\right.$$

$$\left. \cdot\, 0.18^2 \cdot \ln\left(\frac{0.335 + \sqrt{0.335^2 - 0.18^2}}{0.335 - \sqrt{0.335^2 - 0.18^2}}\right)\right] = 0.956\ [m^2]$$

The equation parameters are explained in Appendix VI, while the values used are presented in the table below.

Parameter	Value	Source
$\boldsymbol{a}$	$0.335\ m$	(Oso Hotwater 2016, pers. comm., 11. Feb.)
$\boldsymbol{c}$	$0.18\ m$	(Oso Hotwater 2016, pers. comm., 11. Feb.)

Now that the surface areas of the storage tank are estimated, the U-value can be calculated using equation:

$$U = \frac{E_{24\ hour\ energy\ loss}}{24\ h \cdot \Delta T \cdot A_{tot}} \cdot 1000 = \frac{6.5\ kWh}{24\ h \cdot 45\ K \cdot 3.859\ m^2} \cdot 1000\ {}^{1}/_{k} = 1.58\ W/m^2K$$

The equation parameters are explained in Appendix VI, while the values used are presented in the table below.

Parameter	Value	Source
$\boldsymbol{D_{cylinder}}$	$0.65\ m$	(Oso Hotwater 2016, pers. comm., 11. Feb.)
$\boldsymbol{H_{cylinder}}$	$1.4\ m$	(Oso Hotwater 2016, pers. comm., 11. Feb.)
$\boldsymbol{A_{cylinder}}$	$2.859\ m^2$	Calculated with the equation below $A_{sylinder} = D_{sylinder} \cdot H_{sylinder} \cdot \pi = 0.65m \cdot 1.4m \cdot \pi = 2.859m^2$
$\boldsymbol{A_{top\ and\ bottom}}$	$0.956\ m^2$	
$\boldsymbol{A_{tot}}$	$3.815\ m^2$	
$\boldsymbol{E_{24\ hour\ energy\ loss}}$	$6.5\ kWh$	(OSO Hotwater, 2016b)
$\boldsymbol{\Delta T}$	$45\ K$	(Standard Norge, 2006)

Chapter 4.3.2: Calculation of EVC

Equation 1 is used:

$$\lambda_{eff} = \frac{4 \cdot A_{wall} \cdot \lambda_{wall}}{\pi \cdot D^2} + \lambda_{fluid} = \frac{4 \cdot 0.0038 \cdot 23}{\pi \cdot 0.80^2} + 0.6 = 0.772 \left[\frac{W}{mK}\right]$$

The equation parameters are explained in Appendix VI, while the values used are presented in the table below.

Parameter	Value	Source
$\boldsymbol{A_{wall}}$	$0.0038\ m^2$	The cross sectional area of the wall are calculated below, where the thickness of the walls (t) are given by a source that is not named in this thesis (Oso Hotwater 2016, pers. comm., 11. Feb.). $$A_{wall} = \pi \left(\frac{D}{2}\right)^2 - \pi \left(\frac{D-t}{2}\right)^2 = \pi \left(\frac{0.8}{2}\right)^2 - \pi \left(\frac{0.8-0.003}{2}\right)^2 = 0.0038\ [m^2]$$
$\boldsymbol{D}$	$0.80\ m$	(Oso Hotwater 2016, pers. comm., 11. Feb.)
$\boldsymbol{\lambda_{wall}}$	$23\ \frac{W}{mK}$	(UGINE & ALZ, 2005)
$\boldsymbol{\lambda_{fluid}}$	$0.6\ \frac{W}{mK}$	Typical value for water (Zijdemans, 2012)

Chapter 4.3.2: Calculation of EVC

Equation 1 is used:

$$\lambda_{eff} = \frac{4 \cdot A_{wall} \cdot \lambda_{wall}}{\pi \cdot D^2} + \lambda_{fluid} = \frac{4 \cdot 0.002 \cdot 23}{\pi \cdot 0.65^2} + 0.6 = 0.741 \left[\frac{W}{mK}\right]$$

The equation parameters are explained in Appendix VI, while the values used are presented in the table below.

Parameter	Value	Source
$\boldsymbol{A_{wall}}$	$0.0020\ m^2$	The cross sectional area of the wall are calculated below, where the thickness of the walls (t) are given by a source that is not named in this thesis (Oso Hotwater 2016, pers. comm., 11. Feb.). $$A_{wall} = \pi \left(\frac{D}{2}\right)^2 - \pi \left(\frac{D-t}{2}\right)^2 = \pi \left(\frac{0.65}{2}\right)^2 - \pi \left(\frac{0.65-0.002}{2}\right)^2 = 0.0020\ [m^2]$$
$\boldsymbol{D}$	$0.65\ m$	(Oso Hotwater 2016, pers. comm., 11. Feb.)

$\boldsymbol{\lambda_{wall}}$	$23\ \frac{W}{mK}$	Typical value for steel (Zijdemans, 2012)
$\boldsymbol{\lambda_{fluid}}$	$0.6\ \frac{W}{mK}$	Typical value for water (Zijdemans, 2012)

Chapter 6.6.2.2: Calculation of space between nodes

Equation 6 is used in the calculations, and the results of the calculations can be found in the table below the equation.

$$r_h = r_{h-1} + (r_m - r_1) \cdot \frac{1-f}{1-f^{m-1}} \cdot f^{h-2}$$

$\boldsymbol{r_1}$	0.0575 m
$\boldsymbol{r_2}$	0.0594 m
$\boldsymbol{r_3}$	0.0643 m
$\boldsymbol{r_4}$	0.0765 m
$\boldsymbol{r_5}$	0.1068 m
$\boldsymbol{r_6}$	0.1828 m
$\boldsymbol{r_7}$	0.3726 m
$\boldsymbol{r_8}$	0.8472 m
$\boldsymbol{r_9}$	2.0337 m
$\boldsymbol{r_{10}}$	5.0000 m

The values that have been used to calculate the radiuses is shown in the table below

Parameter	Value	Source
$\boldsymbol{h}$	$2-10$	A integer between 2 and the amount of nodes in radial direction for the calculation
$\boldsymbol{r_1}$	$0.0575\ m$	Radius of the borehole divided by two (found in the mask of the GSHE): $r_1 = \frac{0.115\ m}{2} = 0.0575\ m$
$\boldsymbol{r_m}$	$5\ m$	The maximum radius of the nodes. Given as the half of the distance between the boreholes (found in the mask of the GSHE): $r_m = \frac{10\ m}{2} = 5\ m$
$\boldsymbol{f}$	2.5	The default grid factor
$\boldsymbol{m}$	10	The number of nodes in radial direction

Appendix VIII – Energy meters for the hydronic system

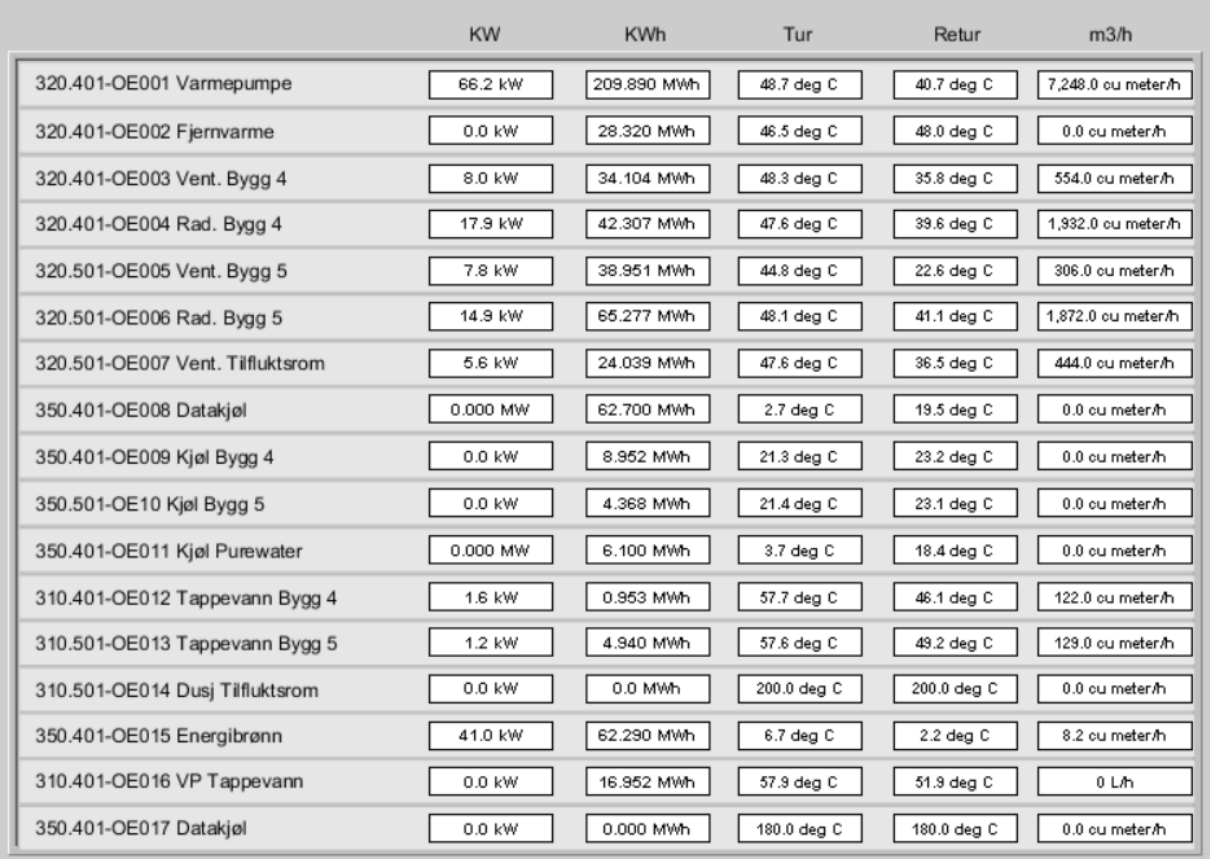

	KW	KWh	Tur	Retur	m3/h
320.401-OE001 Varmepumpe	66.2 kW	209.890 MWh	48.7 deg C	40.7 deg C	7,248.0 cu meter/h
320.401-OE002 Fjernvarme	0.0 kW	28.320 MWh	46.5 deg C	48.0 deg C	0.0 cu meter/h
320.401-OE003 Vent. Bygg 4	8.0 kW	34.104 MWh	48.3 deg C	35.8 deg C	554.0 cu meter/h
320.401-OE004 Rad. Bygg 4	17.9 kW	42.307 MWh	47.6 deg C	39.6 deg C	1,932.0 cu meter/h
320.501-OE005 Vent. Bygg 5	7.8 kW	38.951 MWh	44.8 deg C	22.6 deg C	306.0 cu meter/h
320.501-OE006 Rad. Bygg 5	14.9 kW	65.277 MWh	48.1 deg C	41.1 deg C	1,872.0 cu meter/h
320.501-OE007 Vent. Tilfluktsrom	5.6 kW	24.039 MWh	47.6 deg C	36.5 deg C	444.0 cu meter/h
350.401-OE008 Datakjøl	0.000 MW	62.700 MWh	2.7 deg C	19.5 deg C	0.0 cu meter/h
350.401-OE009 Kjøl Bygg 4	0.0 kW	8.952 MWh	21.3 deg C	23.2 deg C	0.0 cu meter/h
350.501-OE10 Kjøl Bygg 5	0.0 kW	4.368 MWh	21.4 deg C	23.1 deg C	0.0 cu meter/h
350.401-OE011 Kjøl Purewater	0.000 MW	6.100 MWh	3.7 deg C	18.4 deg C	0.0 cu meter/h
310.401-OE012 Tappevann Bygg 4	1.6 kW	0.953 MWh	57.7 deg C	46.1 deg C	122.0 cu meter/h
310.501-OE013 Tappevann Bygg 5	1.2 kW	4.940 MWh	57.6 deg C	49.2 deg C	129.0 cu meter/h
310.501-OE014 Dusj Tilfluktsrom	0.0 kW	0.0 MWh	200.0 deg C	200.0 deg C	0.0 cu meter/h
350.401-OE015 Energibrønn	41.0 kW	62.290 MWh	6.7 deg C	2.2 deg C	8.2 cu meter/h
310.401-OE016 VP Tappevann	0.0 kW	16.952 MWh	57.9 deg C	51.9 deg C	0 L/h
350.401-OE017 Datakjøl	0.0 kW	0.000 MWh	180.0 deg C	180.0 deg C	0.0 cu meter/h

Print screen taken 12.16.2015.

The text in the figure is written in Norwegian, so here are some glossaries that can help make of the figure.

Norwegian	**English**
Bygg	Building
Datakjøl	Computer cooling
Energibrønn	Borehole (or directly: “energy well”)
Fjernvarme	District heating
Kjøl	Cooling
Rad. (short for “radiator”)	Radiator
Tappevann	Domestic water
Varmepumpe	Heat pump
Vent. (short for “ventilasjon”)	Ventilation

Appendix IX – Timeline for the boreholes

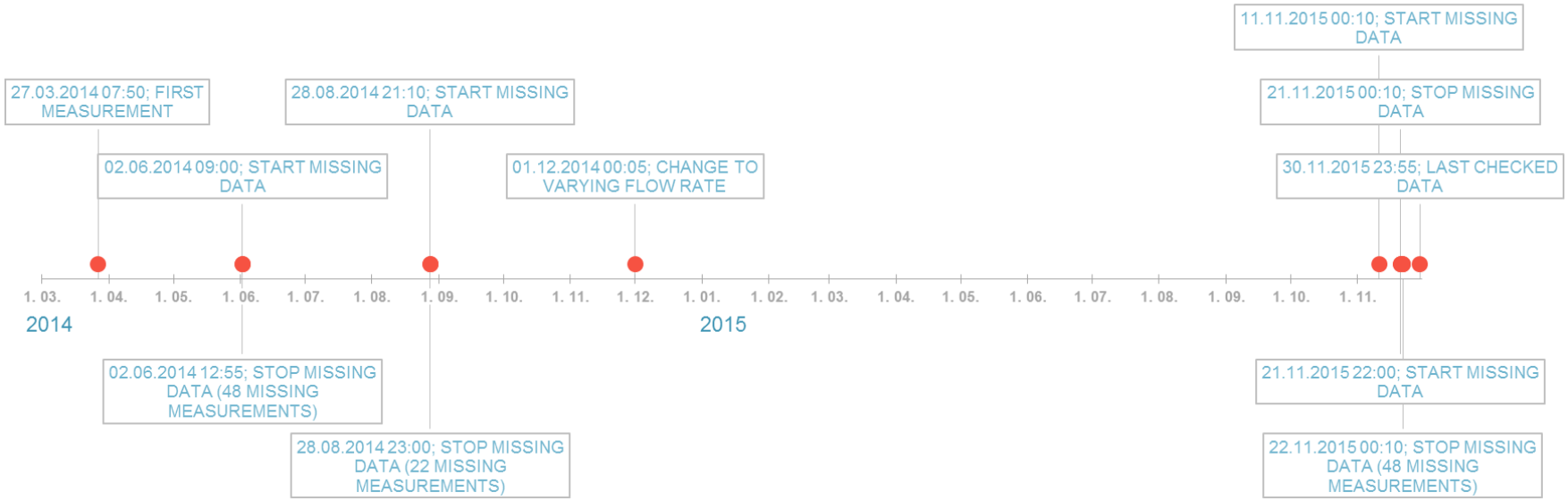

The figure above shows a timeline for the boreholes gathered from the measurements in the CC-system. In Chapter 3 it is mentioned that the in inauguration of the building was in April 2014, and it is therefore believed that there is measurements for the supply and return temperatures and volume flow of brine for the whole lifetime of the boreholes. There might be some missing measurements in the period 22.11.2015 to the date of this writing, but this is not investigated since this period are not used in the simulations performed on the ground source heat exchanger block.

Appendix X – Missing measurements

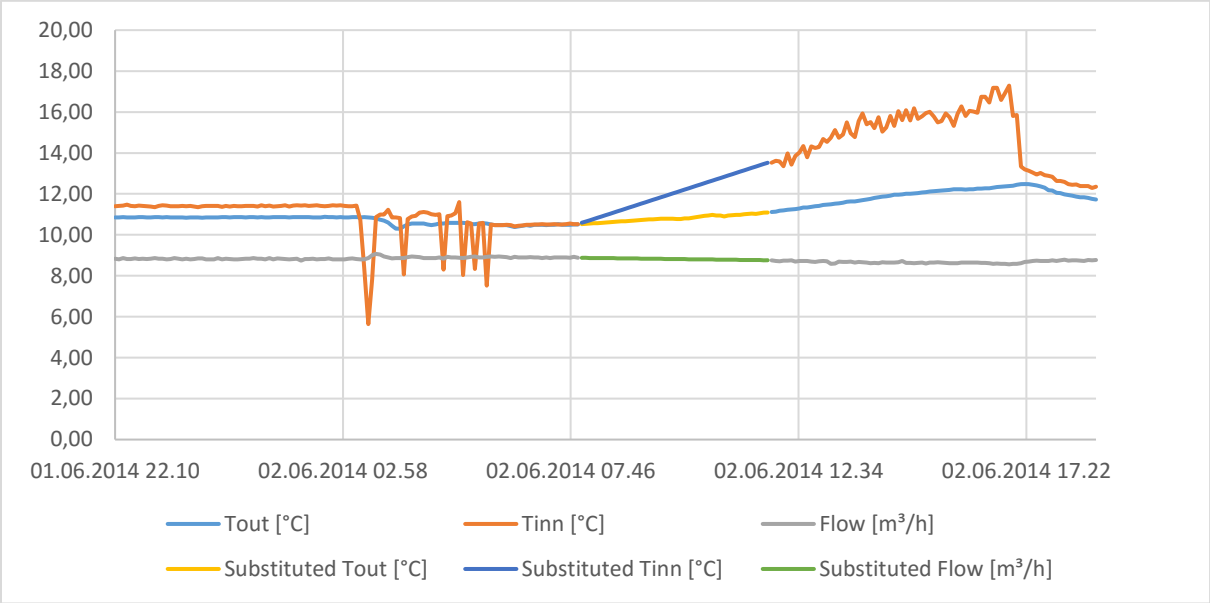

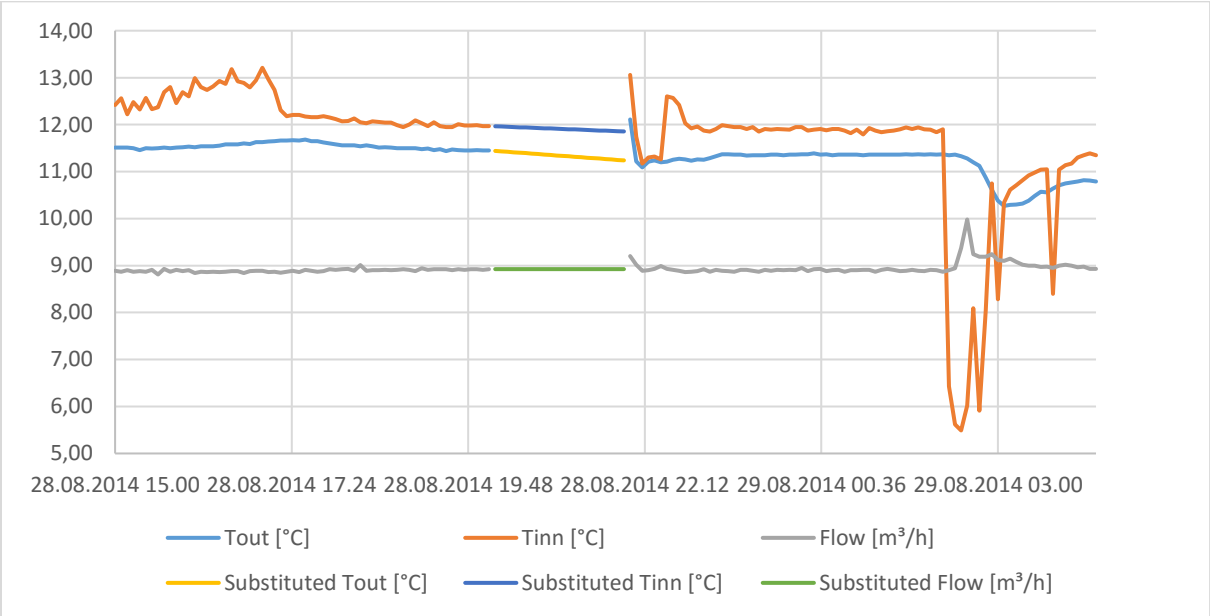

Appendix XI – Volume flow for the boreholes

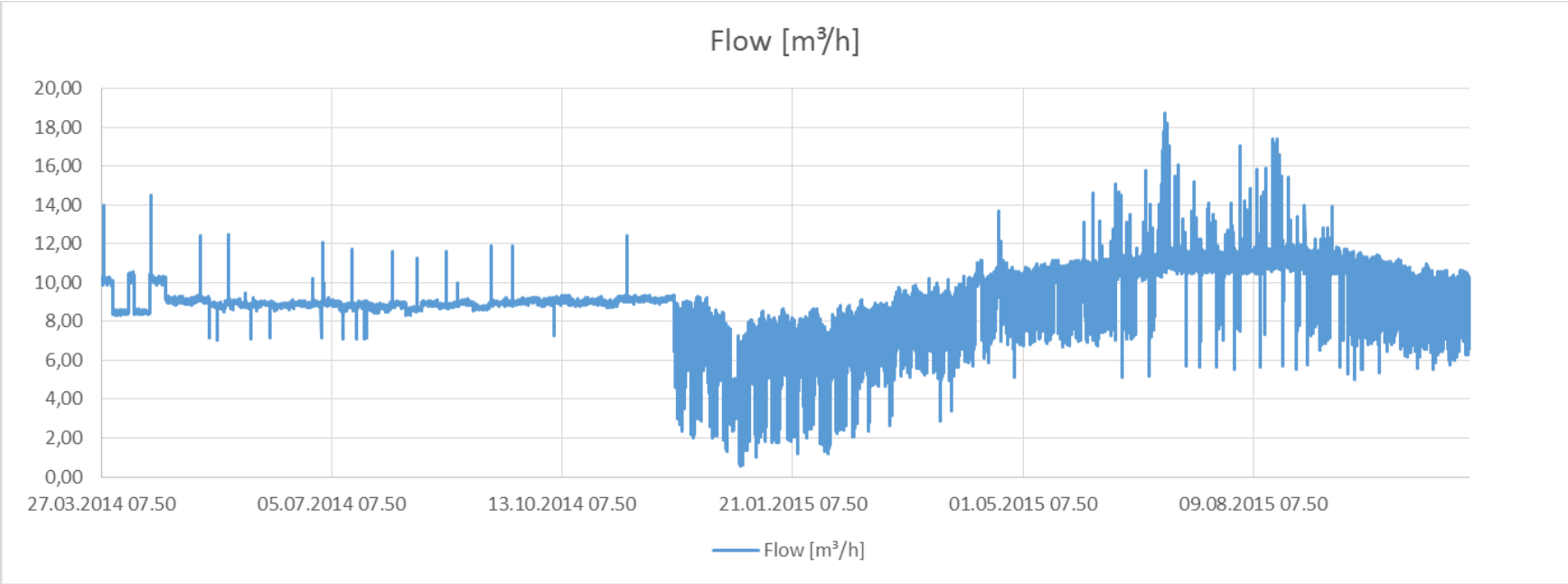

Appendix XII – Heat pump models

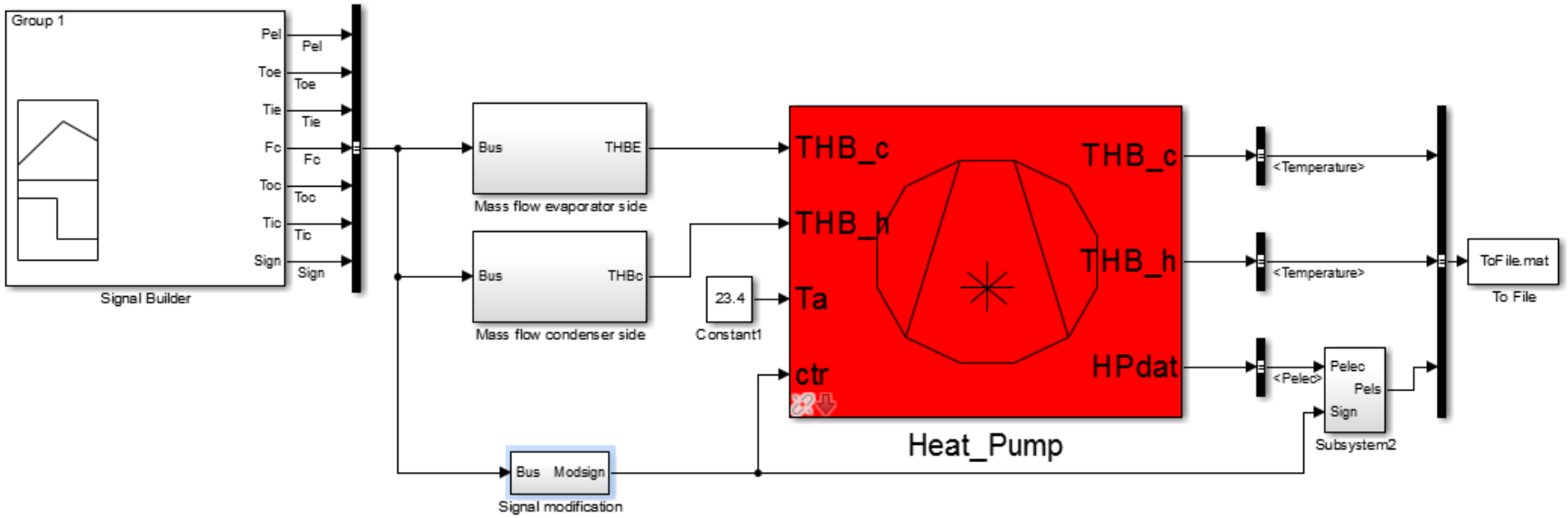

Appendix XIII – Storage tank model

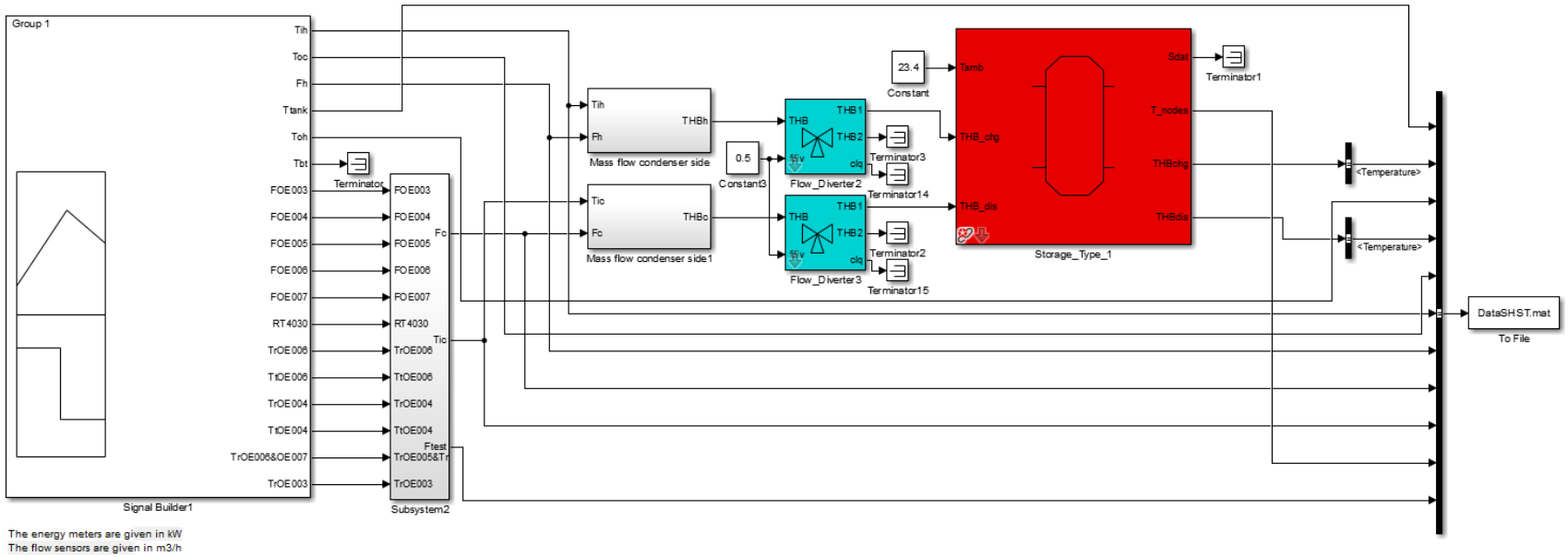

Appendix XIV – GHE simulation model

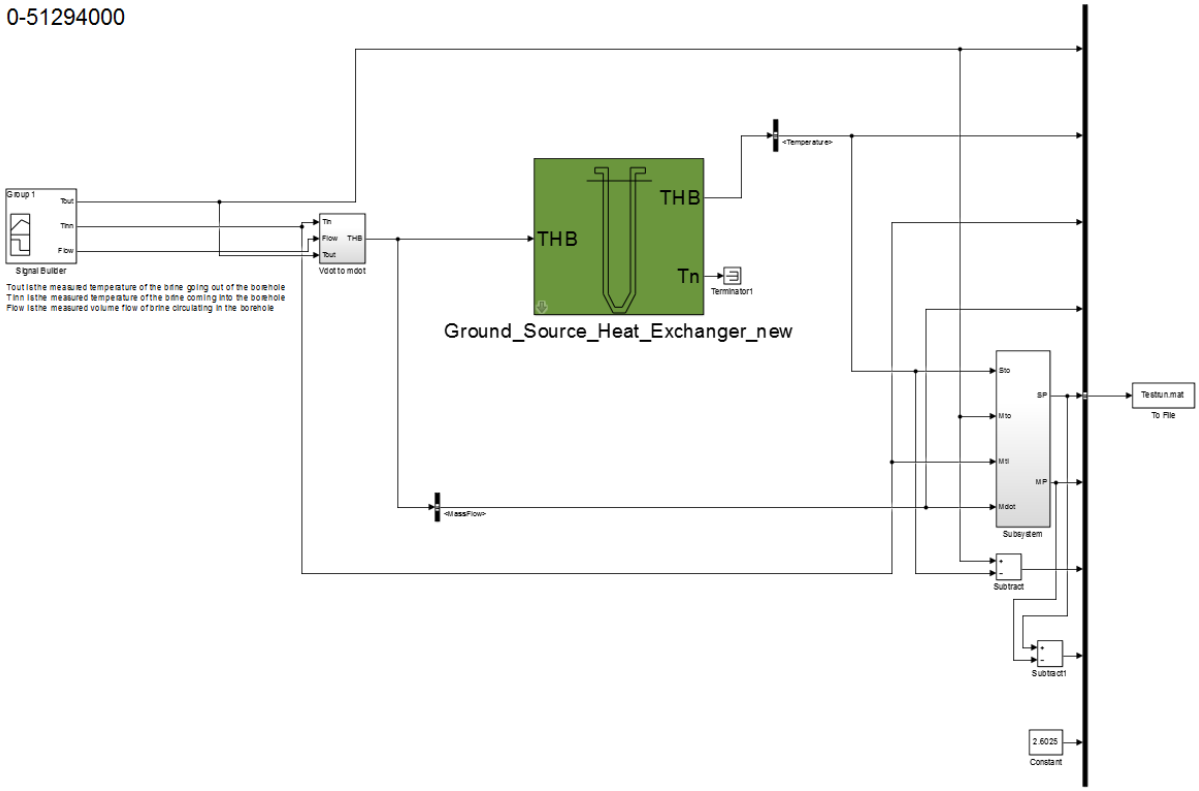

Appendix XV– Space heating system model

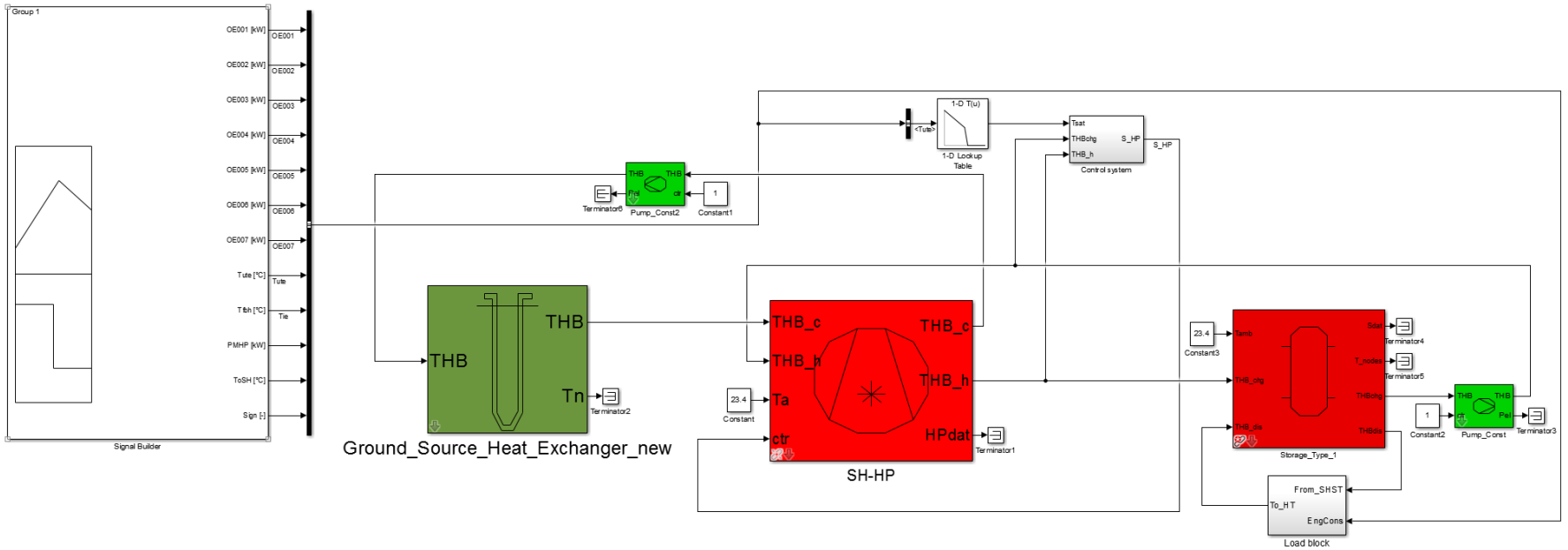

Appendix XVI – Capacity control of the heat pump block

In order to demonstrate that the heat pump block has the ability to be capacity controlled, a simulation has been performed. The simulation uses the heat pump block from the Carnot library, without changing any input parameters of the block. The THB inputs into the evaporator is produced in a basic_create_THB block, and the input parameters into the block is Pressure [Pa] =10000, fluid=5, fluid mixture is 0.35 for the evaporator and 0 for the condenser, diameter [m]=0.1, Geodetic height in m=0 and the calculation mode is 1. For the evaporator, the mass flow is set to 1.68 kg/s and the incoming temperature is set to 5℃. For the condenser, the mass flow is set to 1.12 kg/s and the incoming temperature is set to 40℃.

The signal into the simulation can be seen in the lower graph below. As it can be seen, the signal starts at 0.1, and goes 0.1 up for every 1000 seconds for a period of 10000 seconds.

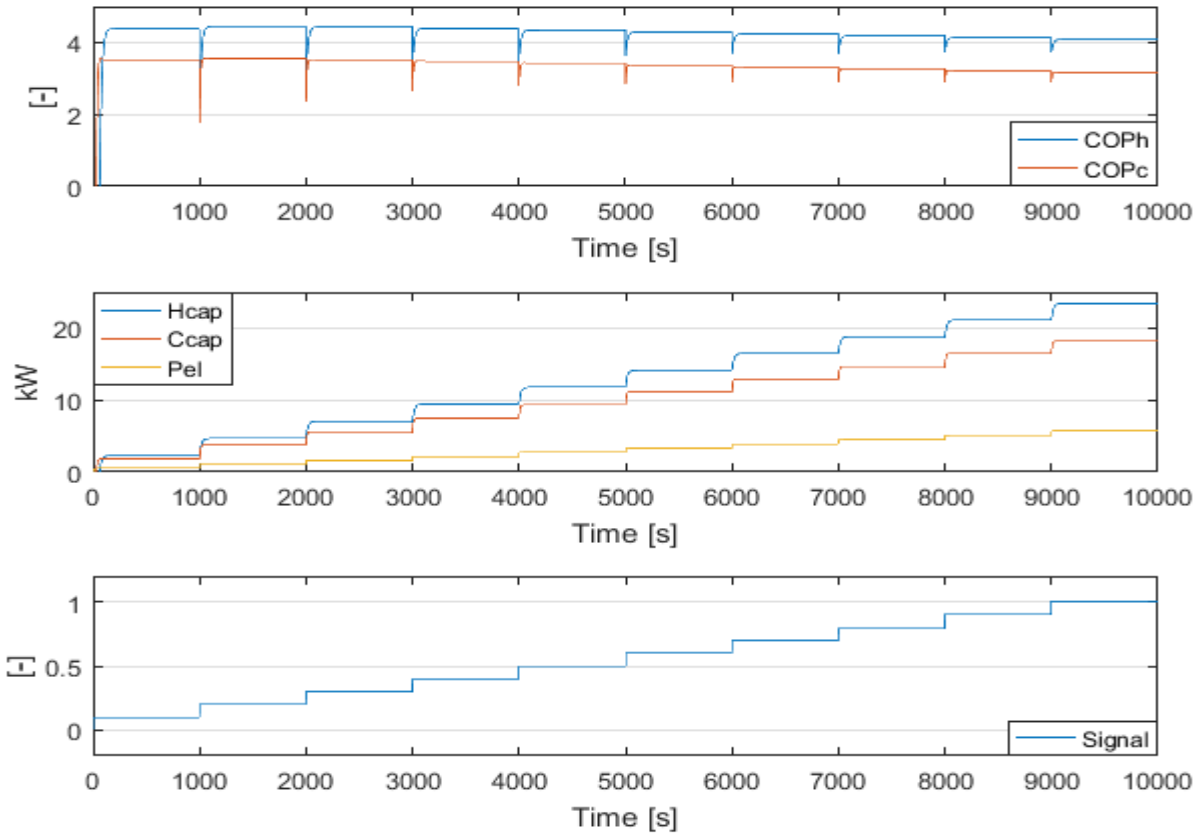

The result of the simulation is shown in the upper and middle figures above. From the upper figure, it is possible to see that the COP's is higher when the heat pump has a low signal. The downward peaks in this figure are caused by the thermal capacity of the condenser or evaporator. The middle figure shows that the power usage and the heating and cooling capacities can be controlled by the incoming control signal.